Proceedings of the I·R·E

APRIL 1942

VOLUME 30 NUMBER 4

Institute of Radio Engineers

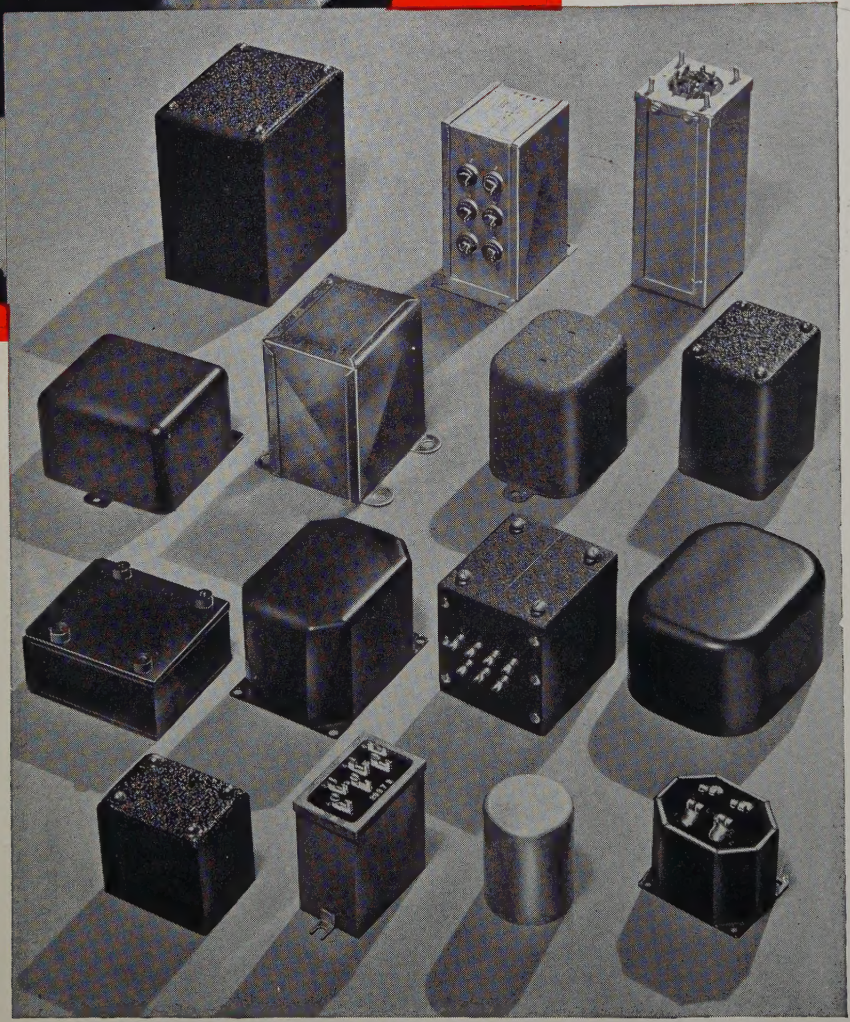

Illustrated are a few (just a very few) typical cases as supplied for some special applications

Proceedings *of the* I·R·E

Published Monthly by
The Institute of Radio Engineers, Inc.

VOLUME 30 — *April, 1942* — NUMBER 4

Entered as second-class matter October 26, 1927, at the post office at Menasha, Wisconsin, under the Act of February 28, 1925, embodied in Paragraph 4, Section 538 of the Postal Laws and Regulations. Publication office, 450 Ahnaip Street, Menasha, Wisconsin. Editorial and advertising offices, 330 West 42nd St., New York, N. Y. Subscription, $10.00 per year; foreign, $11.00.

THE INSTITUTE OF RADIO ENGINEERS
INCORPORATED

New York Meeting—May 6, 1942

Summer Convention, Cleveland, Ohio, June 29, 30, and July 1, 1942

SECTION MEETINGS

ATLANTA	CLEVELAND	DETROIT	LOS ANGELES
May 15	May 28	May 15	May 19

PHILADELPHIA	PITTSBURGH	WASHINGTON
May 7	May 11	May 11

SECTIONS

ATLANTA—Chairman, A. W. Shropshire; Secretary, G. M. Howard, 856 St. Charles Ave., N. E., Atlanta, Ga.

BALTIMORE—Chairman, V. D. Hauck; Secretary, G. J. Gross, Pa. Water & Power Co., 1611 Lexington Bldg., Baltimore, Md.

BOSTON—Chairman, J. M. Henry; Secretary, R. O. Oberg, Northeastern Univ., Boston, Mass.

BUENOS AIRES—Chairman, P. J. Noizeux; Secretary, L. C. Simpson, RCA Victor Argentina, Bartolome Mitre, 1961.

BUFFALO-NIAGARA—Chairman, E. H. Roy; Secretary, Leroy Fiedler, 53 Rosedale Ave., Hamburg, New York.

CHICAGO—Chairman, R. A. Kay; Secretary, Walter Kenworth, RCA Institutes, Inc., 1154 Merchandise Mart. Chicago, Ill.

CINCINNATI—Chairman, W. L. Schwesinger; Secretary, Howard Leppele, 4432 Raceview Ave., Cincinnati, Ohio.

CLEVELAND—Chairman, P. L. Hoover; Secretary, A. S. Nace, 3209 Archwood Ave., Cleveland, Ohio.

CONNECTICUT VALLEY—Chairman, F. G. Webber; Secretary, C. I. Bradford, 187 Glenarden Dr., Fairfield, Conn.

DALLAS-FORT WORTH—Chairman, D. A. Peterson; Secretary, P. C. Barnes, Radio Station WFAA-WBAP, Grapevine, Texas.

DETROIT—Chairman, M. Cottrell; Secretary, Paul Frincke, 26686 Kenwood Ave., Royal Oak, Michigan.

EMPORIUM—Chairman, E. J. Hoffman; Secretary, H. D. Johnson, Hygrade Sylvania Corp., Emporium, Pa.

INDIANAPOLIS—Chairman, A. N. Curtiss; Secretary, T. N. Rosser, P. R. Mallory and Company, Indianapolis, Ind

KANSAS CITY—Chairman, H. K. Morgan; Secretary G. L. Taylor, Midland Radio School Power and Light Building, Kansas City, Mo.

LOS ANGELES—Chairman, C. F. Wolcott; Secretary, E. S. Sievers, Room 567, 417 S. Hill St., Los Angeles, Calif.

MONTREAL—Chairman, E. A. Laport; Secretary, W. A. Nichols, Canadian Broadcasting Corp., 1012 Keefer Bldg., Montreal, P. Q., Canada.

PHILADELPHIA—Chairman, C. C. Chambers; Secretary, R. L. Snyder, 103 Franklin Rd., Glassboro, N. J.

PITTSBURGH—Chairman, P. N. Bossart; Secretary, M. G. Jarrett, Bell Telephone Company of Pennsylvania, 416 Seventh Ave., Pittsburgh, Pa.

PORTLAND—Chairman, R. W. Deardorff; Secretary, L. M. Belleville, 361 N. E. 75th Ave., Portland, Ore.

ROCHESTER—Chairman, H. J. Klumb; Secretary, O. L. Angevine, Jr., Stromberg-Carlson Tel. Mfg. Co., Rochester, N. Y.

ST. LOUIS—Temporary Chairman, R. L. Glasgow, Washington University, St. Louis, Mo.

SAN FRANCISCO—Chairman, H. E. Held; Secretary, W. G. Wagener, Heintz and Kaufman, South San Francisco, Calif

SEATTLE—Chairman, K. H. Ellerbeck; Secretary, R. J. Gleason, Pacific Alaska Airways, Inc., 3314 White Bldg., Seattle, Wash.

TORONTO—Chairman, R. H. Klingelhoeffer; Secretary, L. Claude Simmonds, 301 King St., E., Toronto, Ont., Canada.

TWIN CITIES—Chairman, C. A. Culver; Secretary, N. B. Coil, 1664 Thomas St., St. Paul, Minn.

WASHINGTON—Chairman, E. M. Webster; Secretary, J. D. Wallace, Radio Division U. S. Naval Research Laboratory, Bellevue, Anacostia, D. C.

A Secondary Frequency Standard Using Regenerative Frequency-Dividing Circuits*

F. R. STANSEL†, MEMBER I.R.E.

Summary—*A secondary frequency standard is described in which standard frequencies are derived from a 5-megacycle oscillator by a series of frequency dividers. The advantage of obtaining standard frequencies by frequency division rather than by frequency multiplication is pointed out and the characteristics of the regenerative frequency dividers used are discussed.*

In ALL precision methods of frequency measurement in use today one or more standard frequencies are required. These are generally derived from a piezoelectric oscillator operating in the range of 50 to 100 kilocycles by the use of suitable frequency multipliers or dividers.

When a derived frequency is lower than the oscillator frequency, traces of the latter in the output circuit will cause no confusion since the oscillator frequency is a harmonic of the derived frequency and in measuring equipment harmonics are usually intentionally introduced and must always be considered to be present. Harmonics of the oscillator frequency will also cause no difficulty as these harmonics are also harmonics of the derived frequency.

When a derived frequency is higher than the oscillator frequency any traces of the latter in the output circuit are a possible source of confusion as this oscillator frequency, is extraneous and not harmonically related to the derived frequency. Harmonics of the oscillator frequency may also cause confusion since, in general, they are not harmonics of the derived frequency. An example of such confusion has been reported by Finden.[1] Both he and Thomas[2] found it necessary to interpose a synchronized oscillator in their chain of frequency multipliers to eliminate this residual oscillator frequency.

For measurements at higher radio frequencies, standards of 100 kilocycles, 1 megacycle, and even 10 megacycles are desirable. Piezoelectric oscillators operating at 100 kilocycles possess a greater degree of stability than those operating at higher frequencies and hence are more suited for primary standards, yet the degree of stability of a 5-megacycle piezoelectric oscillator is sufficient to warrant its use as a secondary frequency standard. The National Bureau of Standards now makes available a 5-megacycle standard frequency by transmitting it on an extensive schedule from radio station WWV and if the maximum accuracy is required, the secondary standard may be monitored continuously against this transmission. In this manner an accuracy differing not greatly from that of the transmissions from WWV, namely, one part in ten million, can be obtained.

Fig. 1 shows the block diagram of a secondary frequency standard. The piezoelectric oscillator uses a low-temperature-coefficient-type crystal (Western Electric

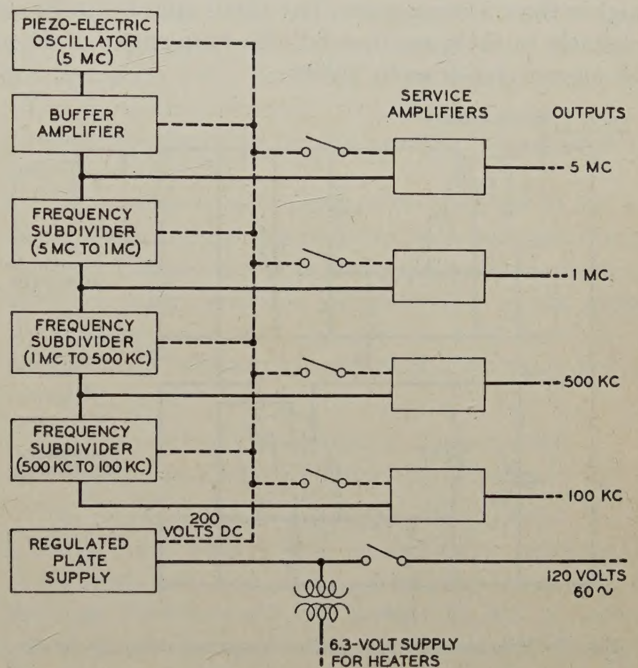

Fig. 1—Block diagram of secondary frequency standard.

type 5AA quartz plate) operating at 5 megacycles in an oscillator circuit of conventional type. This oscillator is followed by a buffer amplifier and a frequency-dividing circuit which is adjusted to deliver an output of 1 megacycle. This 1-megacycle output energizes a second frequency divider which produces 500 kilocycles. A third frequency divider operating from this 500-kilocycle supply produces a frequency of 100 kilocycles. Each of the four frequencies, the 5-megacycle standard and the 1-megacycle, 500-kilocycle, and 100-kilocycle derived frequencies are provided with service amplifiers which make these frequencies available for external use.

Frequency-Dividing Circuits

The frequency-dividing circuits used are of the "regenerative submultiple generator" or "quasi-stable" type proposed by Horton[3] and Longo[4] and discussed

* Decimal classification: R 213. Original manuscript received by the Institute, August 15, 1941; revised manuscript received, October 15, 1941.

† Bell Telephone Laboratories, Inc., New York, N. Y.

[1] H. J. Finden, "Frequency standardization equipment," *Wireless Eng.*, vol. 14, pp. 117–126; March, 1937.

[2] H. A. Thomas, "Frequency measurement, a new equipment for range 1 to 70 Mc/s," *Wireless Eng.*, vol. 14, pp. 299–305; June, 1937.

[3] J. W. Horton, United States Patent No. 1,690,299.

[4] G. Longo, "Multiplication of a frequency by simple fractional numbers," *L'Onde Elec.*, vol. 13, pp. 97–100; February, 1934.

by Sterky,[5] Miller[6] and Fortescue.[7] Frequency-dividing circuits used heretofore have usually consisted of a multivibrator synchronized at one of its harmonic frequencies. Sabaroff,[8] Bollman[9] and Essen[10] have reported the successful operation of multivibrators at a fundamental frequency of 1 megacycle. These investigators all agree that for operation at this frequency all stray capacitances must be carefully controlled and "acorn"-type vacuum tubes are essential. In contrast, the regenerative frequency-dividing circuits of Fig. 1 use vacuum tubes of the type used in broadcast receivers and tuned circuits which contain appreciable capacitance. No experimental data are available on the operation of this type of circuit at frequencies higher than 5 megacycles, but there appears to be no obstacle to their use to subdivide frequencies of 30 to 50 megacycles or even higher.

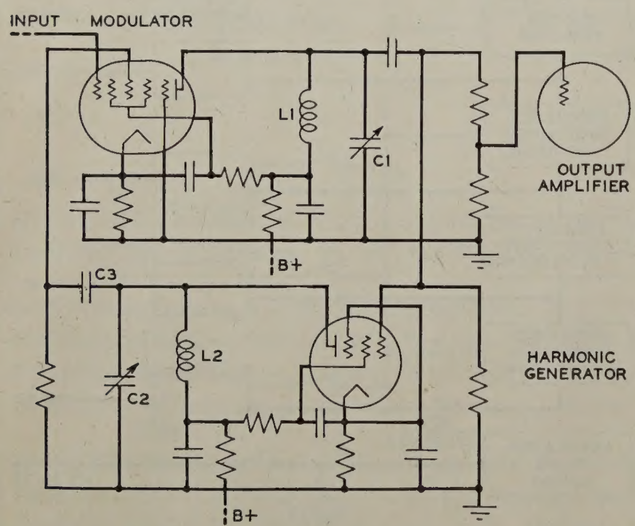

Fig. 2—Schematic of regenerative frequency-dividing circuit.

Fig. 2 shows the circuit of one of the frequency dividers. It consists essentially of two vacuum tubes. The first, designated as the modulator, is of the pentagrid converter type (6SA7) while the second, designed as the harmonic generator, is a pentode (6SJ7). The input frequency f is applied to the first grid of the modulator. The plate of the modulator is connected to the parallel resonant circuit $L1$-$C1$ which is tuned to the submultiple frequency f/n which it is desired to produce.

Assume that the output of the modulator contains a component of the frequency f/n This component will be selected by the tuned circuit $L1$-$C1$ and applied to the output amplifier and also to the grid of the harmonic generator. This tube is adjusted to multiply its input frequency by the factor $n-1$ producing in its plate circuit the frequency component

$$\frac{n-1}{n}f = (1 - 1/n)f.$$

This component, selected by the tuned circuit $L2$-$C2$, is impressed on the third grid of the modulator tube through the condenser $C3$. In the modulator, intermodulation between this component and the original input frequency f produces the sum and difference frequencies

$$\frac{2n-1}{n}f \quad \text{and} \quad \frac{f}{n}.$$

The second of these is the frequency component which was assumed to exist in the output of the modulator and, hence, the circuit once started is self-sustaining.

As an alternative, the harmonic generator may be adjusted to multiply its input frequency by the factor $n+1$. The frequency applied to the third grid of the modulator is then $(1+1/n)f$ and the output of the modulator contains the frequency components

$$\frac{2n+1}{n}f \quad \text{and} \quad \frac{f}{n}.$$

The problem of starting a frequency-dividing circuit of this type is similar in many respects to the problem of starting an oscillator although the mechanism is more complex. In some cases special starting circuits are required, although this was not found to be necessary in this application.

Table I lists a number of possible circuit combinations with which submultiple frequencies from $f/2$ through $f/5$ may be obtained. In addition to the submultiple frequency there is always present in the plate circuit of the modulator the second modulation frequency $(2n\pm1)f/n$ and the two impressed frequencies f and $(n\pm1)f/n$ which are passed through the modulator tube by amplifier action. These additional frequencies, which are listed in Table I for the various circuit combinations, represent other fractional values of the input frequency and if desired may be obtained in addition to the submultiple frequency by means of suitable selective circuits.

TABLE I
REGENERATIVE FREQUENCY-DIVIDING CIRCUITS
(2ND-ORDER MODULATION)

Modulator Plate Circuit Tuned To	Harmonic Used	Frequency Fed Back	Output	
			Sum Frequency	Difference Frequency
f	2nd	$2f$	$3f$	f
$f/2$	Fundamental	$f/2$	$3f/2$	$f/2$
$f/2$	3rd	$3f/2$	$5f/2$	$f/2$
$f/3$	2nd	$2f/3$	$5f/3$	$f/3$
$f/3$	4th	$4f/3$	$7f/3$	$f/3$
$f/4$	3rd	$3f/4$	$7f/4$	$f/4$
$f/4$	5th	$5f/4$	$9f/4$	$f/4$
$f/5$	4th	$4f/5$	$9f/5$	$f/5$
$f/5$	6th	$6f/5$	$11f/5$	$f/5$

[5] H. Sterky, "Frequency multiplication and division," Proc. I.R.E., vol. 25, pp. 1153–1173; September, 1937.

[6] R. L. Miller, "Fractional-frequency generators utilizing regenerative modulation," Proc. I.R.E., vol. 27, pp. 446–457; July, 1939.

[7] R. L. Fortescue, "Quasi-stable frequency dividing circuits," *Jour. I.E.E.* (London), vol. 84, pp. 693–698, June, 1939; discussion, vol. 85, pp. 646–647; November, 1939.

[8] S. Sabaroff, "An ultra-high-frequency measuring assembly," Proc. I.R.E., vol. 27, pp. 208–212; March, 1939.

[9] J. H. Bollman, "The design, construction and test of a source of precisely controlled high frequencies," Thesis, Polytechnic Institute of Brooklyn, May, 1939.

[10] L. Essen, "A precision frequency-meter of range zero to 2000 mc/sec," *Proc. Phys. Soc.*, vol. 52, pp. 616–624; September, 1940.

Since the reason for adopting a high standard frequency followed by frequency dividers is to avoid nonharmonic frequencies, it is necessary to examine the output of such a frequency divider to ascertain that no components that are not multiples of the derived frequency are present. Present in the plate circuit of the modulator and hence in the output, even though attenuated by the selective circuit, are the following frequencies:[11]

Frequencies due to the modulator tube acting as an amplifier

Frequency applied to 1st grid f or $\frac{n}{n}f$

Frequency applied to 3rd grid $\frac{n \pm 1}{n}f.$

Frequencies due to 2nd-order modulation

2nd harmonic of f	$2f$ or $\frac{2n}{n}f$
2nd harmonic of $(n \pm 1)/nf$	$\frac{2(n \pm 1)}{n}f$
Sum product	$\frac{2n \pm 1}{n}f$
Difference product	$\frac{f}{n}.$

Each of these products has the form $(m/n)f$, where m is an integer, and hence is a multiple or harmonic of the derived frequency f/n.

Higher-order modulation in the modulator tube gives rise to several types of products. Harmonics of the applied frequencies f and $(n \pm 1)nf$ will always be in harmonic relation with the derived frequency f/n. Sum and difference products of the type

$$pf + q\left[\frac{n \pm 1}{n}f\right] \quad \text{and} \quad pf - q\left[\frac{n \pm 1}{n}f\right]$$

where p and q are any integer, may be rewritten

$$\frac{f}{n}\left[pn + q(n \pm 1)\right] \quad \text{and} \quad \frac{f}{n}\left[pn - q(n \pm 1)\right].$$

All quantities in the brackets are integers and hence any such components in the output will be harmonically related to f/n.

There remains to be considered the effect of the presence of other harmonics than the $(n \pm 1)$th in the output of the harmonic producer. It has already been shown that each component in the plate of the modulator is a multiple of f/n. Hence, any product of any type in the output of the harmonic producer will also be a multiple of f/n. Finally, any product arising from interaction of these products in the modulator tube will still be in harmonic relation with f/n.

[11] In this tabulation plus or minus signs are used because the $1/n$th submultiple can be produced by two different circuit adjustments using either the $(n+1)$th harmonic or the $(n-1)$th harmonic. For any one adjustment only one sign is used throughout.

From this analysis it is established that if a pure frequency f is applied to the input of this type of frequency divider, the output will consist of the frequency f/n and frequencies which are multiples of f/n. It should be noted further that the introduction of harmonics of f in the input to the frequency divider will still not alter this statement. If the input contains harmonics of f, these frequencies will be also harmonics of f/n and all products generated by these harmonics will also be in harmonic relation to f/n. These statements must, however, be restricted to frequency-dividing circuits such as those heretofore discussed in which the output is of type f/n. In the following section frequency dividers using higher-order modulation and adjusted to give outputs of the type mf/n are discussed. If m and n are different, the input frequency f is not a harmonic of the output frequency mf/n. Frequency dividers of this type are, as a consequence, less desirable for use as a part of a standard-frequency assembly.

The absence of nonharmonic frequencies in divider circuits of this type has been checked on several occasions by the use of a sensitive radio receiver equipped with a beating oscillator. All harmonics of f/n within the frequency range of the receiver were found to be present but in no case was any nonharmonic frequency found.[12]

Fractional-Frequency Generators Using Higher-Order Modulation

The regenerative frequency-dividing circuits tabulated in Table I all depend on 2nd-order components in the modulator and produce fractional frequencies of the type f/n where n is any integer. If 3rd- or higher-order terms in the modulator are considered, fractional frequencies of the type mf/n may be obtained. Such a generator was demonstrated experimentally using the 500- to 100-kilocycle frequency divider of the frequency standard described above. In this frequency divider the output circuit is tuned to 100 kilocycles and the harmonic generator to its fourth harmonic, e.g., 400 kilocycles. After the circuit had been adjusted to operate satisfactorily under normal conditions with an input frequency of 500 kilocycles, the input frequency was changed to 250 kilocycles. With this input frequency, an output of 100 kilocycles, 2/5 the input frequency, was obtained by modulation between the 4th harmonic of the output and twice the input frequency. As a further experiment the input frequency was changed to 150 kilocycles and 100 kilocycles was again obtained, this time as 2/3 the input frequency. Here again the 4th harmonic of the output frequency was modulated with twice the incoming frequency to

[12] When two or more frequency dividers are cascaded as in Fig. 1 there is always the possibility that nonharmonic frequencies from the second divider may, through imperfect shielding between elements in the modulator, be impressed on the input of the preceding service amplifier. These stray components may be eliminated either by careful isolation of the circuits or by de-energizing the dividers following the service amplifier in use.

TABLE II

Regenerative Frequency-Dividing Circuits to Produce mf/n (3rd- and 4th-Order Modulation)

Order of Modulation	Plate Circuit Tuned to	Harmonic Used	Frequency Fed Back	Output	
				Sum Frequency	Difference Frequency
3rd (a)	$2f/3$	2	$4f/3$	$10f/3$	$2f/3$
3rd (a)	$2f/3$	4	$8f/3$	$14f/3$	$2f/3$
3rd (a)	$2f/5$	4	$8f/5$	$18f/5$	$2f/5$
3rd (a)	$2f/5$	6	$12f/5$	$22f/5$	$2f/5$
4th (b)	$2f/3$	Fundamental	$2f/3$	$10f/3$	$2f/3$
4th (b)	$2f/3$	2	$4f/3$	$14f/3$	$2f/3$
4th (b)	$2f/5$	2	$4f/5$	$18f/5$	$2f/5$
4th (b)	$2f/5$	3	$6f/5$	$22f/5$	$2f/5$
4th (c)	$3f/2$	Fundamental	$3f/2$	$9f/2$	$3f/2$
4th (c)	$3f/2$	3	$9f/2$	$15f/2$	$3f/2$
4th (c)	f	2	$2f$	$5f$	$3f/3=f$
4th (c)	f	4	$4f$	$7f$	$3f/3=f$
4th (c)	$3f/4$	3	$9f/4$	$21f/4$	$3f/4$
4th (c)	$3f/4$	5	$15f/4$	$27f/4$	$3f/4$
4th (c)	$3f/5$	4	$12f/5$	$27f/5$	$3f/5$
4th (c)	$3f/5$	6	$18f/5$	$33f/5$	$3f/5$

(a) Twice input frequency plus or minus fed-back frequency.
(b) Twice input frequency plus or minus twice fed-back frequency.
(c) Three times input frequency plus or minus fed-back frequency.

produce, by 3rd-order modulation, the desired output.

Table II lists a number of fractional frequencies of the type mf/n which may be produced by 3rd- and 4th-order modulation. Third-order modulation produces fractional frequencies of type $2f/n$, such as 2/3, 2/5, 2/7, etc., of the input frequency, while 4th-order modulation produces among other fractional frequencies those of the type $3f/n$, such as 3/4, 3/5, and 3/7 of the input frequency. Table II can be extended to higher orders of modulation and, in general, it will be found that nth-order modulation will produce among other fractional frequencies those of the type $(n-1)f/n$. As in the case of Table I, in addition to the difference frequency, a harmonic of which must be fed back in each case to sustain the circuit operation, there are present in the plate circuit of the modulator other components, particularly the sum frequency, which may be obtained if desired by additional selective circuits.

TABLE III

Regenerative Frequency-Dividing Circuits to Produce f/n (3rd- and 4th-Order Modulation)

Order of Modulation	Plate Circuit Tuned to	Harmonic Used	Frequency Fed Back	Output	
				Sum Frequency	Difference Frequency
3 (a)	f	Fundamental	f	$3f$	f
3 (a)	$f/3$	Fundamental	$f/3$	$5f/3$	$f/3$
3 (a)	$f/3$	2	$2f/3$	$7f/3$	$f/3$
3 (a)	$f/5$	2	$2f/5$	$9f/5$	$f/5$
3 (a)	$f/5$	3	$3f/5$	$11f/5$	$f/5$
3 (b)	f	Fundamental	f	$3f$	f
3 (b)	$f/2$	3	$3f/2$	$7f/2$	$f/2$
3 (b)	$f/2$	5	$5f/2$	$9f/2$	$f/2$
3 (b)	$f/3$	5	$5f/3$	$11f/3$	$f/3$
3 (b)	$f/3$	7	$7f/3$	$13f/3$	$f/3$
3 (b)	$f/4$	7	$7f/4$	$15f/4$	$f/4$
3 (b)	$f/4$	9	$9f/4$	$17f/4$	$f/4$
3 (b)	$f/5$	9	$9f/5$	$19f/5$	$f/5$
3 (b)	$f/5$	11	$11f/5$	$21f/5$	$f/5$
4 (c)	$f/2$	Fundamental	$f/2$	$5f/2$	$f/2$
4 (c)	$f/4$	Fundamental	$f/4$	$7f/4$	$f/4$
4 (c)	$f/5$	2	$2f/5$	$11f/5$	$f/5$
4 (d)	$f/2$	5	$5f/2$	$11f/2$	$f/2$
4 (d)	$f/2$	7	$7f/2$	$13f/2$	$f/2$
4 (d)	$f/3$	8	$8f/3$	$17f/3$	$f/3$
4 (d)	$f/3$	10	$10f/3$	$19f/3$	$f/3$
4 (d)	$f/4$	11	$11f/4$	$23f/4$	$f/4$
4 (d)	$f/4$	13	$13f/4$	$25f/4$	$f/4$
4 (d)	$f/5$	14	$14f/5$	$29f/5$	$f/5$
4 (d)	$f/5$	16	$16f/5$	$31f/5$	$f/5$

(a) Input frequency plus or minus twice fed-back frequency.
(b) Twice input frequency plus or minus fed-back frequency.
(c) Input frequency plus or minus three times fed-back frequency.
(d) Three times input frequency plus or minus fed-back frequency.

Fractional frequencies of the type f/n such as those submultiples already considered in Table I can also be generated by higher-order modulation by the circuit combinations tabulated in Table III. Table IV compiled from the data in Tables I and III and extensions of these tables shows the harmonic required to produce frequency ratios from 1:2 through 1:6 using 2nd-, 3rd-, 4th-, or 5th-order modulation.

The presence of submultiple components due to higher-order modulation may sometimes explain discrepancies in experimental observations, particularly when the coupling between the harmonic generator and modulator consists of a single tuned circuit with somewhat limited selectivity. An example of this was noted when observing the phase relation between the input and output frequency of a certain divider as the amplitude of the input frequency was varied. Considering only the effect of 2nd-order modulation, this phase relation should have been constant, but experimental observations showed a variation. The frequency

TABLE IV

Regenerative Frequency-Dividing Circuits—Harmonics Required for Various Frequency Ratios

Frequency Ratio	Order of Modulation			
	2nd	3rd	4th	5th
1:2	1, 3	3, 5	1, 5, 7	1, 7, 9
1:3	2, 4	1, 2, 5, 7	8, 10	1, 4, 5, 11, 13
1:4	3, 5	7, 9	1, 11, 13	3, 15, 17
1:5	4, 6	2, 3, 9, 11	2, 14, 16	1, 3, 7, 8, 19, 21
1:6	5, 7	11, 13	17, 19	23, 25

divider in question was designed to obtain a 1:5 ratio by feeding back the 4th harmonic. From Table IV it may be seen that this ratio may be produced not only by the 4th harmonic (2nd-order modulation) but also, among other combinations, by 2nd and 3rd harmonics (3rd-order modulation). In this manner additional components of the output frequency were generated which had different amplitudes and phases at different levels of input frequency and thus caused the observed variation in phase between the input and output frequencies.

It has been suggested that the presence of additional output components due to higher-order modulation may have some bearing on the question of stability of the circuit. This question has not yet been investigated.

Generation of False Output Frequencies in Regenerative Frequency-Dividing Circuits

Miller, Fortescue, and other writers have pointed out the important advantage of regenerative frequency-dividing circuits over multivibrators and other synchronized circuits in that regenerative frequency dividers, possessing no natural frequency, can never give out a false frequency due to falling out of synchronism. While this statement is true for a correctly adjusted circuit, experimental observations have shown that circuits similar to Fig. 2, if misadjusted, may deliver a false frequency which bears no fixed relationship

to the input frequency. It should be emphasized that these false frequencies occur only in misadjusted circuits and once the circuit is correctly adjusted it is highly stable and will operate without readjustment for an indefinite length of time.[13]

These false output frequencies were observed when the circuit was adjusted as follows: The feedback circuit was opened either by disconnecting the condenser $C3$ or by substituting a tube with an open heater for the harmonic generator. An oscillator tuned to the desired output frequency was applied to the input of the modulator and the plate circuits of the modulator and any following amplifiers were tuned to this frequency. The feedback circuit was then replaced, the input frequency applied, and the tuned circuit of the harmonic generator adjusted until an output of the desired frequency was obtained as shown by the correct Lissajous figure on a cathode-ray oscilloscope connected between the input and output of the frequency divider.

While making this last adjustment it was observed that over a large portion of the scale of the harmonic-generator tuning condenser $C2$ there was, as might be expected, no output. Over a small portion of the scale corresponding to the $(n-1)$th harmonic and again over a second portion of the scale corresponding to the $(n+1)$th harmonic the desired submultiple frequency was obtained. The transition from the condition of no output to the condition of the desired output was in many cases abrupt but in some cases on one or both sides of the setting of $C2$ there was a region in which the oscilloscope showed the presence of an output which bore no definite relation to the input frequency. When such regions of false frequencies were present the range of $C2$ over which they were present was often found to be dependent on the care taken in making the initial adjustment of $C1$. If $C1$ were deliberately misadjusted, the possibility of obtaining a false frequency was greatly increased.

These false frequency outputs were due to any one of several mechanisms. In the frequency region between f/n and $(n-1)f/n$ the tuned circuit $L1$-$C1$ of the modulator has a negative reactance while the tuned circuit $L2$-$C2$ of the harmonic generator has a positive reactance. At some frequency in this range the phase angles of the two circuits will be equal[14] and if there is sufficient gain around the loop, a singing condition will be set up. Such singing is independent of the amplitude of the input frequency and continues even when the input frequency has been removed.

A second possible mechanism for false output frequency is modulation between the input frequency and some spurious frequency generated in the harmonic generator itself due to stray coupling between its input and output or some similar cause. In this case the output behaves in exactly the same manner as would a true derived frequency, the output disappearing completely if the input is removed. An abrupt change is sometimes observed as a pattern changed from a blur to a distinct Lissajous figure which suggests that there is a strong synchronizing action when the frequency of the spurious oscillation is brought close to the frequency of a harmonic of the desired output.

Among the modulation products present in the modulator there is always a direct-current component. This current flowing through the cathode resistor will shift the operating point of the modulator. If the new operating point is unstable the modulator will shift back to the original point and relaxation oscillations will be set up. Such relaxation oscillations, having the characteristic saw-tooth wave-shape and frequencies ranging from approximately 5 to 25 kilocycles, have been observed in frequency dividers. These relaxation oscillations generally appear as a modulation on the true output frequencies but in many cases these spurious sidebands are so strong and numerous as to make the identification of the true submultiple frequency impossible.

Additional Experimental Observations

During the development of the frequency standard described above regenerative frequency-dividing circuits of the type shown in Fig. 2 were operated at ratios[15] of 1:2, 1:3, 1:4, 1:5, and 1:6. No experimental work was performed on higher ratios but there is reason to believe that higher ratios may also be practical. In addition to these simple ratios the circuit previously described using 3rd-order modulation was operated at ratios of 2:3 and 2:5. The adjustment of all of these circuits followed the procedure described in the previous section.

No special devices were found necessary to start these circuits. The normal transient in the circuit apparently supplied sufficient excitation to start the regenerative action. If, after starting, the input voltage was reduced below a critical value, or if one of the variable condensers was slightly misadjusted, the circuit would often continue to function normally but would fail to restart if turned off. Such a condition could be remedied by restoring the input voltage to its former value or resetting the condenser.

Theoretically, any subdivision can be obtained using either the $(n-1)$th or $(n+1)$th harmonic. Several circuits, in which the range of the tuned circuit of the harmonic generator was sufficient, were operated by

[13] The reader may ask, if these false frequencies are possible what, if any, advantage has the regenerative frequency divider over the multivibrator? In a correctly adjusted regenerative divider, on the failure of the input voltage the output drops to zero, while in even a correctly adjusted multivibrator, the output continues, giving the operator without warning a false frequency. The author has discussed the merits of these two circuits with several of his associates who have had experience with both types of circuits and the opinion is unanimous that the likelihood of misadjustment is vastly greater in the multivibrator.

[14] The effect on the phase angle of $C3$ and input capacitance of the modulator must also be considered in any exact analysis.

[15] Since the preparation of this manuscript V. J. Weber has constructed a frequency divider of this type which operates at a ratio of 1:10. Three of these frequency dividers have been used in tandem to step down from 100 kilocycles to 100 cycles.

feeding back the $(n-1)$th harmonic and then readjusted to operate by feeding back the $(n+1)$th harmonic. There appeared to be no marked advantage in the use of one over the other of these settings.[16]

The subdivider circuit shown in Fig. 2 using 6SA7 and 6SJ7 vacuum tubes required an input of from 1 to 4 volts for operation. In the 5- to 1-megacycle frequency divider the gain through the circuit was slightly less than unity, that is, for a 5-megacycle input of 1.8 volts applied to the first grid of the modulator, a 1-megacycle voltage of approximately 1.2 volts appeared at the plate of the modulator.

No difficulty was encountered in cascading these subdivider circuits. Each circuit was followed by a tuned amplifier stage which acted as a buffer and insured an dequate supply of the derived frequency for exciting both the following stage and the service amplifier shown in Fig. 1.

[16] Later experience has shown that there is a small improvement in stability when using the $(n-1)$th harmonic. This is theoretically to be expected as any small frequency increment in the modulator plate circuit on being fed back appears with a reversed sign in the $(n-1)$th harmonic circuit and with the same sign in the $(n+1)$th harmonic circuit. In order to observe this unstability, it was necessary to use two 1:10 stages, a total frequency division of 1:100. The Lissajous figure between the input and output of these dividers showed a slight "jitter" corresponding to a random phase shift back and forth of about 10 to 20 degrees when one of the two stages was adjusted to the $(n+1)$th harmonic. When both stages were adjusted to the $(n-1)$th harmonic no "jitter" could be observed. When the three frequency-dividing stages referred to in footnote 15 were used the 100-cycle output obtained was quite free from "jitters" and other signs of instability.

Acknowledgment

The development of the frequency standard and frequency-dividing circuits described in this paper were carried on under the auspices of the Polytechnic Institute of Brooklyn. The author wishes to express his appreciation to the faculty of this institution and particularly to Professor E. Weber for making this work possible.

Color Television—Part I*

P. C. GOLDMARK†, MEMBER, I.R.E., J. N. DYER†, ASSOCIATE, I.R.E.,
E. R. PIORE†, ASSOCIATE, I.R.E., AND J. M. HOLLYWOOD†, ASSOCIATE, I.R.E.

Summary—*A brief history of color television and the reasons leading up to the Columbia Broadcasting System color television system have been presented. A general theory for color television, including color, flicker, and electrical characteristics, is also given. Equipment for color-television transmission and reception has been designed and constructed based on these principles.*

Introduction

MUCH of the significance of color in television is striking, even to the casual observer. Aside from the most obvious effect, namely, that color introduces a sense of reality and a lifelike quality into the picture, comparison of a color-television picture with the corresponding black-and-white image makes it apparent that not only are small objects more perceptible but outlines in general seem to be more clearly defined. As has been experienced with other media, color in television also seems to introduce a certain perception of depth. This is partly due to the increased ability of color to reproduce the contrasts and shadows as well as high lights and reflections in different hues, while the degree of color saturation, which is a function of distance, especially outdoors, strongly enhances the three-dimensional quality.

Effects such as those mentioned here became apparent immediately after initial experimentation with color television and were encouraging enough to warrant an extensive investigation of that field with the objective of producing a practical color-television system.

At the outset it was realized that the transmission and reception of live objects as well as motion-picture film in natural color entailed the use of a trichromatic system.

History

Before proceeding further, a brief summary of color-television developments in the past will be presented. In view of the large number of proposals for color-television systems, only those are mentioned which, to the knowledge of the authors, have been demonstrated.

A complete color-television bibliography, which is almost identical to that compiled by Panel 1 of the National Television System Committee, is appended to this paper.

Color television was demonstrated for the first time in July, 1928, by John L. Baird in England. Both at the transmitter and at the receiver, a three-spiral scanning disk was employed. Each of these spirals consisted of a succession of holes which were covered with red, green, or blue filters, which scanned the picture completely in the three primary colors. At the transmitter photocells were employed, while at the receiver

* Decimal classification: R583. Original manuscript received by the Institute, September 2, 1941; revised manuscript received, November 17, 1941. Presented, in part, New York Meeting, October 3, 1940; Rochester Fall Meeting, November 12, 1940; Chicago Section, October 17, 1941; Emporium Section, October 30, 1941; Baltimore Section, November 28, 1941; New York Winter Convention, January 12, 1942; Montreal Section, March 11, 1942; and Toronto Section, March 23, 1942.

† Television Engineering Department, Columbia Broadcasting System, Inc., New York, N. Y.

two gas-discharge tubes controlled by a commutator were used. One of the tubes was filled with neon and acted on the red spiral, while the other tube, filled with a mixture of helium and mercury vapor, appeared through the blue and green spirals. The transmission employed a bandwidth of the order of 10 kilocycles and the pictures corresponded to a number of lines somewhere between 20 and 30 per frame.[1]

In July, 1929, the Bell Telephone Laboratories in New York demonstrated a three-color television system employing three independent channels. The live-pickup equipment consisted of three banks of cells with the three primary-color responses. A flying spot scanned the object and a scanning disk served on the receiving end to reconstitute the image. Three discharge tubes furnishing red, green, and blue light and superimposed by mirrors behind the scanning disk served as the light source.[2]

It is interesting to note that while the Bell Laboratories employed a three-channel system which obviously occupies three times the frequency spectrum over the corresponding black-and-white picture and requires three times the facilities, Baird, though similarly requiring three times the frequency space, employed rotating filters and was thus the first one to demonstrate the sequential, additive method of color in television.

Early in 1938, John L. Baird demonstrated in England a 9- ×12-foot 120-line color-television picture using sixfold interlacing, employing a flying spot, mirror drum, and rotating filters at the transmitter. At the receiving end also a mirror drum was employed, rotating at the rate of 6000 revolutions per minute and using a Kerr cell as modulator in conjunction with rotating color-filter slots.

In July, 1939, a demonstration with similar transmitting equipment was reported.[3] At the receiver there was a projection cathode-ray tube combined with a rotating color filter. The system was a two-color system using alternately orange and blue-green filters. The color-picture frequency was $16\frac{2}{3}$ per second employing 102 lines.

Finally, on August 28, 1940, a three-color, high-definition television system employing electronic scanning both at the transmitter and at the receiver was broadcast for the first time over Station W2XAB in New York City. The subject of transmission was motion-picture color film. Soon after live pickup employing the same trichromatic system was demonstrated.

This paper will deal largely with the color-television system demonstrated on those two occasions, as well as its subsequent development up to the summer of 1941. Beginning on June 1, 1941, daily color transmissions over Station WCBW of the Columbia Broadcasting System inaugurated a field-test period for the purpose of determining the practicability of color television as presented in this paper.

Columbia Broadcasting System Color Television

At the outset of research activities in color television a number of conditions were set down upon fulfillment of which depended the success of practical color television. These were:

1) For a given bandwidth the loss in monochromatic definition due to the introduction of color should not be excessive.
2) The system should be based on three primary colors.
3) Within any given bandwidth the performance of the color system decided upon should give at least as much satisfaction as the corresponding black-and-white system.

In the color-television system under discussion the following terms will be used:

color-field frequency—the highest vertical scanning frequency employed in the system

color-frame frequency—color-repetition time per second, i.e., trichromatic-repetition rate per second, corresponding to the color-field frequency divided by three

color-picture frequency—number per second of the coincidence of one and the same primary color with one and the same area of the image

frame frequency—identical to the term used in monochromatic television, i.e., completion of the scanning of the entire picture area per second in black and white.

Before the choice for a final system was narrowed down, several alternatives were considered. These all had in common sequential, additive-color scanning where the primary-color impulses of varying ratio, following in rapid succession, are integrated by the observer's eyes. The three primary colors employed were red, blue, and green, the characteristics of which will be discussed later. Rotating color disks or drums in front of the pickup device and the receiving tube, suitably synchronized and phased, produced the color analysis at the transmitter and the synthesis at the receiver.

The various systems combining different interlace ratios, color fields, color-frame and color-picture frequencies as well as lines, are tabulated in Table I.

System 1, as can be seen, is a straight adaptation of the black-and-white standards. Though the monochromatic definition was unimpaired, the resulting flicker due to the low color-frame frequency (20) was intolerable even at low illumination values. The effect, known as "color breakup," which is purely a

[1] A. Dinsdale, "Recent advances in television: television by daylight and television in colors," *Television*, vol. 1, pp. 9–10, 26; August, 1928.

[2] "Television in colors; Bell Telephone engineers transmit and reproduce scenes in their natural hues," *Tel. and Tel. Age.*, no. 14, pp. 315–318; July 16, 1929.

[3] F. W. Marchant, "New Baird colour-television system," *Telev. and Short Wave World*, vol. 12, pp. 541–542; September, 1939.

physiological one and increases with decreasing color-frame frequency, was objectionable. A white object which moved across the screen with sufficient velocity would show red, blue, and green color fringes. Only empirically could it be determined at which color-frame frequency the color breakup for the most commonly transmitted objects in motion became negligible.

TABLE I

System	1	2	3	4	5
Color fields—(c)	60	120	120	180	120
Color frames	20	40	40	60	40
Frames—(f)	30	120	60	45	30
Color pictures	10	40	20	15	10
Interlace ratio—(c/f)	2:1	1:1	2:1	4:1	4:1
Lines per frame, corresponding to 441 black-and-white, nearest practical value	441	240	315	350	441
Horizontal (line) frequency	13,230	28,800	18,900	15,750	13,230
Lines per frame, corresponding to 525 black-and-white, nearest practical value	525	260	375	450	525
Horizontal (line) frequency	15,750	31,200	22,500	20,250	15,750
Color breakup conditions	Unsatisfactory	Satisfactory	Satisfactory	Satisfactory	Satisfactory
Interline flicker conditions	Unsatisfactory	Satisfactory	Satisfactory	Doubtful	Unsatisfactory
Picture flicker conditions	Unsatisfactory	Satisfactory	Satisfactory	Satisfactory	Satisfactory

In System 1 the color-picture frequency is 10, which gives rise to interline flicker. It will be obvious when considering the subsequent systems that for a constant frame frequency the color-picture frequency also remains the same. This is an important factor when considering interlace ratios higher than 2.

System 2 employs sequential scanning in order to eliminate interline flicker. The frame frequency is 120 and thus the color-field frequency becomes 40 per second. Flicker and color-breakup conditions are satisfactory. However, the loss in definition is excessive.

It became evident that in order to increase definition, interlacing had to be introduced. This led to a system which has a color-field frequency of 120, a color-frame frequency of 60, and color-picture frequency of 20 per second. Due to a 2:1 interlace ratio the frame frequency remains at 50 per second and the number of lines at 343. This system gave freedom from flicker with screen brilliancies up to 2 apparent foot-candles

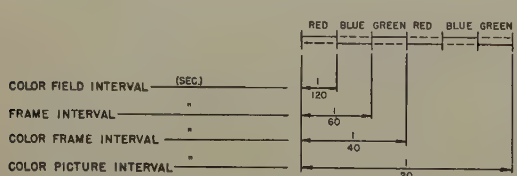

Fig. 1—Diagrammatic representation of CBS System 3.

and showed no interline flicker. It was subsequently chosen as the most satisfactory compromise for the present 6-megacycle band at the same time increasing the number of lines to 375 which corresponds to the 525 lines used in monochromatic television.

System 4 is a compromise between Systems 3 and 5 inasmuch as the color-picture frequency is 15 with a corresponding color-frame frequency of 60 and color-field frequency of 180 per second. The frame frequency of 45 per second will permit a number of lines approximating $525\sqrt{30/45}$. In this system flicker even at the highest brilliances is eliminated; however, the interline flicker still appears somewhat excessive.

System 5 uses the same horizontal-scanning frequency as monochromatic television; however, it utilizes quadruple interlacing to increase the field frequency to 120 per second. Thus flicker conditions are satisfactory and resolution is excellent. However, due to the low color-picture frequency (10 per second) interline flicker appears excessive.

In order to avoid the so-called "line-crawling" effect the quadruple interlacing in Systems 4 and 5 is of the staggered type where the sequence of lines is 1, 3, 2, 4 instead of 1, 2, 3, 4.

Conditions in these two systems are aggravated by the fact that the color-field frequency of 180, and respectively 120, per second, being a multiple of the power-supply frequency, would show a distinct breakdown of the line structure emphasizing a raster of approximately 100 lines in case 60-cycle components were not completely eliminated from the vertical scanning.

The final decision in favor of System 3, with System 4 as a close second, had to be made in view of the discouraging results, confirmed by other experimenters, in attempting to reach a satisfactory solution of the quadruple interlacing problem in general.

In Systems 1, 3, 4, and 5 the number of color fields over frames per second was an even number. If in a trichromatic system all areas of the image are to be scanned in all three primary colors, then the following conditions must be fulfilled:

$$\frac{c}{f} = 3n \pm 1 \quad \text{where } c = \text{color fields per second}$$

$$f = \text{frames per second, and}$$

$$n = \text{any whole number } 0, 1, 2, 3, \text{etc.}$$

For sequential scanning $n=0$ and thus $c/f=1$, for $n=1$, c/f becomes either 2 or 4, which corresponds to double and, respectively, quadruple interlacing. Fig. 1 is a diagrammatic representation of System 3.

Color

The color-television method under discussion is based on the eye's retentivity of light of all colors and its ability to recognize mixtures of several colors as a single one. Because of the fact that theoretically all colors are reproducible by a suitable set of three primaries, a trichromatic system was chosen as the basis for color television.

The experimental fact that the stimulant $E(\lambda)$ produces a sensation equivalent to a mixture of three primaries can be expressed as

$$E(\lambda) = w_1(\lambda)I_1 + w_2(\lambda)I_2 + w_3(\lambda)I_3 \quad (1)$$

where the w's are coefficients and the I's are the three primary colors.

Before proceeding to the discussion of the application of (1) and the choice of primaries in reproducing color in television, it is best to introduce some concepts used in standard colorimetry. It can be shown that although the w's can be determined experimentally, there is nothing unique about a given set of primaries and their respective coefficients. The present practice is to use coefficients determined by the International Commission on Illumination in 1931, for the standard observer.[4]

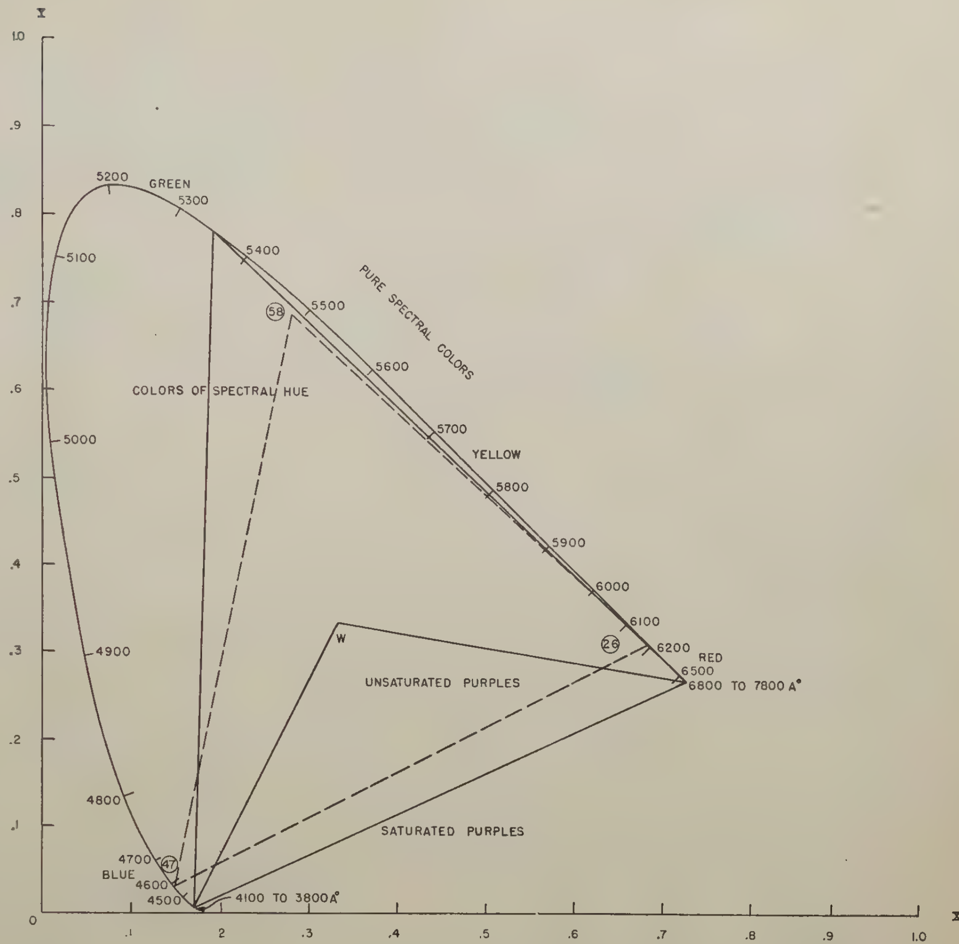

Fig. 2—Unified trichromatic coefficient diagram (color triangle).

These coefficients, known as the ICI tristimulus values of the spectrum colors, are usually designated by $\bar{x}(\lambda)$ dominant in the red region of the spectrum, $\bar{y}(\lambda)$ in the green, and $\bar{z}(\lambda)$ in the blue region. The tabulated values and the curves for these tristimulus values can be found in several places.[5,6] The primaries associated with $\bar{x}$, $\bar{y}$, and $\bar{z}$ are fictitious in the sense that they have no physical counterpart. However, they never assume negative values. Purposely $\bar{y}(\lambda)$ was chosen to coincide with the luminosity curve or the standard visibility function and thus represent the energy of the light source in terms of the eye or the brilliance of the color.

With the aid of the tristimulus values $\bar{x}$, $\bar{y}$, $\bar{z}$ a graphic representation of all colors can be constructed. This is known as the color triangle or the unified trichromatic coefficient diagram, and is shown in Fig. 2. The locus of pure spectral colors is shown with a solid curve. This curve is obtained by the so-called unified coefficients; i.e.,

$$x = \frac{\bar{x}}{\bar{x}+\bar{y}+\bar{z}} \qquad y = \frac{\bar{y}}{\bar{x}+\bar{y}+\bar{z}} \qquad z = \frac{\bar{z}}{\bar{x}+\bar{y}+\bar{z}}$$

as a result $x + y + z = 1$.

To determine the tristimulus values for a light source $E(\lambda)$, an integration must be performed; i.e.,

$$X' = \int_0^\infty E(\lambda)\bar{x}(\lambda)d\lambda, \qquad Y' = \int_0^\infty E(\lambda)\bar{y}(\lambda)d\lambda,$$

$$Z' = \int_0^\infty E(\lambda)\bar{z}(\lambda)d\lambda. \qquad (2)$$

For these values the unified trichromatic coefficients are

$$X = \frac{X'}{X'+Y'+Z'}, \qquad Y = \frac{Y'}{X'+Y'+Z'},$$

$$Z = \frac{Z'}{X'+Y'+Z'}.$$

The light source $E(\lambda)$ can now be represented by a point in the color triangle. The operation shown in (2)

[4] "Commission internationale de l'eclairage, *Comptes Rendus des Seances*, 1931, Cambridge University Press, New York, N. Y., 1932, p. 25.

[5] A. C. Hardy, "Handbook of Colorimetry," Technology Press, Massachusetts Institute of Technology, Cambridge, Massachusetts, 1936.

[6] C. D. Hodgman, "Handbook of Chemistry and Physics," Chemical Rubber Company, Cleveland, Ohio, 1937.

can be carried out on luminants of any spectral distribution, such as fluorescent materials, illumination sources with or without color filters, etc., after which their respective positions in the color triangle can be determined. The second equation in the group determines the luminosity of the color. In Fig. 2, point w represents white and grays; i e.,

$$X = Y = Z.$$

The gamut of colors which a given set of primaries will reproduce can be determined with the aid of the color diagram. (The primaries in this discussion are used only with positive coefficients.) Only those colors enclosed within the triangle, the corners of which are represented by the primaries, can be reproduced by the afore-mentioned primary colors. Two such triangles are drawn in Fig. 2. In order to reproduce the largest possible gamut, the three primary colors must be so chosen that the resulting triangle encloses most of the colors commonly used. Usually this entails a compromise, with a sacrifice of some of the blue-green region.

The limitations encountered in any two-color system are obvious when examining Fig. 2. Employing only two primaries, the colors that can be reproduced are only those found along the straight line joining the location of the two primaries in the color triangle.

Color Characteristics at the Receiver

In the television system under discussion the primaries at the receiver are determined by the color filters, red, green and blue, and the fluorescent material in the tube. The largest gamut of colors is produced with primaries which fall on the locus of monochromatic colors in the color triangle. One such choice is red 7000, green 5350, and blue 4000 angstrom units, shown in Fig. 2.

Unfortunately, monochromatic primaries can only be obtained at the sacrifice of light intensity. Thus one finds that in television, as in certain color-reproducing processes, a compromise must be found between light intensity and the best choice of primaries. In addition, there is a restricted choice in available phosphors. The decay time of the fluorescent powder used in the receiving tube must be such that its intensity becomes negligible after one color-field period.

Of the commercially available phosphors the zinc and calcium sulphides possess sufficient luminescent efficiency and also satisfy the decay requirements. The luminescent spectrum of the phosphor must cover the entire range of the three filters in order to provide a light source for each primary. The precise character of the spectrum desired is contingent upon the choice of filters. The most desirable characteristic would be to furnish maximum light in those blue, green, and red regions that fit the maximum transmission portions of the blue, green, and red filters. Commercial tubes usable for color television employ, for the most part, two component mixtures utilizing a zinc-sulphide with a spectral emission maximum in the blue and blue-green region, and a zinc-cadmium sulphide with a maximum in the yellow and yellow-red region.[7] The spectral curve of such a mixture is shown in Fig. 3.

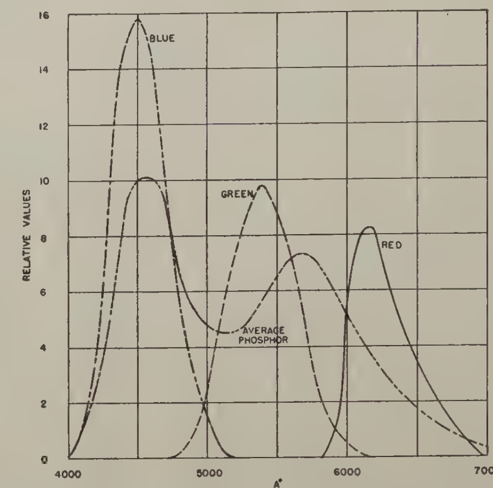

Fig. 3—Color characteristics at the receivers; filters Nos. 47, 58, and 26 combined with the phosphor. The fourth curve represents an average phosphor.

An inexpensive source of spectroscopically reproducible filters, with a wide selection of color, is the Wratten series, available in gelatin or acetate stock. The choice of the filters is determined by the wavelength at which the maximum transmission occurs, the width of the transmission band, and the total transmission. It is desirable to have filters and phosphor so chosen as to produce white corresponding to daylight fluorescent lamps with equal signals on the grid of the picture tube during the red, blue, and green periods. Thus, if a white surface of 6000 to 6500 degrees Kelvin is transmitted, it should be received as the same shade of white and also should be identical to the receiver's own color when operated without a signal.

The filters finally chosen for use at the receiver were Wratten No. 26 for red, No. 47 for blue, and No. 58 for green. The emission curves for the phosphor mixture used for the experimental tubes combined with filters Nos. 47, 58, and 26 are given in Fig. 3. The resultant blue, green, and red primaries yield a new color triangle represented with broken lines in Fig. 2; the location of the new primaries is marked with the corresponding filter numbers.

A satisfactory method of specifying the color composition of the phosphor, which is a mixture of blue, yellow, and orange zinc and zinc-cadmium sulphides, without resorting to actual spectral curve data, was to specify the transmission through filters Nos. 47, 58, and 26 as recorded with a Weston photocell No. 2.

[7] H. W. Leverenz and F. Seitz, "Luminescent materials," *Jour. Appl. Phys.*, vol. 10, pp. 479–493; July, 1939.

The relative values which proved satisfactory were No. 47-1.0, No. 58-1.25, and No. 26-0.75. Of the commercially available tubes, the General Electric and Baird have been found quite useful. RCA Radiotron and National Union have supplied special tubes that have proved satisfactory. In the Columbia Broadcasting System laboratories, tubes have been built using a phosphor mixture containing 60 per cent of a blue zinc-sulphide, 35 per cent of a yellow-green zinc-cadmium sulphide, and 5 per cent of a reddish zinc-cadmium sulphide. The final color characteristic of the tube, however, depends to a large extent on the various processing schedules.

The range of colors obtainable with this choice of phosphors and filters (shown in Fig. 2 with a dotted triangle) is as large as is encountered in color photography. The white produced with three equal signals appears somewhat bluish. Very recently, however, satisfactory "white" tubes were made in the laboratories, which show consistently good color characteristics and permit transmitter operation with equal blanking pulses. Spectral curves for these tubes are in preparation and will be available shortly for standardization purposes.

Transmitter Color Characteristics

While the performance of the receiver was based on the color theory of vision, the study of the color characteristics at the transmitting end of the system had to be guided by the desirability of producing all colors encountered in nature. At the receiver three properly chosen narrow bands in the spectrum were sufficient; at the transmitter, the bands must be wide enough and sufficiently overlapping to produce a signal from every color. The exact character of the three spectral curves at the transmitter is determined by the filter and phosphor combination at the receiver.

The spectral characteristics at the transmitter are composed of the spectral sensitivity of the pickup tube in the camera, the transmission curves of the filters and the spectral emission of the light source. The filters and light source must be so chosen as to produce negligible signals in the infrared (beyond 7000 angstrom units) and the near-ultraviolet (below 4000 angstrom units) regions of the spectrum.

The general relationship between the color characteristics of the transmitter and the receiver can be derived from an analysis developed by Hardy and Wurzburg in connection with photographic reproduction in color.[8]

The tristimulus values for any object at the transmitter, the spectral reflection of which is represented by $E(\lambda)$, was given by (2). At the receiver the tristimulus values are represented by

$$\left.\begin{aligned} X'' &= r\int_0^\infty P(\lambda)F_r(\lambda)\bar{x}(\lambda)d\lambda + g\int_0^\infty P(\lambda)F_g(\lambda)\bar{x}(\lambda)d\lambda \\ &\quad + b\int_0^\infty P(\lambda)F_b(\lambda)\bar{x}(\lambda)d\lambda \\ Y'' &= r\int_0^\infty P(\lambda)F_r(\lambda)\bar{y}(\lambda)d\lambda + g\int_0^\infty P(\lambda)F_g(\lambda)\bar{y}(\lambda)d\lambda \\ &\quad + b\int_0^\infty P(\lambda)F_b(\lambda)\bar{y}(\lambda)d\lambda \\ Z'' &= r\int_0^\infty P(\lambda)F_r(\lambda)\bar{z}(\lambda)d\lambda + g\int_0^\infty P(\lambda)F_g(\lambda)\bar{z}(\lambda)d\lambda \\ &\quad + b\int_0^\infty P(\lambda)F_b(\lambda)\bar{z}(\lambda)d\lambda \end{aligned}\right\}. \quad (3)$$

The coefficients r, g, and b are proportional to the light intensities at the picture tube associated with signals generated at the camera through the red, green, and blue filters. $P(\lambda)$ is the spectral emission of the phosphor. $F_r(\lambda)$, $F_g(\lambda)$, and $F_b(\lambda)$ are the spectral transmissions of the red, green, and blue filters at the receiver, and $\bar{x}(\lambda)$, $\bar{y}(\lambda)$, and $\bar{z}(\lambda)$ are the ICI tristimulus values.

r, g, and b are some functions of the light incident at the photosensitive member of the camera tube; i.e.,

$$r = f(S_r) \qquad g = f(S_g) \qquad b = f(S_b). \quad (4)$$

Simplified for further discussion, (3) can be written as

$$\begin{aligned} X'' &= ra_{11} + ga_{12} + ba_{13} \\ Y'' &= ra_{21} + ga_{22} + ba_{23} \\ Z'' &= ra_{31} + ga_{32} + ba_{33}. \end{aligned} \quad (5)$$

For the system to reproduce color faithfully it is necessary for (2) and (3) to be related linearly; i.e.,

$$X' = kX''; \quad Y' = kY''; \quad Z' = kZ''; \quad (6)$$

where k is a constant.

The S_r, S_g, S_b of (4) is that portion of the light at the transmitter which is useful in producing the electrical signal. It can be resolved into three components: $A(\lambda)$, the spectral sensitivity of the photosensitive member of the camera tube, the spectral attenuation of the red, green, and blue filters at the camera tube, $T_r(\lambda)$, $T_g(\lambda)$, and $T_b(\lambda)$, and the spectral distribution of the object $E(\lambda)$ being televised. $E(\lambda)$ will depend on the light source used to illuminate the object. The S's can thus be written as

$$\left.\begin{aligned} S_r &= \int_0^\infty E(\lambda)T_r(\lambda)A(\lambda)d\lambda \\ S_g &= \int_0^\infty E(\lambda)T_g(\lambda)A(\lambda)d\lambda \\ S_b &= \int_0^\infty E(\lambda)T_b(\lambda)A(\lambda)d\lambda \end{aligned}\right\}. \quad (7)$$

[8] A. C. Hardy and F. C. Wurzburg, Jr., "The theory of three-color reproduction." *Jour. Opt. Soc. Amer.*, vol. 27, pp. 227–240; July, 1937.

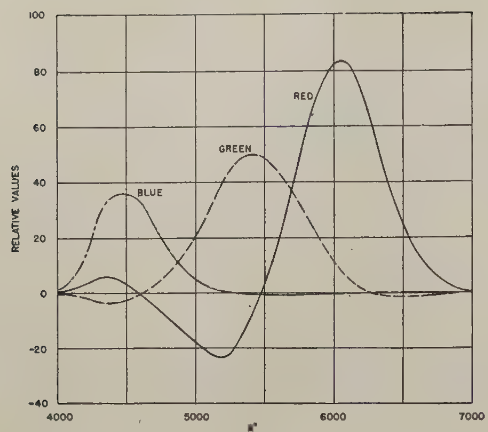

Fig. 4—Color characteristics at the transmitter; these curves are solutions of equation (9) on the basis of receiver characteristics represented in Fig. 3.

The actual functional relation between r and S_r, etc., depends on the relationship between the light input and the signal output at the camera, on the relationship between the voltage on the grid of the receiving picture and the light output from the phosphor; it further depends on the electrical characteristics of the terminal equipment, the transmitter proper, and the receiver.

Equations (2) and (3) permit the determination of $T_r(\lambda)A(\lambda)$, $T_g(\lambda)A(\lambda)$, and $T_b(\lambda)A(\lambda)$ for a given light source, once $P(\lambda)F_r(\lambda)$, $P(\lambda)F_g(\lambda)$, and $P(\lambda)F_r(\lambda)$ have been chosen and provided it is assumed that $r=S_r$, $g=S_g$, and $b=S_b$. This in effect signifies that the gamma of the over-all system is unity. If (5) is substituted in (2) and the new equation is in turn substituted with (7) into (3), and the integral sign and $E(\lambda)$ are cancelled heuristically from both sides, the resulting relationship is

$$\begin{aligned} \bar{x}(\lambda) &= T_r(\lambda)A(\lambda)a_{11} + T_g(\lambda)A(\lambda)a_{12} + T_b(\lambda)A(\lambda)a_{13} \\ \bar{y}(\lambda) &= T_r(\lambda)A(\lambda)a_{21} + T_g(\lambda)A(\lambda)a_{22} + T_b(\lambda)A(\lambda)a_{23} \qquad (8) \\ \bar{z}(\lambda) &= T_r(\lambda)A(\lambda)a_{31} + T_g(\lambda)A(\lambda)a_{32} + T_b(\lambda)A(\lambda)a_{33}. \end{aligned}$$

The color response at the transmitter is contained in the quantities $T_r(\lambda)A(\lambda)$, $T_g(\lambda)A(\lambda)$, and $T_b(\lambda)A(\lambda)$. In (8), the coefficients a_{mn} are known constants that are evaluated in terms of color response at the receiver and the ICI tristimulus values. Equation (8) can thus be written as

$$\left.\begin{aligned} cT_r(\lambda)A(\lambda) &= (a_{22}a_{33} - a_{23}a_{32})\bar{x}(\lambda) \\ &\quad + (a_{13}a_{32} - a_{12}a_{33})\bar{y}(\lambda) \\ &\quad + (a_{12}a_{23} - a_{22}a_{13})\bar{z}(\lambda) \\ cT_g(\lambda)A(\lambda) &= (a_{23}a_{31} - a_{21}a_{33})\bar{x}(\lambda) \\ &\quad + (a_{11}a_{33} - a_{13}a_{31})\bar{y}(\lambda) \\ &\quad + (a_{13}a_{21} - a_{11}a_{23})\bar{z}(\lambda) \\ cT_b(\lambda)A(\lambda) &= (a_{21}a_{32} - a_{22}a_{31})\bar{x}(\lambda) \\ &\quad + (a_{12}a_{31} - a_{11}a_{32})\bar{y}(\lambda) \\ &\quad + (a_{11}a_{22} - a_{12}a_{21})\bar{z}(\lambda) \end{aligned}\right\} \qquad (9)$$

where c is a constant. The solution of (9) in terms of receiver color response as represented in Fig. 3 is shown in Fig. 4. The curves in these figures display the usual characteristics found in all color-reproduction problems, the existence of negative color values for perfect matching. The present color-television system has no mechanism to introduce these negative values; however, they are being partially compensated for with the aid of the color mixer.

The above analysis is valid for the color transmission of live scenes as well as for color slides or motion pictures, provided the latter two contain no color distortion. Once the photographic or printing processes have introduced certain distortions, the filters at the transmitter must be so chosen as to compensate, if possible, for these specific anomalies.

Camera Tubes

Before comparing the results contained in Fig. 4 with actual operating conditions, it is best to consider briefly the color characteristics of the tube used at the transmitting end. They are of two types: the dissector, used for slides and motion pictures, and the orthicon, used in the studio and in outdoor pickups. One of the problems in dissector operation is the elimination of signals produced with infrared radiation. The infrared contaminates all colors as it passes freely through the red, blue, and green filters. Originally the standard dissector was used with a cesiated silver-oxide cathode surface. This surface has a minimum color response in the green portion of the spectrum while it shows rising tendencies both towards the blue and the infrared regions. In order to utilize this tube a carbon arc was used as a light source, combined with the infrared-absorbing Corning glass filter No. 978, 2 millimeters thick. The filters that were used in this setup were Wratten Nos. 47, 58, and 25. Fig. 5 is a graphic representation of the results. The dissector used at present is the so-called daylight dissector (developed especially for color television by the Farnsworth Television and Radio Corporation) with a maximum in the green portion of the spectrum falling off towards the blue and the red end. This dissector was also used with a carbon

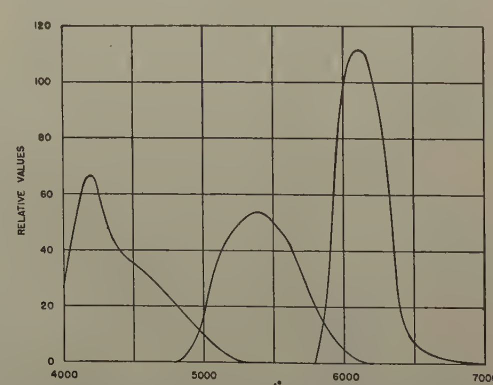

Fig. 5—Color characteristics at the transmitter; the curves combine the standard dissector, the carbon arc, 2 millimeters of Corning glass No. 978, and Wratten filters Nos. 25, 47, and 58.

arc but with a Corning filter No. 978 only 1 millimeter thick. The color filters were again Nos. 47, 58, and 25. In both cases a water cell was used to secure protection for the slides and film. Fig. 6 gives the operating conditions for the daylight dissector. There is no question of the superiority of this type of tube over the standard dissector for this work. The signal-to-noise ratio is improved partly because of the greater photoelectric response in the pertinent portion of the spectrum and also because of the reduction in thickness of the infrared filter.

The spectral characteristics of the orthicon have not

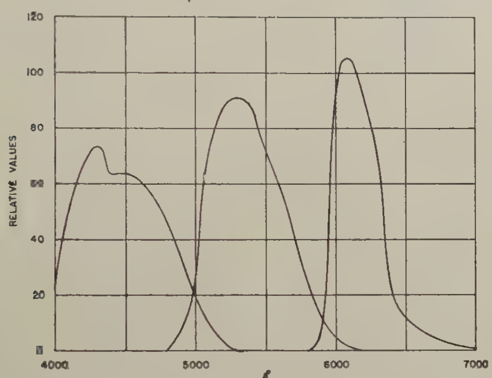

Fig. 6—Color characteristics at the transmitter; the curves combine the light dissector with the carbon arc, 1 millimeter of Corning glass No. 978, and Wratten filters Nos. 25, 47, 58.

been measured under operating conditions. However, from measurements of the signal obtained through various Wratten filters it can be stated very generally that the spectral response of the color orthicon does not conform to the standard cesiated silver-oxide surface. It was found that specifications of the color characteristics of the orthicons used can be summed up in terms of the signal obtained through Wratten filters Nos. 47, 57, and 25. The ratio of the signals through No. 47 to No. 57 using daylight fluorescent light source is approximately 1.25 and the ratio of No. 47 to No. 25 is 0.85. To obtain a general view of the color characteristics at the transmitter a daylight fluorescent-light source attenuated through filters Nos. 47, 57 and

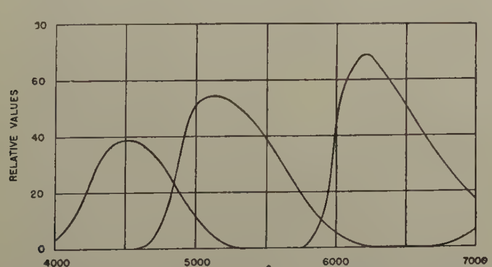

Fig. 7—Color characteristics at the transmitter; Wratten filters No. 25, 47, and 57 combined with daylight fluorescent light source as used with orthicons.

25 has been plotted in Fig. 7. The inclusion of the characteristics of the orthicon in this figure will reduce the red curve roughly by 30 per cent. It may shift the maxima slightly but it will not change the limits of the individual curves. Thus the extent of filter overlapping remains the same.

Lighting

The color characteristics at the transmitting end of the system depend to a large extent on the illumination

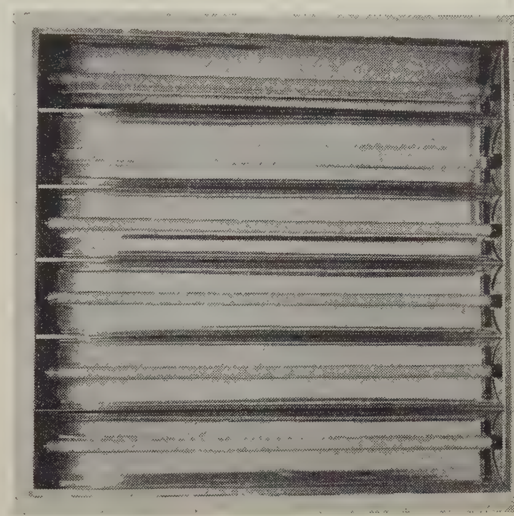

Fig. 8—A fluorescent-light unit, used in color work.

source. For slides and motion pictures, the carbon arc is used and the filters are chosen to match the carbon arc. For direct pickup it is desirable to have a light source such as not to necessitate the change of filters

Fig. 9—A view of a bank of fluorescent lights.

when the camera is moved outdoors. A good approximation to such a light source can be obtained with incandescent lamps where the infrared is attenuated with properly chosen glass filters, such as Aklo glass. However, this type of source is very inefficient. Fluorescent lamps of the daylight type are a fair approximation to the requirements. The lamps contain 30-watt bulbs mounted in specially designed reflectors,

developed for color television to give the maximum light flux for a minimum ceiling area. A single unit is shown in Fig. 8 and a bank in Fig. 9.

Fig. 10 gives the spectral emission curve for the daylight fluorescent lamps. The spectral distribution of light as received from the sun on a horizontal plane under various cloud conditions and at different times of day also is shown.[9]

It can be seen that the daylight fluorescent lamps are down in the red and slightly down in the blue portions of the spectrum as compared to outdoor illumination. It was found that when switching from studio pickup to outdoor scenes it is necessary to reduce the red signal by means of the electrical color mixer.

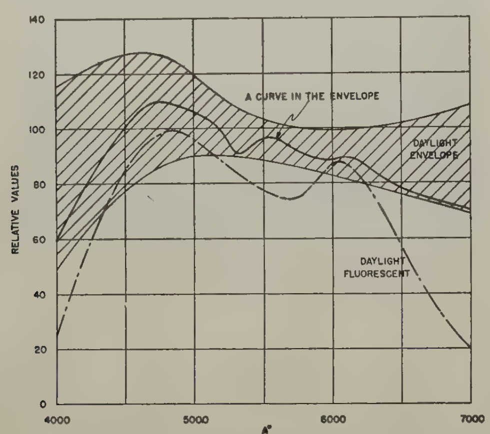

Fig. 10—Comparison of daylight fluorescent-light source with actual daylight.

Comparison of Figures

The calculations culminating in Fig. 4 have been purposely kept in general terms using a light source of uniform energy distribution over the visible spectrum. Figs. 5 through 7 take into consideration the actual light source in order to show the signal magnitude through the filters and the attenuation of the infrared component.

It follows that the comparison of Fig. 4 with Figs. 5 to 7 must be very general. The spectral characteristics of operational equipment lack the negative value. The maxima are roughly in the same region, and the limits (principally determined by the Wratten filters), of the blue and green curves correspond quite closely. A certain discrepancy exists in the reds, where in Fig. 4 the cutoff is at 5500 angstrom units and in Fig. 7 at 5800 angstrom units. When examining Fig. 5 carefully, one can see that monochromatic sources between 4000 and 4800 angstrom units will appear as the same blue, between 5400 and 5800 angstrom units will appear as the same green, and between 6300 and 6700 angstrom units will appear as the same red at the receiver. However, these imperfections are not too serious, since only rarely do objects reflect colors of such narrow bands.

As has been pointed out previously, the present television system does not permit introducing the negative values (which are common to all color-reproducing systems) as shown in Fig. 4. Nevertheless, the color mixer permits partial compensation by changing the ratio between signals r, g, and b. The system itself is unaware of whether the change takes place in the spectral characteristics of the light source at the transmitting end or in light emission of the receiver. Changing the relative amounts of the red, blue, and green signals electrically in effect changes the solution of (9). Thus the manipulation of the color mixer changes the ratio of positive to negative signal. Color deterioration resulting from the lack of negative signal is thus partially reduced.

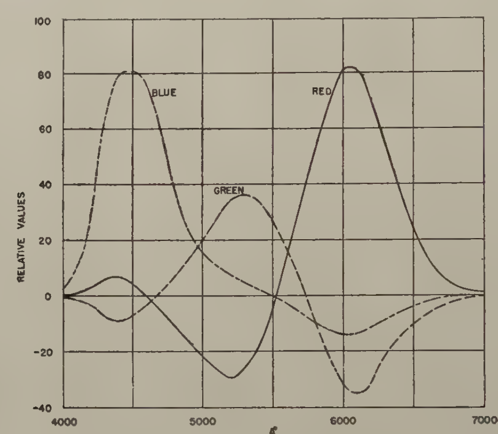

Fig. 11—Solution of equation (9), including a decay of 1/5 from one color field to the next in the orthicon.

In this analysis, the persistence of a signal from one color field to the following ones, as experienced in the orthicon under certain conditions, has been neglected. Curves similar to those in Fig. 4 have been calculated, taking into account hangover of 1:5 and 1:10 of the original signal into the next field for a color sequence red-blue-green, and are shown in Figs. 11 and 12. The same receiver color characteristics as in Fig. 4 were assumed. The most outstanding feature of these curves is the increased amplitude and width of the negative portions. A hangover of 1:5 (Fig. 11) would require much broader filters at the transmitter and the color contamination would be appreciable. A hangover of 1:10 (Fig. 12) shows less deviation, as compared with conditions in Fig. 4, where no hangover was assumed. The blue filter is wider than in Fig. 4 and has a negative component in the red region. On the whole, however, Fig. 12 matches Fig. 4 reasonably well.

The color mixer has been used to compensate for different lighting conditions, to correct for color contamination resulting from lack of negative signal, and thus also indirectly for hangover. There is no assurance that all these corrections require the same

[9] A. H. Taylor and G. P. Kerr, "The distribution of energy in the visible spectrum of daylight," *Jour. Opt. Soc. Amer.*, vol. 31, pp. 3–8; January, 1941.

adjustment. The mixer permits a partial removal of color contamination from a number of sources and in actual operations a compromise is made for the best over-all effect.

This analysis has been based on a linear relationship between light output at the receiver; i.e., a system with unity gamma, which conditions may not be obtained with present equipment.

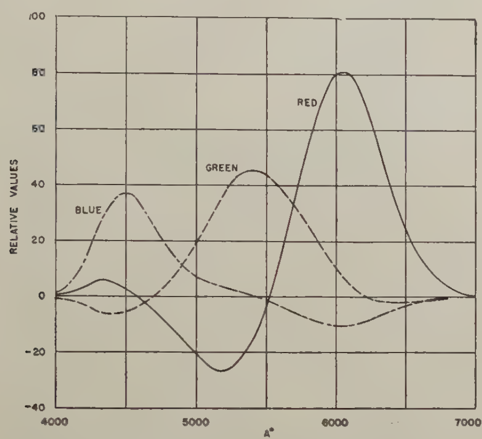

Fig. 12—Solution of equation (9), including a decay of 1/10 from one color field to the next in the orthicon.

Flicker in Color Television

The well-known Ferry-Porter[10,11] law states that the critical frequency is proportional to the logarithm of the illumination intensity. Porter was the first to establish the fact that the critical fusion frequency is independent of wavelength, provided the apparent brilliance remains constant. Based on this law he derived the well-known color-intensity curve of the eye using a flicker photometer. It follows that with constant irradiation over the visual spectrum the eye's sensitivity to flicker follows the color-intensity curve.

In the sequential color-television system under consideration the worst flicker condition would occur if only the primary color with the highest luminosity were received while the other two primary colors were suppressed completely. Such a condition hardly ever occurs in practice unless the color camera picks up a green object, the limits of its chromaticity being between 5400 and 5800 angstrom units (see Fig. 5). The flicker frequency for this case would be 40 per second. An attempt will be made to calculate the maximum permissible brilliance of such a green picture before flicker becomes perceptible.

The validity of Talbot's law has been checked for all colors by Porter[11] and others. Thus, applying Talbot's law to the special case of color television as discussed here, the apparent brilliance of the image at the receiver would be

$$I_A = \frac{1}{T_c}\int_0^T L(t)dt \tag{10}$$

where T_c is the duration of a complete color cycle (color frame) and T the duration of a color field. $L(t)$ is the decay function of the screen material. This is assumed to be exponential, with a luminosity not greater than 1/10th of the initial brilliance after the duration of one field period (T).

Thus for the transmission of green between 5400 and 5800 angstrom units the apparent brilliance of the received picture becomes

$$I_g = \frac{1}{T_c}\int_0^T Y_g L(t)dt \tag{11}$$

where the luminosity at the receiver has been expressed in terms of the Y component of the tristimulus coefficients, representing the combination of the receiver's green filter and the screen material, as shown in Fig. 2, and the decay with time of the screen material.

For a picture tube made in the laboratories especially for color reception the following ratios of the luminosity values of the three color primaries were found:

$$\frac{Y_{\text{green}}}{Y_{\text{blue}}} = 23 \quad \text{and} \quad \frac{Y_{\text{red}}}{Y_{\text{blue}}} = 10.3. \tag{12}$$

Equation (11) can be rewritten

$$I_g = \frac{Y_g}{T_c}\int_0^T L(t)dt$$

Using equation (12) we obtain

$$I_g = \frac{23 Y_b}{T_c}\int_0^T L(t)dt \tag{13}$$

In order to determine at what apparent brilliance a 40-cycle television picture will just begin to show flicker we consult the curve shown in Fig. 11, which is from the article by Engstrom.[12] The curves were

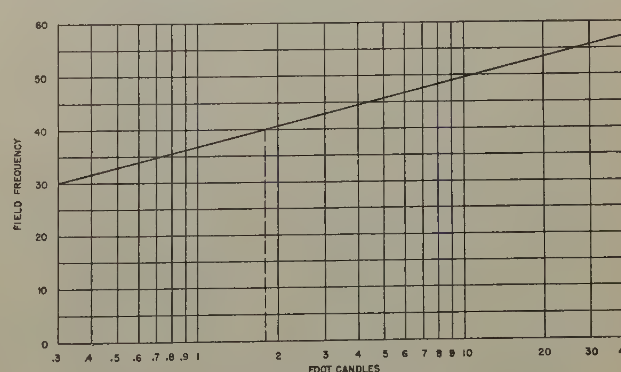

Fig. 13—Relationship between critical flicker frequency and picture brilliance.

[10] E. S. Ferry, *Amer. Jour. Sci.*, vol. 44, p. 192, 1892.
[11] T. C. Porter, "Study of 'flicker'," *Proc. Roy. Soc.* (London), vol. 70, pp. 313–329; July 29, 1902.

[12] E. W. Engstrom, "A study of television image characteristics," Proc. I.R.E., vol. 23, pp. 295–310; April, 1935.

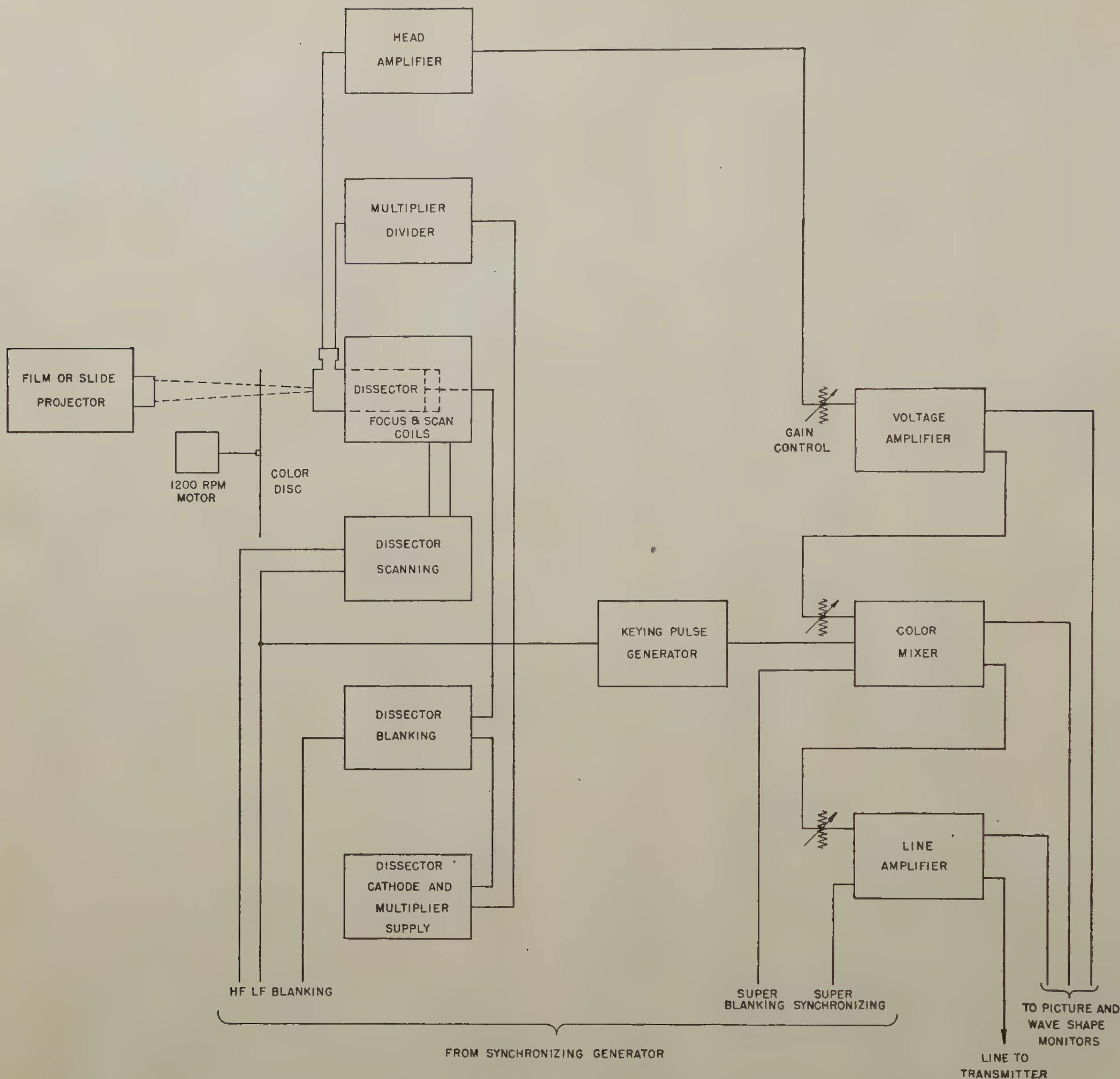

Fig. 14—Dissector block diagram.

obtained by using a special film which corresponded to certain decay characteristics of screen materials. It was decided to choose film No. 1, the decay characteristic of which is sufficiently fast to correspond to a screen material usable in color television, where at the end of one frame the screen brilliance decays practically to zero. Thus, according to Fig. 13, a repetition frequency of 40 per second will permit a screen illumination of 1.8 apparent foot-candles.

So far we have considered the most unfavorable case from a flicker point of view. More favorable conditions will occur if white with three equal electrical impulses during the red, green, and blue periods is transmitted and received.

In order to obtain the total apparent illumination at the receiver, (11) will be expanded into

$$I_w = \frac{I}{T_c}\int_0^T Y_g L(t)dt + \int_0^T Y_r L(t)dt + \int_0^T Y_b L(t)dt \quad (14)$$

assuming that $L(t)$ is independent of color, equation (14) can be written as

$$I_w = \frac{(Y_g + Y_r + Y_b)}{T_c}\int_0^T L(t)dt \quad (15)$$

using the substitutions in (12) we obtain

$$I_w = \frac{34.3 Y_b}{T_c}\int_0^T L(t)dt. \quad (16)$$

Comparing this with (13) it is found that

$$\frac{I_w}{I_g} = \frac{34.3}{23}. \quad (17)$$

The meaning of this expression is that the apparent brilliance of the receiver screen increases only in the ratio of 34.3/23 when white is transmitted, even though it is produced by three equal electrical impulses, one during each color field. Since in this case a light impulse is received during each of the color fields, flicker conditions improve rapidly. However, the apparent

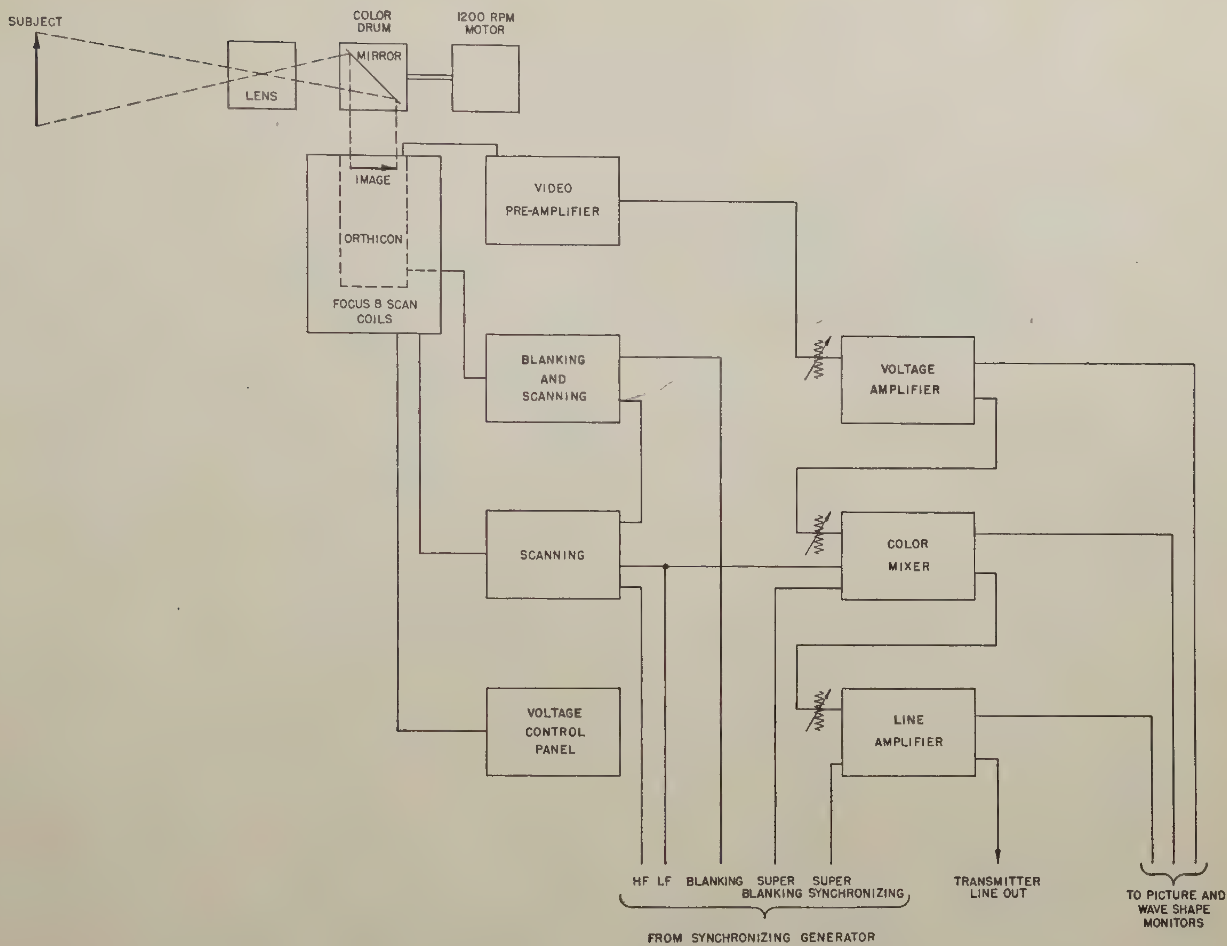

Fig. 15—Orthicon block diagram.

Fig. 16—Orthicon camera on tripod; direct-pickup color camera.

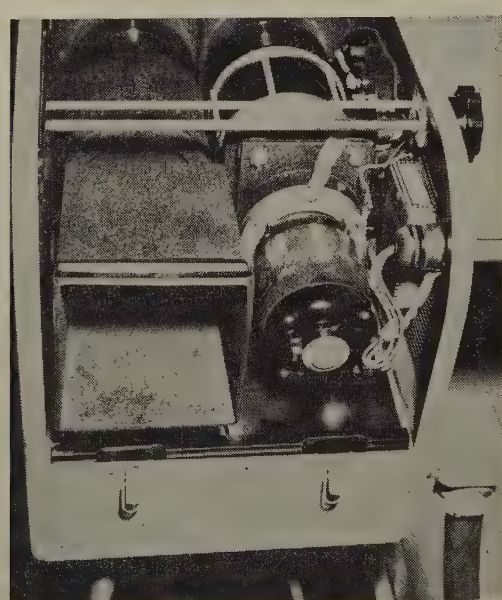

Fig. 17—Orthicon color camera; inside view, showing filter drum with synchronous driving motor.

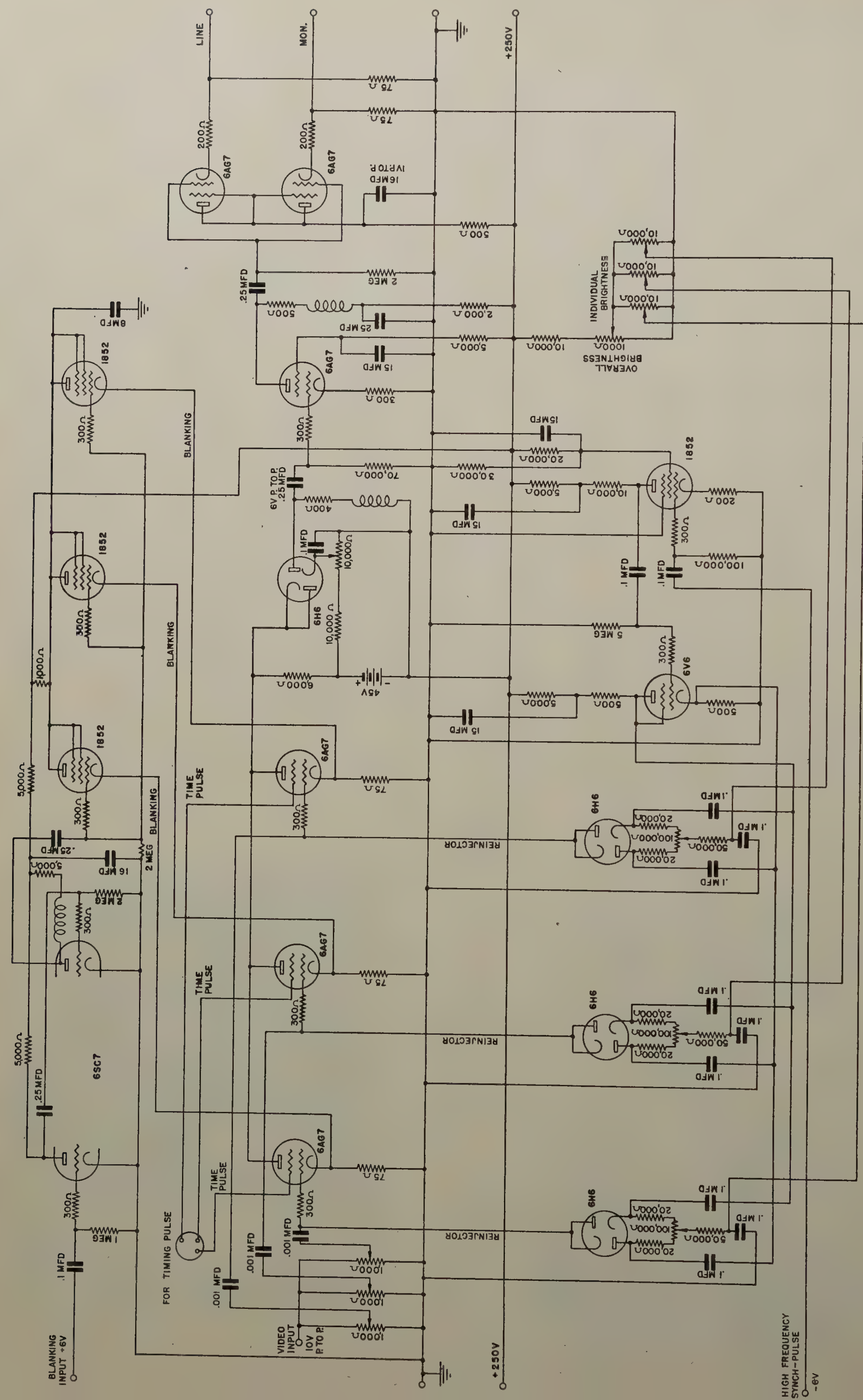

Fig. 18—Color-mixer amplifier.

brilliance should not be higher than 1.8 times 34.3/23, which is 2.7 apparent foot-candles if one wishes to make sure that in the singular case of the transmission of a narrow band of green no flicker is present. This top value of 2.7 foot-candles is not a serious limitation. Present black-and-white pictures with such a high-light brilliance give satisfactory viewing in darkness. The same black-and-white receiver, however, will not permit satisfactory viewing with surrounding illumination of any appreciable magnitude.

Color-television pictures produced with the aid of rotating filters do not deteriorate appreciably in the surrounding illumination due to the fact that the room light which passes through the filters twice is attenuated by the square of the filter loss factor, while the picture itself is only attenuated by the first power of the filter factor.[13] As a result the unmodulated screen of a color receiver appears nearly black even in a well-illuminated room. Thus the 2.7-foot-candle maximum brilliance will furnish a more satisfactory image than a conventional black-and-white receiver even with 10-foot-candle high-light illumination.

Equipment for Color Television

Studio

Certain electrical requirements must be met by pickup tubes if they are to be used in color television. It is important that the signals produced during any one color field should not be adulterated by a signal left over from a previous field. Storage-type camera tubes must, therefore, be designed so that the entire electrical charge on the mosaic is removed within one field period.

A constant black level must be established in the camera tube, and spurious signals such as "shading" should be absent. The dissector is the only commercial camera tube that meets all of the above requirements though its usefulness is limited to the transmission of film or slides due to its low sensitivity.

The orthicon as modified for color television with lower mosaic capacitance was developed through the co-operation of the RCA Radiotron Division and has been found to produce very acceptable color pictures with incident light of 150 foot-candles on the subject. A certain amount of "hangover," which may be defined as the amount of signal remaining on the mosaic after the scanning beam has completed one field, appears to be unavoidable, but is only troublesome at lower light levels. The hangover occurs when the potentials on the mosaic are small enough to be within range of the random velocity distribution of the scanning beam. Under this condition the charge is not completely removed until the mosaic has been scanned several times. A lower mosaic capacitance permits the voltage on the mosaic (for a given illumination) to build up to higher levels.

[13] A black-and-white receiver with an equivalent neutral filter will resist room illumination to the same extent.

It might be expected that difficulty would be experienced with interlaced scanning on a storage-type camera tube such as the orthicon. In an ideal storage tube, where the scanning spot is only one line wide, it will be apparent that at the end of one field-scanning period only one-half the lines will be scanned and the hangover will be 100 per cent. Actually, in practice, hangover ratios of from 1:5 to 1:10 are obtained with the orthicon, indicating that either leakage, defocusing, or other effects are present to such an extent as to remove most of the unscanned picture at the end of one field scansion.

The gamma of a camera tube need not necessarily be unity, as correction may be made for any particular characteristic later on, if desired. In general, a tele-

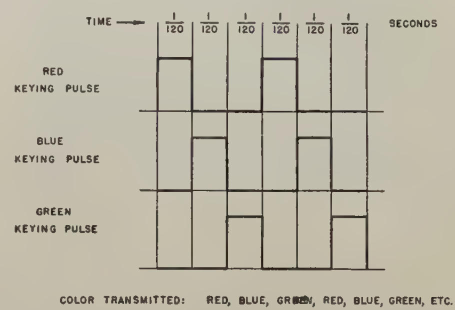

Fig. 19—Color-mixer pulse diagram.

vision system employing a linear pickup tube such as an orthicon, will have an over-all gamma higher than unity, due to the cathode-ray tube. A reduction in the gamma may be more satisfactorily made with tubes of the dissector type, where the noise is negligible in the black portions of the picture, than in a tube of the orthicon type, where the noise is determined by the impedance of the tube and the first amplifier stage. A reduction of gamma in the latter case results in increased noise in the blacks, if all other factors remain equal.

The introduction of color does not change many of the design requirements which are ordinarily encountered in monochromatic television studio equipment. Certain factors, however, are worthy of mention. The color-field frequency of 120 per second necessitates freedom from 60-cycle hum in the synchronizing generator and scanning equipment and, to a lesser degree, in video amplifiers. Sixty-cycle components present in the synchronizing generator or scanning equipment cause loss of interlace and in the video equipment cause flicker at a 20-cycle rate resulting from the beat between the 60-cycle hum and the 40-cycle picture components. Hum may be eliminated easily by operating the equipment from a 120-cycle power source.

Good low-frequency response is necessary in video amplifiers to pass the 40-cycle picture components properly. The video control equipment for color is somewhat more complex than for black-and-white transmission, as it seems advantageous to control the

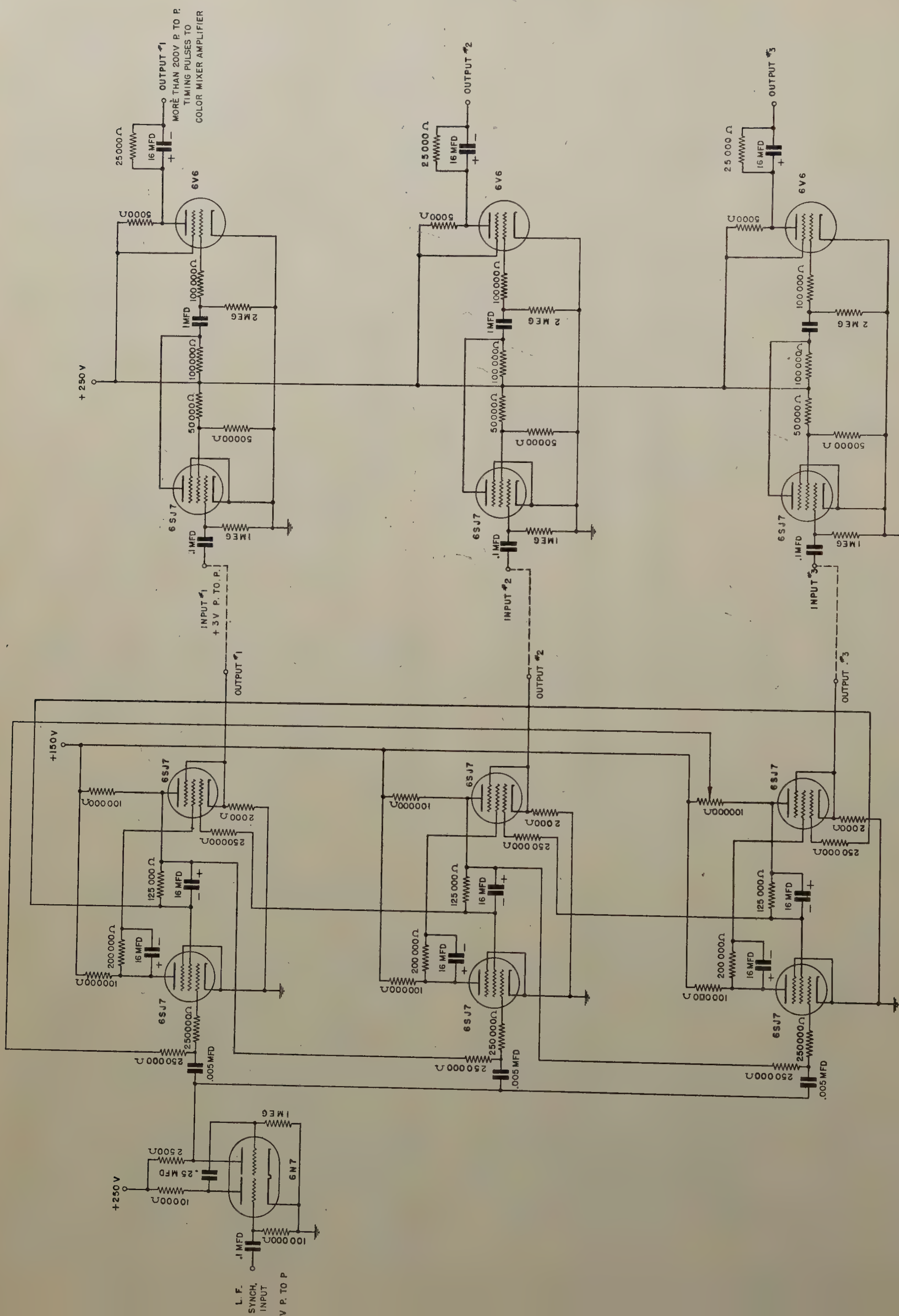

Fig. 20—Color-mixer pulse generator.

gain and possibly the background of each color independently, as previously mentioned.

Block diagrams of a color-television system using dissector and orthicon camera tubes are shown in Figs. 14 and 15. Photographs of the orthicon direct-pickup color camera are shown in Figs. 16 and 17.

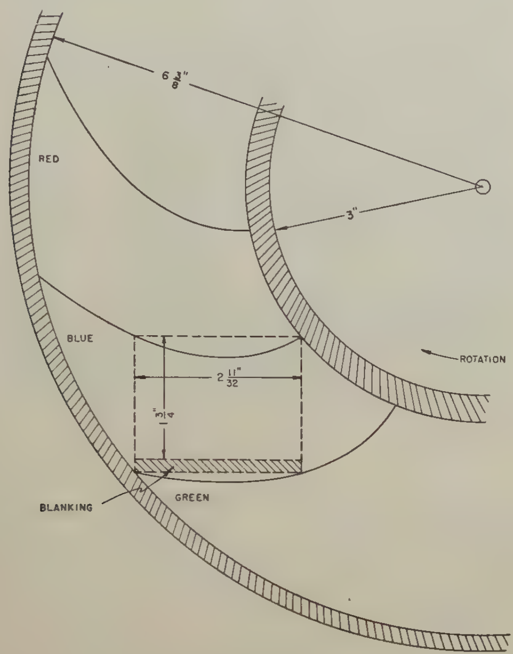

Fig. 21—Filter disk for orthicon.

As previously mentioned, it is essential that the black level be established at the camera since manual control of the direct-current level for each color would seem a tremendous task. This is done by applying the blanking pulses to the grid of the orthicon and to the cathode of the dissector.

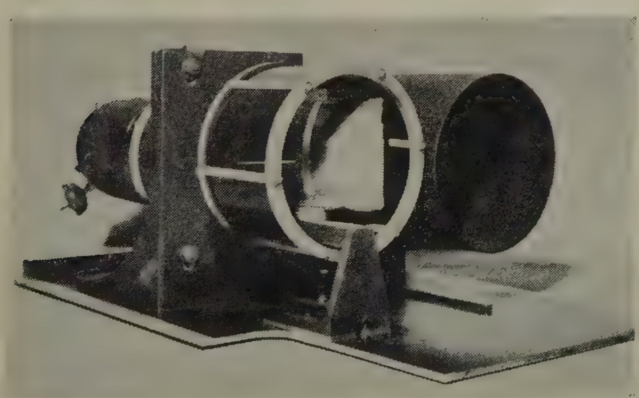

Fig. 22—Orthicon color camera; filter drum assembly.

The video amplifiers in a color-television camera channel are conventional except for the color mixer. Manual control of gain and brightness for each color are achieved by the equipment shown in Fig. 18. The color-mixer amplifier may be described as an electronic switch combined with three separate amplifiers, each with its own gain and brightness controls. The video signal is switched by means of suitable timing pulses (Fig. 19) applied to the screen grids of the 6AG7 switch-

Fig. 23—Nine-inch color-television receiver; front view.

ing amplifier tubes. The pulses are so timed as to operate each amplifier in succession, turning on one as another is turned off. This switching occurs during the blanking period, and switching transients are removed by subsequent clipping of the recombined signals. Blanking is injected on the cathode of each switching amplifier tube and the individual brightness of

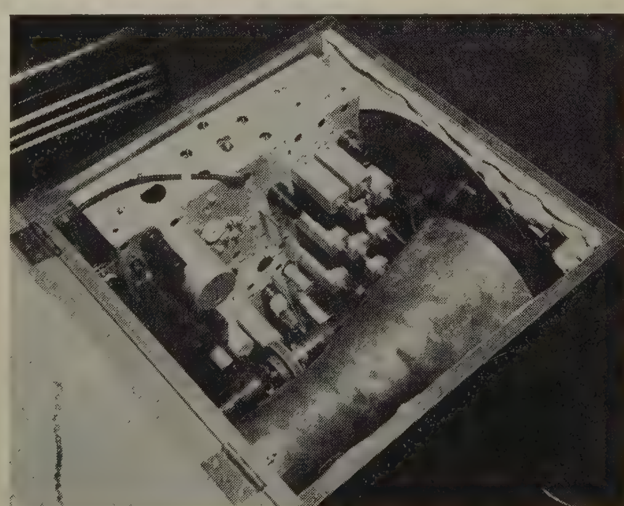

Fig. 24—Nine-inch color-television receiver; top view, open.

each color is adjustable by bias controls. The switching pulses are generated by the "ring frequency divider" circuit shown in Fig. 20.

The nonstorage dissector is more easily adapted to a filter disk, since it is necessary that the optical image on the cathode be of the correct color only at the

point which is being scanned. The orthicon, on the other hand, being of the storage type, requires that only one color can be present in the optical image for one complete scanning-field period, prior to the actual scansion of a given point. It is possible to design a disk to fulfill this requirement, but it will be of considerably larger diameter than the filter disk for the dissector. Fig. 21 shows the filter disk for the orthicon, where the contamination of colors due to the curvature of the filter segments is not more than 10 per cent. A filter drum, as shown in Fig. 22, accomplishes the same purpose with less contamination and less space. The drum is phased so that the shadow of the slotted rods holding the filters follows the scanning line.

Fig. 25—Seven-inch color-television receiver; front view.

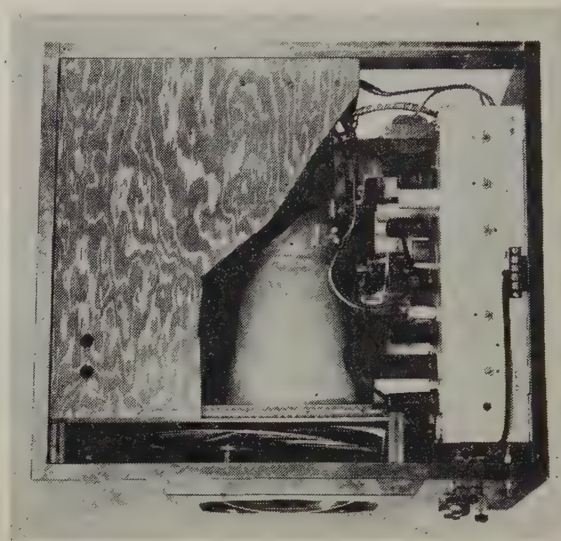

Fig. 26—Seven-inch color-television receiver; top view, open.

Receiving Equipment

Practically any good black-and-white television receiver design may be made the basis of a color-television receiver. Typical color receivers are shown in Figs. 23, 24, 25, and 26. The additional equipment required will be the color disk, with its driving and synchronizing means.

Usually additional precautions should be taken to insure complete direct-current component insertion and freedom from hum. The cathode-ray tube should be magnetically shielded to minimize pairing due to 60-cycle hum. It is fully as important, however, that attention be paid to sources of hum in the scanning circuit, such as common ground returns carrying alternating current, insufficient power-supply filtering, or magnetic coupling from power equipment into scanning transformers. It has sometimes been found economical to inject hum in opposing phase to neutralize alternating-current fields that otherwise may be difficult to remove. This is only possible when the

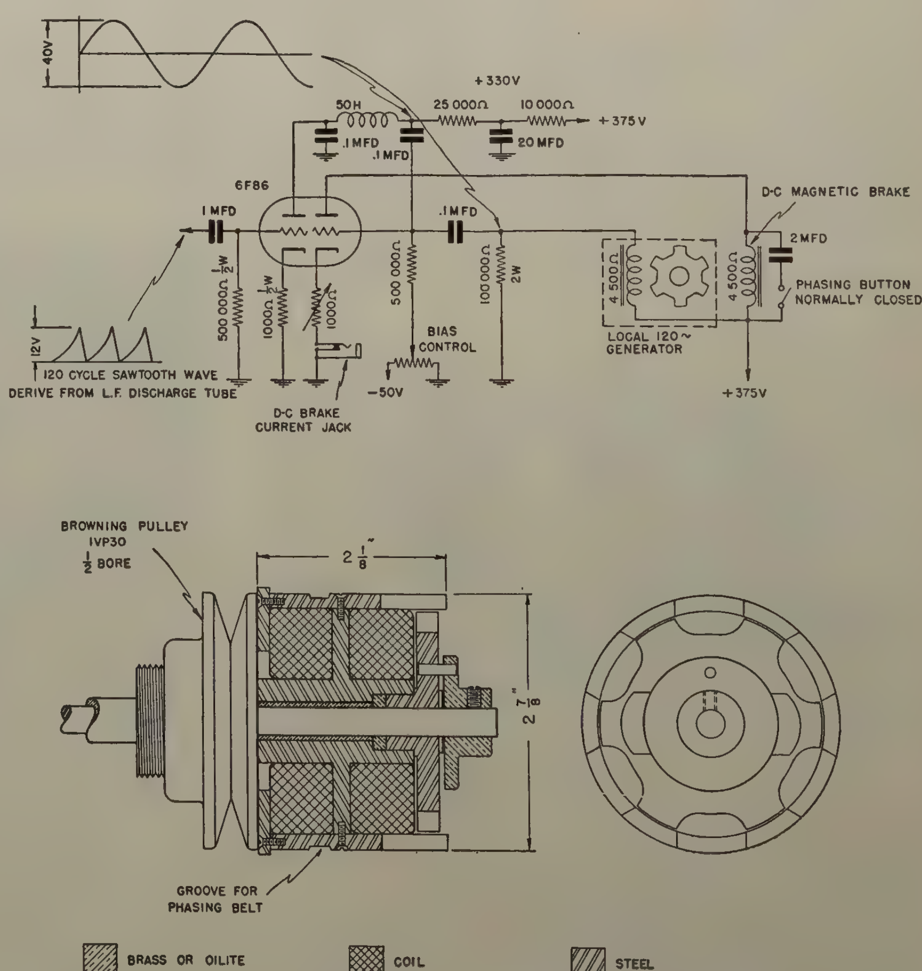

Fig. 27—Seven-inch-receiver brake circuits and design.

interfering hum remains constant in phase and amplitude with respect to the neutralizing components. Another effect which sometimes tends to destroy interlacing is due to electrostatic charges which accumulate on the rapidly moving color disk. Variations in the charge over the surface of the disk produce movement of the scanning lines as the disk rotates. It is possible to remove the charge with a semiconductive coating on the cathode-ray-tube face or with other electrostatic means of screening.

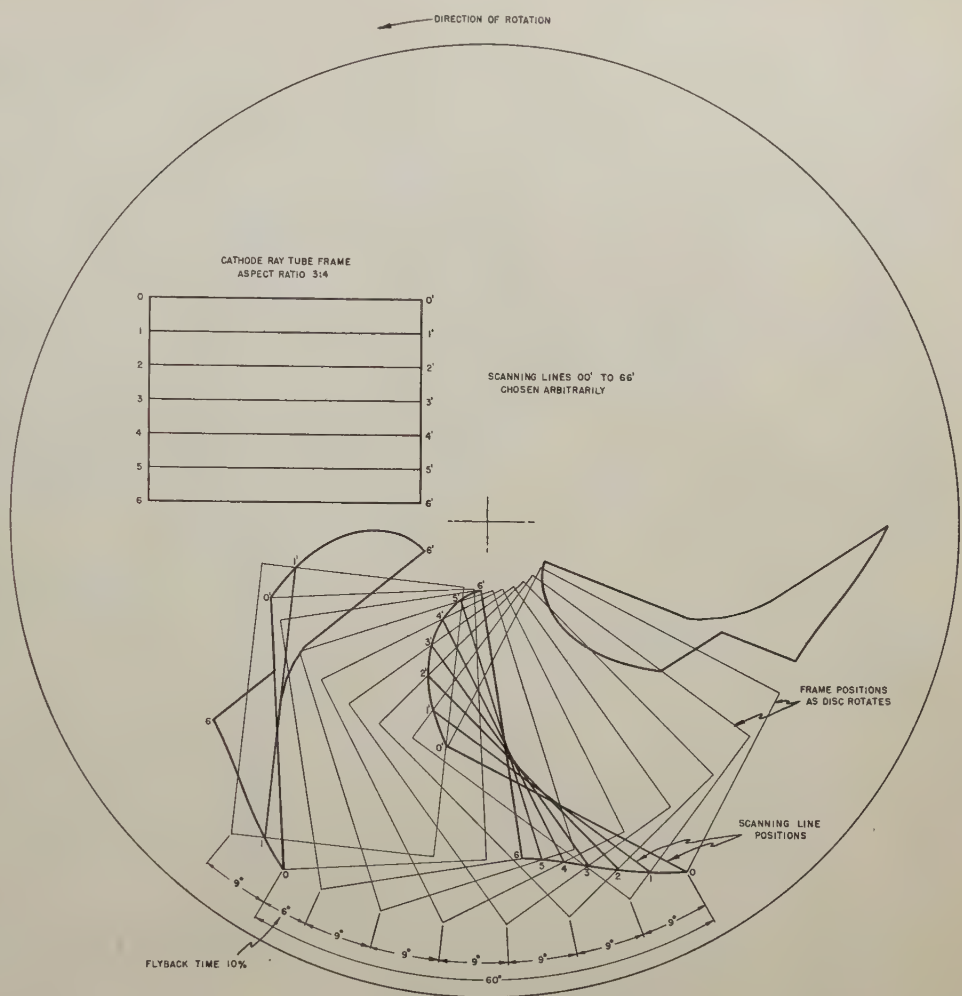

Fig. 29—Generation of filter shapes.

Color disks have been made of metal or of transparent plastics such as Lucite, Plexiglass, etc. Wratten filters may be obtained coated on a 10/1000-inch acetate stock which can be rivited to the plastic or metal disk. The disk may be rotated by a synchronous motor or by an asynchronous motor with auxiliary synchronizing means. Owing to lack of synchronism between the power supplies of New York, Connecticut, and New Jersey, and also owing to lack of standard synchronous motors of 1200-revolution-per-minute type, it was found desirable to drive the disk with an inexpensive induction-type motor and synchronize it by means of a phonic motor or a magnetic brake. Satisfactory phonic motors have been constructed which are driven by a single 6V6 tube, but the brake arrangement is preferred, Fig. 27. A photograph of the same brake assembly as used on the receiver of Fig. 25 is shown in Fig. 28. The 120-cycle voltage is derived from the low-frequency scanning circuit and is mixed with a similar voltage from a small generator on the disk shaft. The sum of the voltages is then rectified and the resulting direct current applied to the magnetic brake. A departure in the disk phase with respect to the scanning produces a corresponding correction on the part of the brake.

Fig. 28—Seven-inch color-television receiver, showing synchronizing brake and driving-motor assemblies.

The generation of a properly shaped filter disk is shown in Fig. 29. This type of shape is suitable for a receiving or transmitting tube with short decay or storage times. The curve which is obtained in Fig. 29 is an envelope of the position of a scanning line as traced onto the filter which is moving with the line. The required filter shape for a given mechanical arrangement is obtained by developing curves which make allowance for positive and negative tolerances to take care of fluctuation in the disk position, viewing angle, and screen decay, Fig. 30. Generally, the minimum disk diameter is about twice the outside diameter of the tube plus 1 or 2 inches. The optimum location will be determined by such factors as the distance

Fig. 30 (*right, top*)—Typical receiver filter-disk design.

Fig. 31 (*left, below*)—Drum receiver.

Fig. 32 (*right, middle*)—Rectangular flat-screen cathode-ray tube for color.

Fig. 33 (*right, bottom*)—Projector for color film showing lamp housing, projector, filter disk, and dissector housing.

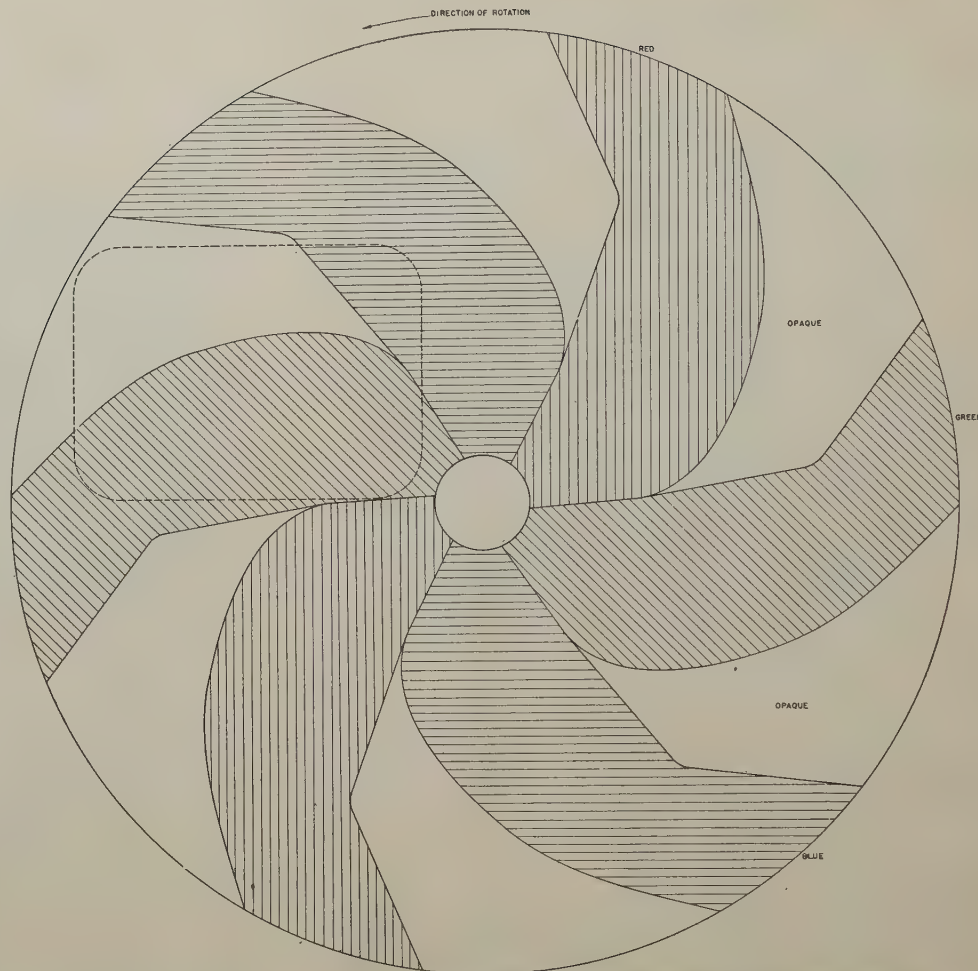

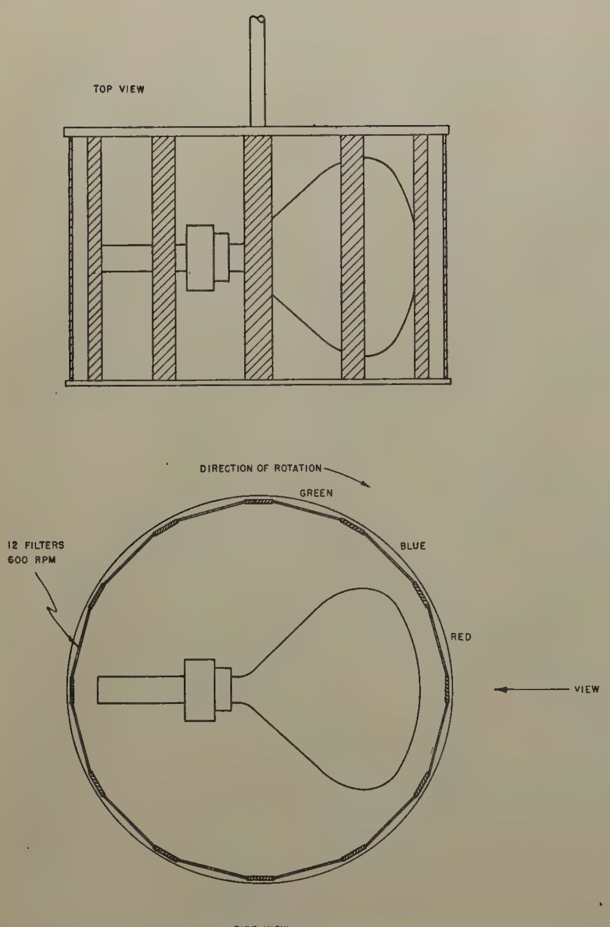

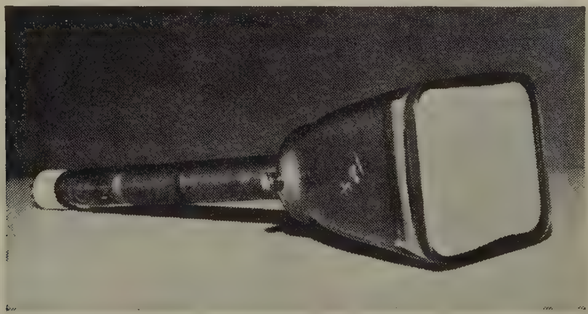

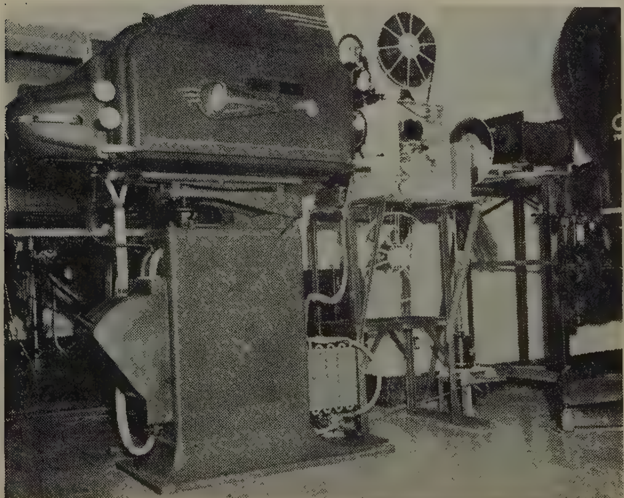

from the disk shaft to the picture frame, but can be determined for any particular arrangement.

Color drums have been used at the receiver as well as at the transmitter instead of color filters. A short cathode-ray tube can be placed within the drum (Fig. 31). The drum is designed for a lower speed of revolution than is usually possible with the disk. Successful drums have been built to operate at a speed of 600 revolutions per minute or one half the usual disk speed.

The small table-model receiver shown in Fig. 25 utilizes a cathode-ray tube developed especially for color pictures. The screen of the tube is flat and has the exact shape of the final image (Fig. 32). The tube produces a picture equivalent in size to that of a conventional 7-inch round tube. Thus the color disk is 15 inches in diameter. A 10-inch lens with a focal length of 12 inches, which is built into the receiver, increases the image to correspond to that of a conventional 9-inch tube. Owing to low magnification, distortion and decrease of the viewing angle are appreciably reduced.

Acknowledgment

All members of the Columbia Broadcasting System television engineering department have been concerned with this development. In particular, the active co-operation of Messrs. Goetz, Freundlich, Harcher, Erde, Doncaster, Reeves, and Haas is gratefully acknowledged.

The CBS television program department has unselfishly contributed by preparing suitable test and demonstration material.

Thanks are due to Mr. Adrian Murphy for his constructive criticism, active encouragement, and enthusiastic support throughout the entire developmental period.

Bibliography

Section I—Patents

(1) Otto von Bronk, No. 155,528 (German) 10/22/04. Method and device for making visible at a distance pictures or objects under temporary decomposition of the picture into parallel rows of points.
(2) W. von Jaworski and A. Frankenstein, No. 172,376 (German) 6/21/06. Method and device for reproducing at a distance pictures and objects by means of selenium cells through color filters and decomposition of the pictures in groups of points by means of mirrors.
(3) Johannes Adamian, No. 7219 (British) 1908. Improvement in electrically controlled apparatus for seeing at a distance.
(4) A. C. Andersen and L. S. Andersen, No. 30188 (British) 1909. Television apparatus.
(5) V. K. Zworykin, No. 255,057 (British) 7/3/26. Television apparatus.
(6) R. D. Kell, No. 308,277 (British) 11/21/29. Television apparatus.
(7) R. D. Kell, No. 1,748,883 (U. S.) 2/25/30. Transmission of pictures.
(8) Siemens-Schuckertwerke, No. 387,206 (British) 5/30/31. Cathode-ray tubes.
(9) M. von Ardenne, No. 388,623 (British) 6/8/32. Television method.
(10) John Hays Hammond, Jr., No. 1,725,710 (U. S.) 8/20/29. System and method of television.
(11) H. E. Ives, No. 390,158 (British) 9/28/31. Television.
(12) J. L. Baird, No. 418,527 (British) 5/25/33. Television. (Noted in *Telev. and Short Wave World*, vol. 8, p. 385, July, 1935.)
(13) D. S. Loewe and K. Schlesinger, No. 426,138 (British) 9/29/33. Cathode-ray tubes. (Noted in *Telev. and Short Wave World*, vol. 8, p. 458; August, 1935.)
(14) Fernseh, G.m.b.H., No. 432,989 (British) 3/6/34. Television receivers and cathode-ray tubes. (Noted in *Telev. and Short Wave World*, vol. 8, p. 715; December, 1935.)
(15) Fernseh, G.m.b.H., No. 434,868 (British) 3/6/34. Color television and cathode-ray tubes. (Noted in *Telev. and Short Wave World*, vol. 8, p. 28; January, 1936.)
(16) W. S. Hewitt, No. 439,494 (British) 6/5/34. Television. (Noted in *Telev. and Short Wave World*, vol. 9, p. 208; April, 1936.)
(17) L. C. Jesty, (General Electric Co.) No. 443,896 (British) 10/6/34. Television.
(18) J. L. Baird, No. 473,323 (British) 5/9/36. Television.
(19) Standard Telephones and Cables, Ltd., No. 500,005 (British) 2/18/38. Cathode-ray tubes. (Noted in *Telev. and Short Wave World*, vol. 12, p. 346; June, 1939.)
(20) A. Carpmael, No. 502,358 (British) 9/14/37. Television.
(21) C. N. Smyth, No. 508,037 (British) 12/24/37. Television. (Noted in *Telev. and Short Wave World*, vol. 12, p. 647; November, 1939.)
(22) J. L. Baird, No. 508,039 (British) 12/24/37. Television. (Noted in *Telev. and Short Wave World*, vol. 12, p. 648; November, 1939.)
(23) J. L. Baird, No. 512,855 (British) 3/22/38. Television.

Section II—Articles and Papers

(1) "Der Fernseher der Gebrüder Andersen (Television apparatus of Andersen and Andersen)," *Zeit. für Schwachstrom Tech.*, vol. 4, no. 17, pp. 452–454; 1910.
(2) H. D. Hubbard, "Colored scenes, motion, sound are envisaged," *Radio World*, vol. 11, p. 13; April 23, 1927.
(3) "Motion pictures in color radio's next," *Radio Digest*, vol. 20, p. 13; March 11, 1927.
(4) "Colored television due," *Radio World*, vol. 12, p. 7; February 4, 1928.
(5) A. Dinsdale, "Recent advances in television: television by daylight and television in colors," *Television*, vol. 1, pp. 9–10, 26; August, 1928.
(6) J. C. Jevons, "Television in colour," *Pop. Wireless*, vol. 13, p. 829; August 25, 1928.
(7) C. Tierney, "My impressions of daylight and colour television," *Television*, vol. 1, pp. 7–8; August, 1928.
(8) R. F. Tiltman, "Television in natural colors demonstrated," *Radio News*, vol. 10, pp. 320–374; October, 1928.
(9) "How colour television images are obtained," *Television*, vol. 1, p. 25; September, 1938.
(10) E. T. Larner, "Practical television" (Book review signed A. R.), *Nature*, vol. 122, pp. 232–234; August 18, 1928.
(11) C. S. Gleason, "High frequencies for color television," *Radio News*, vol. 10, pp. 632, 633, 679, 680; January, 1929.
(12) H. E. Ives, "Television in color," *Bell Lab. Rec.*, vol. 7, pp. 439–444; July, 1929. Reprint: *Instrument World*, vol. 2, no. 17, pp. 133–34; 1929.
(13) E. Andersen, "Ein Vorschlag zum Fernsehen in natürlichen Farben (A suggestion for television in natural color)," *Fernsehen*, vol. 1, pp. 179–180; April, 1930.
(14) A. Neuberger, "Farbiges Fernsehen (Color television)," *Fernsehen*, vol. 1, pp. 62–68; February, 1930.
(15) H. E. Ives, "Television in color," *Tel. Engr.*, vol. 33, 8, pp. 19–20; August, 1929.
(16) "Television in colors; Bell Telephone Laboratories engineers transmit and reproduce scenes in their natural hues," *Tel. and Tel. Age*, vol. 14, pp. 315–318; July 16, 1929.

References on same subject

Sci. News Letter, vol. 16, p. 3; July 6.
Telephony, vol. 97, pp. 23–25; July 6.
Wireless World, vol. 25, p. 37; July 10.
Science, vol. 70, supp. p. x; July 5.
Radio World, vol. 15, p. 11; July 20.
Elec. Record, vol. 46, p. 91, August.
Pop. Science, vol. 115, p. 25, September.
Radio News, vol. 11, p. 203; September.
Pop. Wireless, vol. 16, pp. 11–12; September 14.
Bell Tel. Quart., vol. 8, p. 344; October.
Radio, vol. 11, pp. 35–36; October.
Nature, vol. 124, p. 241; August 10.

(17) "Color television," *Western Elec. News*, vol. 18, pp. 18–19; August, 1929.
(18) H. E. Ives and A. L. Johnsrud, "Television in colors by a beam scanning method," *Jour. Opt. Soc. Amer.*, vol. 20, pp. 11–12; January, 1930.
(19) "Color television reported on way," *Tel. Engr.*, vol. 34, p. 40; March, 1930.

(20) S. P. Cook, "On an electromagnetic theory of sight and color vision," *Phys. Rev.*, p. 790, 1930. (Abstract.)
(21) Gradenwitz, "Ahronheim's television in natural colors," *Television*, vol. 3, pp. 177–178; June, 1930.
(22) H. E. Ives, "Television in color from motion picture film," *Jour. Opt. Soc. Amer.*, vol. 21, pp. 2–7; January, 1931.
(23) "Photoelectric cells for color television," *Television*, vol. 7, pp. 36–37; January, 1934.
(24) J. C. Wilson, "Trichromatic reproduction in television," *Jour. Roy. Soc. Arts.*, vol. 82, pp. 341–863; June, 1934; *Television*, vol. 7, pp. 268, 270, 272; June, 1934.
(25) R. L. Ashmore, "Color values in television," (A discussion of the pickup of colored scenes and their reproduction in black and white)," *Telev. and Short Wave World*, vol. 8, pp. 516, 517, 519; September, 1935.
(26) "Cheap screen invention reported for television in colors with sound," *Tel. and Tel. Age*, p. 146; July 1, 1935.
(27) "Television development—color broadcasting system," *Electrician*, vol. 114, p. 805; June 14, 1935. (News item.)
(28) "Television in color reported in Belgium," *Motion Pict. Herald*, vol. 119, p. 90; June 8, 1935.
(29) "Natural color television forecast by new patent (U.S. 2,055,557)," *Sci. News Letter*, vol. 30, p. 345; November 28, 1936.
(30) "Natural color television (Patent U.S. 2,055,557 RCA)," *New Prod. Digest*, vol. 2, item no. 1177, December 16, 1936.
(31) "Television pictures shown in color," *Pop. Science*, vol. 131, p. 53; July, 1937.
(32) V. A. Babits, "Television in colors," *Telev. and Short Wave World*, vol. 10, p. 480; August, 1937.
(33) "Baird color television," *Telev. and Short Wave World*, vol. 11, pp. 151–152; March, 1938.
(34) W. L. Prager, "Color in broadcasting studies by new Hollywood television group," *Amateur Cinematographer*, vol. 19, pp. 160–161; April, 1938.
(35) "Television in color covered by new patent (U.S. 2,109,773)," *Sci. News Letter*, vol. 34, p. 70; July 30, 1938.
(36) "Television in color," *Electrician*, vol. 120, p. 197; February 17, 1938.
(37) G. Otterbein, "Ein Farblichtrelais (Colored light relay—Its use in color television)," *Teleg.-Ferns.-und Funk.-Tech.*, vol. 27, spec. issue, pp. 550–551; November, 1938.
(38) H. Pressler, "Über die Bildfeldzerlegung bei der Farbenfernsehübertragung (Resolving the field of the image in color television transmission)," *Fernsehen*, supp. to *Funk. Tech. Monatshefte*, no. 12, pp. 89–93; December, 1938.
(39) F. W. Marchant, "New Baird color television system," *Telev. and Short Wave World*, vol. 12, pp. 541–542; September, 1939.
(40) T. de Nemes, "Color television with electrical color filters," *Telev. and Short Wave World*, vol. 12, pp. 73, 75; February, 1939.
(41) "Grande-Bretagne—La television en couleurs, (Great Britain—Color television)," *Rev. Teleph., Teleg., et Tel.*, vol. 16, pp. 169–170; February, 1939.
(42) J. Pressler, "La television en colores (Television in color)," *Revista Telegrafica*, vol. 27, pp. 169, 171, 187; March, 1939. (Translation of an article in German.)
(43) N. W. Maybank, "Color television—Baird television system described," *Wireless World*, vol. 45, pp. 145–146; August 17, 1939.
(44) W. Reichel, "Der Mehrfachzeilenspring (Multiple interlacing)," *Fernseh.*, vol. 15, pp. 171, 179; August, 1939.
(45) "Television in natural color." *Communications*, vol. 20, pp. 8, 27–28; June, 1940.
(46) CBS Publicity release, "Color television achieves realism," *New York Times*, September 5, 1940.
(47) A. H. Rosenthal, "The Skiatron—a new Scophony development towards large screen television projection," *Electronics and Telev. and Short Wave World*, vol. 13, pp. 52–55; February, and pp. 117–119; March, 1940.
(48) A. H. Rosenthal, "A system of large-screen television reception based on certain electron phenomena in crystals," Proc. I.R.E., vol. 28, pp. 211–212; May, 1940.
(49) "Color television demonstrated by CBS engineers," *Electronics*, vol. 13, pp. 32–34, 73–74; October, 1940.

Characteristic Impedance of Parallel Wires in Rectangular Troughs*

SIDNEY FRANKEL†, ASSOCIATE, I.R.E.

Summary—*The method of conformal transformation and the method of images are employed jointly to deduce the characteristic impedance of a balanced two-conductor transmission line and of a balanced three-conductor transmission line symmetrically surrounded by perfect, rectangular, grounded, conducting surfaces. It is assumed that 1, the wires are of circular cross section, of diameter small compared to the distance between them and small compared to the distance from the wire to any side of the surrounding surface, and 2, the wires are perfect conductors.*

I. Introduction

The characteristic impedance of a transmission line consisting of a system of parallel perfect conductors in air is readily calculated when the capacitance per unit length of the line is known. Thus if

Z_0 = characteristic impedance, in ohms

C = electrostatic capacitance in electrostatic units per centimeter

then[1]

$$Z_0 = \frac{30}{C}. \tag{1}$$

The problem of determining the characteristic impedance thus reduces to a two-dimensional problem in electrostatics otherwise known as the logarithmic potential.[2] Many such problems can be solved directly by finding the potential field due to an assigned distribution of charges and then calculating the capacitance as the ratio of charge on the conductors to potential difference between them.[2–4] The number of solutions available can be extended by various devices,[2,5] among which two will be employed in this paper. The two devices employed here are the method of conformal transformation[2,6] and the method of images.[2,3] Starting with known solutions of simple logarithmic potential

* Decimal classification: R322. Original manuscript received by the Institute, August 8, 1941.
† Federal Telegraph Company, Newark, N. J.
[1] W. R. Smythe, "Static and Dynamic Electricity," first edition, McGraw-Hill Book Company, New York, N. Y., page 472, equation (7).

[2] J. H. Jeans, "Mathematical Theory of Electricity and Magnetism," fifth edition, Cambridge University Press, London, England, pp. 67–68, 73–74, 185–299.
[3] M. Abraham and R. Becker, "Electricity and Magnetism," Blackie and Son, London, England, pp. 53–69.
[4] R. D. Duncan, "Characteristic impedance of grounded and ungrounded open-wire transmission lines," *Communications*, p. 10, June, 1938.
[5] E. Weber, "Mapping of Fields," *Trans. A.I.E.E.*, 1934, vol. 53, p. 1563, 1934. (Extensive Bibliography.)
[6] I. S. Sokolnikoff and E. S. Sokolnikoff, "Higher Mathematics for Engineers and Physicists," first edition, McGraw-Hill Book Company, New York, N. Y., pp. 432–461.

problems (such as, for example, the problem of two circular conductors in free space), a conformal transformation will be used to change these solutions to the solutions of problems involving wires located between parallel infinite planes. Finally, by the method of images these solutions will be transformed to the solutions of problems involving wires in rectangular troughs.

Although the methods used are fairly general, only two definite rectangular-trough problems are solved in this paper: The balanced two-wire transmission line and the balanced three-wire line in which the center lines of the three wires lie in a plane and the inner wire serves as a return for the outer two. In all cases the trough is at zero, or ground, potential. The following assumptions are made:

(1) The wires are of circular cross section, of diameter small compared to the distance between them, and small compared to the distance from the wire to any side of the trough. This assumption is similar and equivalent to the one ordinarily made in computing open-wire lines.

(2) The wires are perfect conductors, so that (1) is valid.

In the method of conformal transformation only points are transformed and not potentials. This means that if the points of the complex Z plane are transformed to points of the complex W plane by means of an analytic transformation

$$w = f(z)$$

then the point

$$w_1 = f(z_1)$$

has the same potential in the W plane that the point z_1 has in the Z plane. For this reason the intermediate step of transforming capacitance is unnecessary; the characteristic impedance may be transformed directly. This, of course, is no longer true when the method of images is introduced.

II. Wires Between Infinite Planes

We begin by considering the conformal transformation from the complex Z plane to the complex W plane,

$$w = u + iv = e^z = e^{x+iy} = e^x \cos y + ie^x \sin y;$$

i.e.,

$$\left.\begin{aligned} u &= e^x \cos y \\ v &= e^x \sin y \end{aligned}\right\} \qquad (12)$$

where $i = \sqrt{-1}$, e = Naperian base = $2.718 \cdots$.

Consider the transformation of points on the u axis. Let $(a, 0)$ be such a point, and first let $a>0$ (Fig. 1(a)). Then we have, from (2),

$$\left.\begin{aligned} e^x \cos y &= a \\ e^x \sin y &= 0 \end{aligned}\right\}, \qquad a > 0.$$

From the second of these we have

$$\sin y = 0, \qquad y = \pm n\pi \qquad (n = 0, 1, 2, \cdots)$$

whence

$$e^x(-1)^n = a, \qquad e^x = (-1)^n a$$

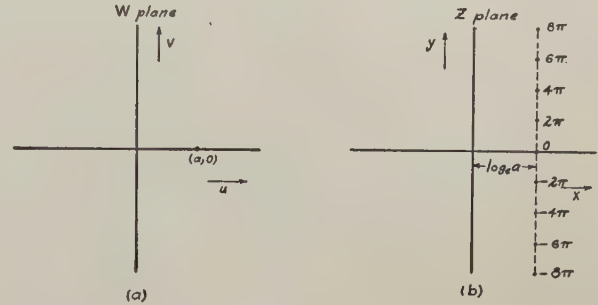

Fig. 1—Transformation of a point in the W plane to points in the Z plane by means of the transformation $w=e^z$, where the point in the W plane lies on the u axis to the right of the origin.

and since $e^x>0$ for real x, we must restrict n to even integers. The result is, therefore,

$$\left.\begin{aligned} y &= \pm 2m\pi \\ x &= \log_e a \end{aligned}\right\} \qquad \begin{aligned} &(m = 0, 1, 2, \cdots) \\ &a > 0. \end{aligned}$$

These transformed points are plotted in Fig. 1(b). Now suppose $a<0$. Then, as before,

$$e^x = (-1)^n a$$

which requires that $n=2m+1$, $(m=0, 1, 2, \cdots)$. The result runs

$$\left.\begin{aligned} y &= \pm (2m+1)\pi \\ x &= \log_e (-a) \end{aligned}\right\} \qquad \begin{aligned} &(m = 0, 1, 2, \cdots) \\ &a < 0. \end{aligned}$$

The situation is shown in Figs. 2(a) and 2(b).

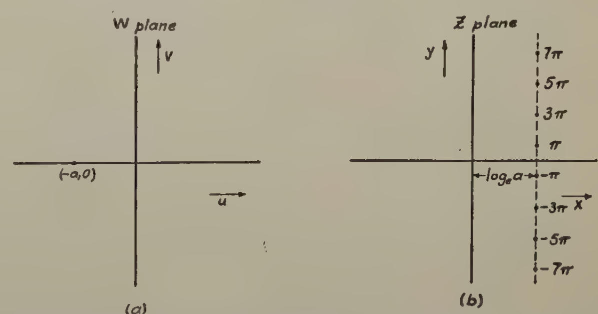

Fig. 2—Transformation of a point in the W plane to points in the Z plane by means of the transformation $w=e^z$, where the point in the W plane lies on the u axis to the left of the origin.

Let $\alpha>0$. If in the W plane we have a charge λ per unit depth at $(\alpha, 0)$ and a charge $-\lambda$ per unit depth at $(-\alpha, 0)$ (Fig. 3(a)), then Fig. 3(b) shows the resultant in the Z plane.

The line $u=0$ transforms to

$$y = \pm (2m+1)\frac{\pi}{2}$$

as is apparent from the equation

$$u = e^x \cos y = 0.$$

In particular, it transforms to $y = \pm\pi/2$. Hence it is apparent that the field to the right of the Y axis transforms (in particular) to the field between the planes whose traces are $y = \pm\pi/2$; i.e., to a field between

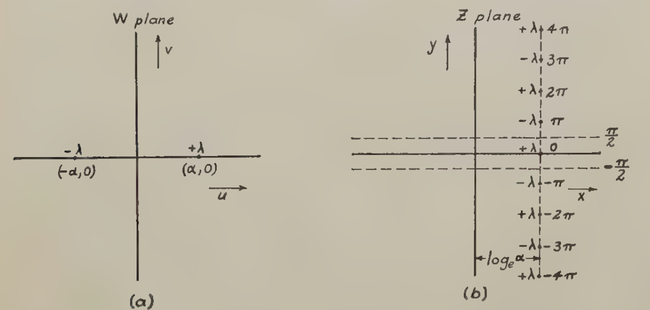

Fig. 3—Transformation of points representing line charges in the W plane to points representing line charges in the Z plane by means of the transformation $w = e^z$, where the line charges in the W plane lie on the u axis, symmetrically disposed with respect to the origin.

infinite conducting plates separated by a distance π when a thin wire is located centrally between them. We get more general solutions by using more general pairs of lines corresponding to the condition

$$y = \pm (2m + 1) \frac{\pi}{2} \qquad (m = 1, 2, 3, \cdots).$$

Before proceeding further it is desirable to generalize the transformation slightly, by changing it to

$$w = e^{kz}, \quad k > 0, \quad \text{real.} \tag{3}$$

In that case we get

$$\left.\begin{aligned} u &= e^{kx} \cos ky \\ v &= e^{kx} \sin ky \end{aligned}\right\}.$$

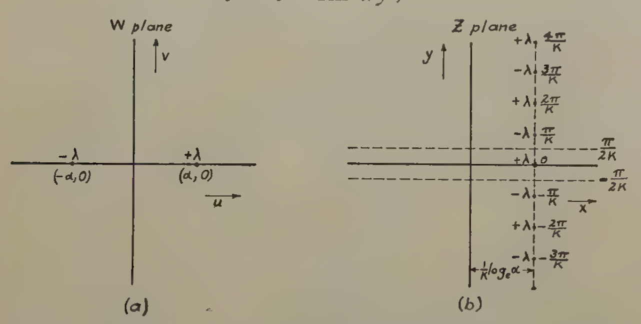

Fig. 4—Transformation of points representing line charges in the W plane to points representing line charges in the Z plane by means of the transformation $w = e^{kz}$, where the line charges in the W plane lie on the u axis, symmetrically disposed with respect to the origin.

The solutions for y become

$$y = \pm n \frac{\pi}{k}$$

while for x, we have

$$x = \frac{1}{k} \log_e \alpha.$$

The configurations are shown in Fig. 4. If $k = \pi/h$ the transformation gives the solution for the field due to a wire between parallel plates separated by a distance h when the solution for two wires in free space is known. This solution will now be obtained.

In the W plane let the radius of the wires be c_α. Then the well-known solution in practical units is

$$Z_0 = 276 \log_{10} \frac{2\alpha}{c_\alpha}. \tag{4}$$

This is the characteristic impedances between wires, in ohms.

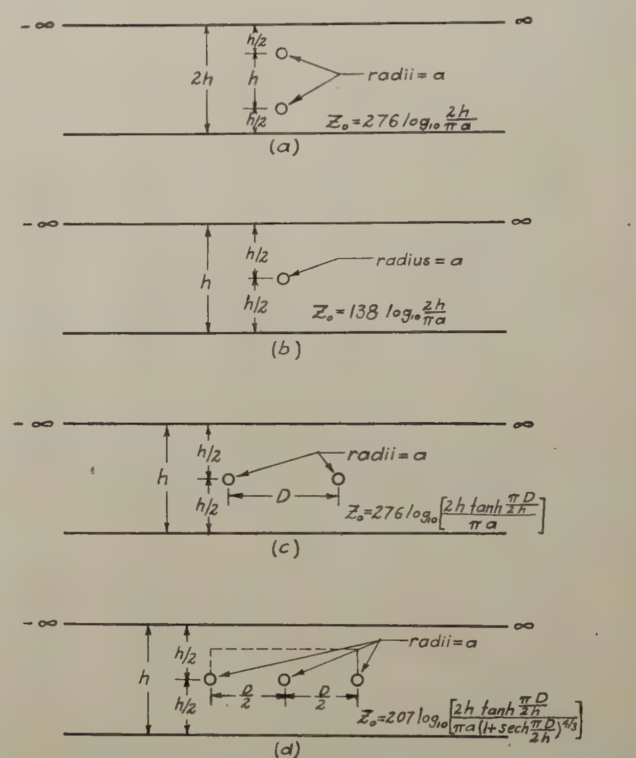

Fig. 5—Characteristic impedance of various configurations of transmission lines located between parallel infinite planes; (a) balanced two-wire line in plane perpendicular to infinite planes, (b) single-conductor line, (c) balanced two-wire line in plane parallel to infinite planes, (d) balanced three-wire line in plane parallel to infinite planes.

In the Z plane let the radius of the wires be a. The distance between two successive wires is h. Now since

$$dz = \frac{dw}{kw}$$

we have, taking $dz = a$, $dw = c_\alpha$ (i.e., a and c_α assumed small)

$$a = \frac{c_\alpha}{k\alpha}; \; a, c_\alpha \text{ small}^7$$

[7] A circle in the Z plane transforms very nearly to a circle in the W plane if the radius of the circle is sufficiently small. Thus, let the equation of a circle in the Z plane be

$$z = \zeta + \rho e^{i\theta}$$

where ζ is the distance from the origin to the center of the circle, ρ is the radius of the circle, and θ is the independent variable angle. In the W plane we have $w = f(z) = f(\zeta + \rho e^{i\theta})$ which by Taylor's expansion theorem may be written $w = f(\zeta) + f'(\zeta)\rho e^{i\theta} + f''(\zeta)/2!\,\rho^2 e^{i2\theta} + \cdots$, where $f^{(n)}(\zeta) = d^n/dz^n f(z)_{z=\zeta} (n = 1, 2, 3, \cdots)$. From this series it is clear that by taking ρ sufficiently small we can approximate W by the first two terms of the series, which, of course, represent another circle.

i.e.,

$$\frac{\alpha}{c_\alpha} = \frac{1}{ak} = \frac{h}{\pi a}.$$

Substituting this value in (4) we find that the characteristic impedance between two wires is

$$Z_0 = 276 \log_{10} \frac{2h}{\pi a} \tag{5}$$

or between a single wire and ground, it is

$$Z_0 = 138 \log_{10} \frac{2h}{\pi a} \cdot \tag{6}$$

These results are shown in Figs. 5(a) and 5(b), respectively.

Next suppose that instead of two wires in the W plane, we have four as shown in Fig. 6(a). Then the disposition of wires in the Z plane is clearly as shown in Fig. 6(b), and a particular solution that can be found is the cases for two parallel balanced wires between infinite planes.

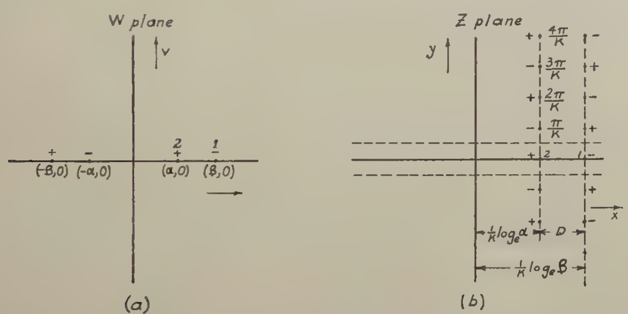

Fig. 6—Transformation of points representing line charges in the W plane to points representing line charges in the Z plane by means of the transformation $w=e^{kz}$, where the line charges in the W plane lie on the u axis, symmetrically disposed with respect to the origin.

Let wires at $(\alpha, 0)$ and $(-\alpha, 0)$ have radii c_α; wires at $(\beta, 0)$ and $(-\beta, 0)$ have radii c_β; while wires in the Z plane all have radii a. Then, by the same method as used previously,

$$a = \frac{c_\alpha}{k\alpha} = \frac{c_\beta}{k\beta} \cdot \tag{7}$$

Furthermore we have, from Fig. 6(b)

$$\frac{1}{k} \log_e \frac{\beta}{\alpha} = D; \frac{\beta}{\alpha} = e^{kD}; \beta = \alpha e^{kD}, \alpha = \beta e^{-kD}. \tag{8}$$

The solution for the characteristic impedance between wires 1 and 2 in the W plane is readily obtained[8] as

$$Z_0 = 276 \log_{10} \left[2 \frac{\beta - \alpha}{\beta + \alpha} \sqrt{\frac{\alpha\beta}{c_\alpha c_\beta}} \right].$$

[8] For the expression of a transformation representing the potential of any number of parallel filaments see E. J. Townsend, "Functions of a Complex Variable," Henry Holt and Company, New York, N. Y., p. 141.

But

$$\frac{\beta - \alpha}{\beta + \alpha} = \frac{\frac{\beta}{\alpha} - 1}{\frac{\beta}{\alpha} + 1} = \frac{e^{kD} - 1}{e^{kD} + 1} = \tanh \frac{kD}{2} \qquad \text{from (8)}$$

and

$$\frac{\alpha\beta}{c_\alpha c_\beta} = \frac{1}{k^2 a^2} \qquad \text{from (7).}$$

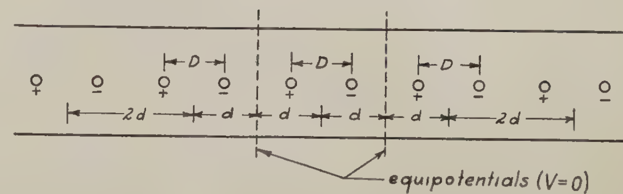

Fig. 7—Substitution of an infinite series of line charges for a finite system of line charges located between two parallel infinite planes.

Hence, the solution runs

$$Z_0 = 276 \log_{10} \left[\frac{2 \tanh \frac{kD}{2}}{ka} \right] \text{ohms.} \tag{10a}$$

In particular, if $k = \pi/h$,

$$Z_0 = 276 \log_{10} \left[\frac{2h \tanh \frac{\pi D}{2h}}{\pi a} \right] \text{ohms.} \tag{10b}$$

The configuration is shown in Fig. 5(c).

III. Wires in Troughs

Balanced Two-Wire Line

In order to establish the characteristic impedance of a balanced line symmetrically placed in a rectangular box, we apply the method of images to the configuration of Fig. 5(c). In order to establish two vertical equipotentials for the vertical walls, it is necessary to use an infinite series of images extending in a straight line from $-\infty$ to $+\infty$ as shown in Fig. 7.

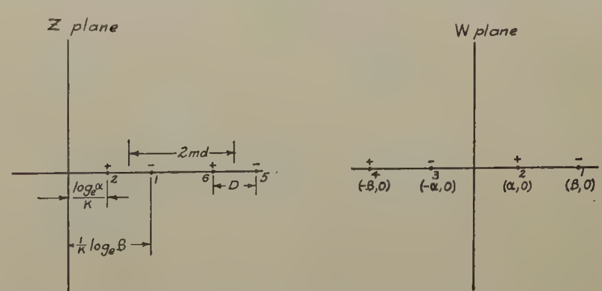

Fig. 8—Transformation of the left m^{th}-image pair of Fig. 7 (points 1 and 2 in the Z plane) to a system of charges in the W plane (compare Fig. 6).

In order to study the effect of this series of images on the potential difference between the wires (which, for fixed charge per unit length λ is proportional to Z_0),

we study the effect of the m^{th} pair to the left of the wires. The m^{th} pair to the right has precisely the same effect on the potential difference, so that the effect of two symmetrically placed pairs is twice the effect of one of them. Finally we sum the effects over m.

In Fig. 8, the left m^{th} image pair is at the points 1, 2, (Z plane) and the wires with charge λ per unit length, are at the points 5, 6. In the W plane the potential at any point is

$$V = -2\lambda \log_e \frac{|w - w_2||w - w_4|}{|w - w_1||w - w_3|}, \quad \text{(subscripts correspond to points)}$$

$$= -2\lambda \log_e \frac{|e^{kz} - e^{kz_2}||e^{kz} - e^{kz_4}|}{|e^{kz} - e^{kz_1}||e^{kz} - e^{kz_3}|}$$

where $\quad w_1 = \beta,\ w_2 = \alpha,\ w_3 = -\alpha,\ w_4 = -\beta.$

Since we are interested only in points on the X axis, and since $e^x > 0$ for all x,

$$V = -2\lambda \log_e \frac{(e^{kx} - \alpha)(e^{kx} + \beta)}{(e^{kx} + \alpha)(e^{kx} - \beta)}.$$

Now

$$\left.\begin{aligned} x_5 &= \frac{1}{k}\log_e \sqrt{\alpha\beta} + 2md + \frac{D}{2};\\ kx_5 &= \log_e \sqrt{\alpha\beta} + \delta_5, \text{ where } \delta_5 = k\left(2md + \frac{D}{2}\right)\\ x_6 &= \frac{1}{k}\log_e \sqrt{\alpha\beta} + 2md - \frac{D}{2};\\ kx_6 &= \log_e \sqrt{\alpha\beta} + \delta_6, \text{ where } \delta_6 = k\left(2md - \frac{D}{2}\right) \end{aligned}\right\}. \quad (11)$$

Hence

$$V_6 = -2\lambda \log_e \frac{(\sqrt{\alpha\beta}\, e^{\delta_6} - \alpha)(\sqrt{\alpha\beta}\, e^{\delta_6} + \beta)}{(\sqrt{\alpha\beta}\, e^{\delta_6} + \alpha)(\sqrt{\alpha\beta}\, e^{\delta_6} - \beta)}$$

which, by virtue of (8), becomes

$$V_6 = -2\lambda \log_e \frac{(e^{\delta_6 + kD/2} - 1)(e^{\delta_6 - kD/2} + 1)}{(e^{\delta_6 + kD/2} + 1)(e^{\delta_6 - kD/2} - 1)}.$$

But by (11),

$$\delta_6 + \frac{kD}{2} = 2mkd, \qquad \delta_6 - \frac{kD}{2} = k(2md - D).$$

Hence

$$V_6 = -2\lambda \log_e \left\{\tanh\,[mkd] \coth\left[k\left(md - \frac{D}{2}\right)\right]\right\}. \quad (12a)$$

Similarly

$$V_5 = -2\lambda \log_e \left\{\tanh\left[k\left(md + \frac{D}{2}\right)\right] \coth\,[mkd]\right\}. \quad (12b)$$

Thus the effect of the left m^{th} pair is

$$(V_6 - V_5)_{ml} = -2\lambda \log_e \frac{\tanh^2\,[mkd]}{\tanh\left[k\left(md - \frac{D}{2}\right)\right] \tanh\left[k\left(md + \frac{D}{2}\right)\right]} \quad (13)$$

while the effect of both (left and right)m^{th} pairs is just twice this value; i.e.,

$$(V_6 - V_5)_m = 2(V_6 - V_5)_{ml}. \quad (14)$$

It is readily shown that

$$\tanh\,(a + b)\tanh\,(a - b) = \tanh^2 a \frac{1 - \left(\dfrac{\sinh b}{\sinh a}\right)^2}{1 + \left(\dfrac{\sinh b}{\cosh a}\right)^2}.$$

Hence (14) becomes

$$(V_6 - V_5)_m = -4\lambda \log_e \frac{1 + \left[\dfrac{\sinh \frac{kD}{2}}{\cosh mkd}\right]^2}{1 - \left[\dfrac{\sinh \frac{kD}{2}}{\sinh mkd}\right]^2}. \quad (15)$$

Summing for m and adding to the original potential in the absence of images, we get for the characteristic impedance

$$Z_0 = 276\left\{\log_{10}\left[\frac{2h \tanh \frac{\pi D}{2h}}{\pi a}\right] - \sum_{m=1}^{\infty} \log_{10}\left[\frac{1 + \left(\dfrac{\sinh \frac{\pi D}{2h}}{\cosh \frac{m\pi d}{h}}\right)^2}{1 - \left(\dfrac{\sinh \frac{\pi D}{2h}}{\sinh \frac{m\pi d}{h}}\right)^2}\right]\right\}. \quad (16)$$

Finally, setting $2d=w$, we get the formula for the configuration of Fig. 9(a),

$$Z_0 = 276\left\{\log_{10}\left[\frac{2h\tanh\dfrac{\pi D}{2h}}{\pi a}\right] - \sum_{m=1}^{\infty}\log_{10}\left[\frac{1+\left(\dfrac{\sinh\dfrac{\pi D}{2h}}{\cosh\dfrac{m\pi w}{2h}}\right)^2}{1-\left(\dfrac{\sinh\dfrac{\pi D}{2h}}{\sinh\dfrac{m\pi w}{2h}}\right)^2}\right]\right\}. \tag{17}$$

Usually, it is unnecessary to go beyond $m=1$ in the summation. Hence for practical purposes,

$$Z_0 = 276\left\{\log_{10}\left[\frac{2h\tanh\dfrac{\pi D}{2h}}{\pi a}\right] - \log_{10}\left[\frac{1+\left(\dfrac{\sinh\dfrac{\pi D}{2h}}{\cosh\dfrac{\pi w}{2h}}\right)^2}{1-\left(\dfrac{\sinh\dfrac{\pi D}{2h}}{\sinh\dfrac{\pi w}{2h}}\right)^2}\right]\right\}. \tag{18}$$

Three Wires in a Trough

We consider the case of three wires in a trough, where the middle conductor acts as a return for the outer two. The problem is entirely similar to the preceding one of two conductors. The configuration in the W plane is shown in Fig. 10(a), while the transformed configuration is shown in Fig. 10(b).

If the wires at points $(\alpha, 0)$, $(\beta, 0)$, and $(\gamma, 0)$ have radii c_α, c_β, c_γ, respectively, while the wires in the Z plane all have radius a, then

$$\left.\begin{aligned} \frac{\beta}{\alpha} = \frac{\gamma}{\beta} = \frac{c_\beta}{c_\alpha} = \frac{c_\gamma}{c_\beta} = e^{kD/2} \\ \frac{c_\alpha}{k\alpha} = \frac{c_\beta}{k\beta} = \frac{c_\gamma}{k\gamma} = a \end{aligned}\right\}. \tag{19}$$

In the W plane the potential function is

$$V = -2\lambda \log_e \frac{|w-w_1|\cdot|w-w_3|\cdot|w-w_5|^2}{|w-w_2|^2\cdot|w-w_4|\cdot|w-w_6|} \tag{20}$$

where λ is the charge per unit length of the outer wires, the charge on the inner (return) wire being -2λ whence

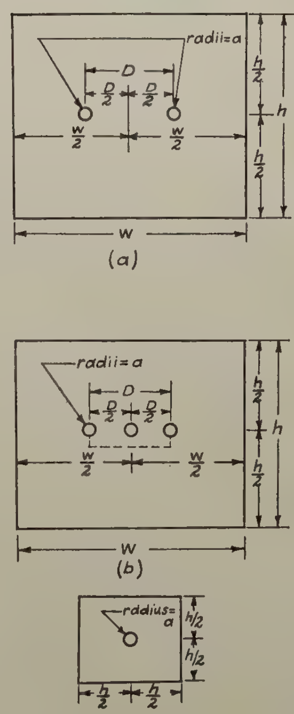

Fig. 9—Rectangular-trough configurations; (a) balanced two-wire line, (b) balanced three-wire line, (c) concentric line. See text for characteristic-impedance formulas.

$$V_1 = -2\lambda\log_e\frac{c_\gamma(\gamma-\alpha)(\gamma+\beta)^2}{(\gamma-\beta)^2(\gamma+\alpha)(2\gamma)}$$

$$V_2 = -2\lambda\log_e\frac{(\gamma-\beta)(\beta-\alpha)(2\beta)^2}{c_\beta^2(\beta+\alpha)(\gamma+\beta)}$$

$$V_1 - V_2 = -2\lambda\log_e\left[\frac{1}{8}\left(\frac{c_\gamma}{\gamma}\right)\left(\frac{c_\beta}{\beta}\right)^2\left(\frac{\gamma+\beta}{\gamma-\beta}\right)^3\left(\frac{\gamma-\alpha}{\gamma+\alpha}\right)\left(\frac{\beta+\alpha}{\beta-\alpha}\right)\right].$$

Making use of (19), we get

$$\frac{c_\gamma}{\gamma}\left(\frac{c_\beta}{\beta}\right)^2 = (ka)^3$$

$$\frac{\gamma+\beta}{\gamma-\beta} = \coth\frac{kD}{4}$$

$$\frac{\gamma-\alpha}{\gamma+\alpha} = \tanh\frac{kD}{2}$$

$$\frac{\beta+\alpha}{\beta-\alpha} = \coth\frac{kD}{4}.$$

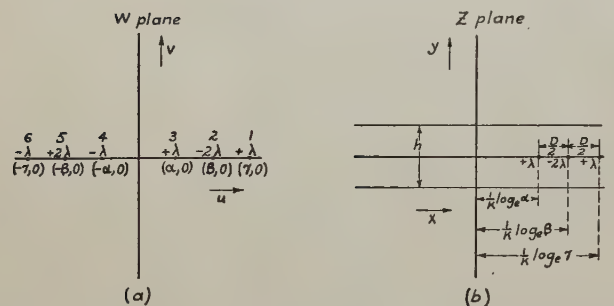

Fig. 10—Transformation of points representing line charges in the W plane to points representing line charges in the Z plane by means of the transformation $w = e^{kz}$, where the line charges in the W plane lie on the u axis, symmetrically disposed with respect to the origin.

Hence

$$V_1 - V_2 = -2\lambda \log_e \frac{k^3a^3}{8}\coth^4\frac{kD}{4}\tanh\frac{kD}{2}$$

$$= 6\lambda \log_e \frac{2h}{\pi a}\sqrt[3]{\frac{\tanh^4\dfrac{\pi D}{4h}}{\tanh\dfrac{\pi D}{2h}}}$$

so that for three wires between infinite planes (Fig. 5(d)) we get

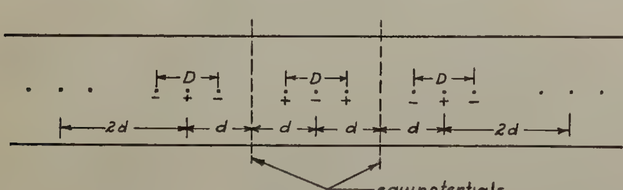

Fig. 11—Substitution of an infinite series of line charges for a finite system of line charges located between two parallel infinite planes.

$$Z_0 = 207 \log_{10}\frac{2h}{\pi a}\sqrt[3]{\frac{\tanh^4\dfrac{\pi D}{4h}}{\tanh\dfrac{\pi D}{2h}}}$$

$$= 207 \log_{10}\frac{2h\tanh\dfrac{\pi D}{2h}}{\pi a\left[1+\operatorname{sech}\dfrac{\pi D}{2h}\right]^{4/3}} \tag{21}$$

In obtaining the image effect of the vertical sides of the rectangular box, we notice (Fig. 11) that on the first-order image the signs of the charges are reversed, on the second-order they are direct again, etc. For the m^{th}-order image on the left the situation is shown in Fig. 12. The potential function is, from (20),

$$V = -(-1)^m 2\lambda \log_e \frac{|w-w_1|\cdot|w-w_3|\cdot|w-w_5|^2}{|w-w_2|^2\cdot|w-w_4|\cdot|w-w_6|}$$

$$= -(-1)^m 2\lambda \log_e \frac{(e^{kx}-\gamma)(e^{kx}-\alpha)(e^{kx}+\beta)^2}{(e^{kx}+\gamma)(e^{kx}+\alpha)(e^{kx}-\beta)^2}$$

for points along the X axis.

Although the wires at 7 and 9 (Fig. 12) are unequally affected by the left-hand m^{th} image, the inequality is exactly reversed by the right-hand m^{th} image, so that the m^{th} pair brings 7 and 9 to exactly the same potential. Therefore we consider the effect on the potential difference between 7 and 8 only. The change in $(V_7 - V_8)$ due to both m^{th}-order images is the same as the *sum* of the effects on 7 and 9 of the left image alone. Therefore we calculate $(V_9 - V_8)$ and $(V_7 - V_8)$ for the left image. Their sum is the effect of the left and right images on $(V_7 - V_8)$. We have

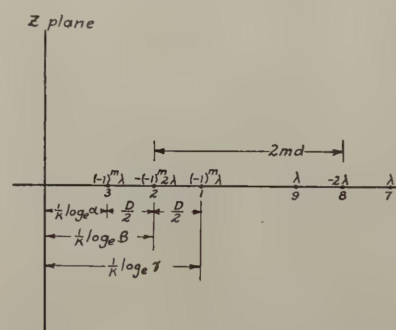

Fig. 12—Representation in the Z plane of the left m^{th}-image group of Fig. 11 (points 1, 2, 3; compare Fig. 6).

$$x_7 = \frac{1}{k}\log_e\beta + 2md + \frac{D}{2};$$

$$kx_7 = \log_e\beta + \delta_7, \text{ where } \delta_7 = k\left(2md + \frac{D}{2}\right)$$

$$x_8 = \frac{1}{k}\log_e\beta + 2md;$$

$$kx_8 = \log_e\beta + \delta_8, \text{ where } \delta_8 = 2kmd$$

$$x_9 = \frac{1}{k}\log_e\beta + 2md - \frac{D}{2};$$

$$kx_9 = \log_e\beta + \delta_9, \text{ where } \delta_9 = k\left(2md - \frac{D}{2}\right).$$

Hence

$$V_7 = -(-1)^m 2\lambda \log_e \frac{(\beta e^{\delta_7}-\gamma)(\beta e^{\delta_7}-\alpha)(\beta e^{\delta_7}+\beta)^2}{(\beta e^{\delta_7}+\gamma)(\beta e^{\delta_7}+\alpha)(\beta e^{\delta_7}-\beta)^2}.$$

But since

$$\beta = \gamma e^{-kD/2} = \alpha e^{kD/2}$$

we get, on substituting and reducing,

$$V_7 = -(-1)^m 2\lambda \log_e \left\{ [\tanh mkd] \left[\tanh k\left(md + \frac{D}{2} \right) \right] \left[\coth k\left(md + \frac{D}{4} \right) \right]^2 \right\}.$$

Similarly

$$V_8 = -(-1)^m 2\lambda \log_e \left\{ \left[\tanh k\left(md - \frac{D}{4} \right) \right] \left[\tanh k\left(md + \frac{D}{4} \right) \right] [\coth mkd]^2 \right\}$$

and

$$V_9 = -(-1)^m 2\lambda \log_e \left\{ \left[\tanh k\left(md - \frac{D}{2} \right) \right] [\tanh mkd] \left[\coth k\left(md - \frac{D}{4} \right) \right]^2 \right\}.$$

By our agreement, the effect of the m^{th} pair on the potential difference is

$$(V_7 - V_8)_m = (V_7 - 8) + (V_9 - V_8) = V_7 + V_9 - 2V_8$$

$$= -(-1)^m 2\lambda \log_e \left\{ \frac{[\tanh mkd]\left[\tanh k\left(md + \frac{D}{2}\right)\right]\left[\coth k\left(md + \frac{D}{4}\right)\right]^2 \left[\tanh k\left(md - \frac{D}{2}\right)\right][\tanh mkd]\left[\coth k\left(md - \frac{D}{4}\right)\right]^2}{\left[\tanh k\left(md - \frac{D}{4}\right)\right]^2 \left[\tanh k\left(md + \frac{D}{4}\right)\right]^2 [\coth mkd]^4} \right\}$$

$$= -(-1)^m 2\lambda \log_e \left\{ [\tanh mkd]^6 \left[\tanh k\left(md + \frac{D}{2}\right)\right]\left[\coth k\left(md + \frac{D}{4}\right)\right]^4 \left[\tanh k\left(md - \frac{D}{2}\right)\right]\left[\coth k\left(md - \frac{D}{4}\right)\right]^4 \right\}$$

which by hyperbolic transformations reduces to

$$(V_7 - V_8)_m = -(-1)^m 2\lambda \log_e \left\{ \left[\frac{1 - \left(\dfrac{\sinh \frac{kD}{2}}{\sinh mkd} \right)^2}{1 + \left(\dfrac{\sinh \frac{kD}{2}}{\cosh mkd} \right)^2} \right] \left[\frac{1 + \left(\dfrac{\sinh \frac{kD}{4}}{\cosh mkd} \right)^2}{1 - \left(\dfrac{\sinh \frac{kD}{4}}{\sinh mkd} \right)^2} \right]^4 \right\}$$

so that the final result for the characteristic impedance is

$$Z_0 = 207 \left\{ \log_{10} \left[\frac{2h \tanh \frac{\pi D}{2h}}{\pi a \left[1 + \operatorname{sech} \frac{\pi D}{2h} \right]^{4/3}} \right] - \frac{2}{3} \sum_{m=1}^{\infty} (-1)^m \log_{10} \left[\frac{1 - \left(\dfrac{\sinh \frac{\pi D}{2h}}{\sinh \frac{m\pi w}{2h}} \right)^2}{1 + \left(\dfrac{\sinh \frac{\pi D}{2h}}{\cosh \frac{m\pi w}{2h}} \right)^2} \right] \left[\frac{1 + \left(\dfrac{\sinh \frac{\pi D}{4h}}{\cosh \frac{m\pi w}{2h}} \right)^2}{1 - \left(\dfrac{\sinh \frac{\pi D}{4h}}{\sinh \frac{m\pi w}{2h}} \right)^2} \right]^4 \right\} \tag{22}$$

for the configuration of Fig. 9(b).

Concentric Line with Circular Inner Conductor and Square Outer Conductor

In Fig. 9(a), a vertical plane that divides the configuration into its two mirror-image halves is an equipotential of potential zero. Accordingly, if we replace half the configuration by a plane conductor in this neutral plane and set $D=h$, $w=2h$, we get the configuration of Fig. 9(c), for which we have, from (17),

$$Z_0 = 138\left\{\log_{10}\frac{2h\tanh\frac{\pi}{2}}{\pi a} - \sum_{m=1}^{\infty}\log_{10}\left[\frac{1+\left(\frac{\sinh\frac{\pi}{2}}{\cosh m\pi}\right)}{1-\left(\frac{\sinh\frac{\pi}{2}}{\sinh m\pi}\right)^2}\right]\right\}. \tag{23}$$

If d is the inner diameter of the outer conductor and a is the outer radius of the inner conductor of the conventional concentric circular transmission line, then

$$Z_0 = 138\log_{10}\frac{d}{2a}. \tag{24}$$

Equations (23 and (24) are equal if

$$d = 1.079h. \tag{25}$$

For the same characteristic impedance the diameter of the circular conductor exceeds the side of the square conductor by only 7.9 per cent.

Water and Forced-Air Cooling of Vacuum Tubes*

Nonelectronic Problems in Electronic Tubes

I. E. MOUROMTSEFF†, ASSOCIATE, I.R.E.

Summary—*General laws of heat transfer from a hot wall to a moving fluid are applied to water and forced-air cooling of vacuum tubes. The calculated data are compared with experimental results. The practical importance of various factors constituting the mechanism of heat transfer is analyzed; the role of the internal structure of the tube on the dissipation limits is discussed generally. Rules for designing finned air coolers are outlined, and the "optimum" design is discussed. Numerical examples are given. Some limiting factors in cooler design are analyzed.*

WITHOUT exaggeration one may state that in designing electronic tubes there are many more mechanical, metallurgical, and heat engineering problems than those of pure electronic character. One may also admit that quite frequently nonelectronic problems are solved by the cut-and-try method rather than by calculation. One of such questions is the anode cooling; in spite of the fact that water cooling of vacuum tubes has found enormous application since 1923, even now there is no complete agreement among individual experimenters regarding diverse factors involved in efficient cooling of the tubes. In this paper an attempt is made to give a common basis for analyzing and comparing practical results obtained by various experimenters. This is done by simply applying to our specific case data long since known in heat engineering.

* Decimal classification: R139. Original manuscript received by the Institute, January 24, 1941; revised manuscript received, November 6, 1941. Presented, Fifteenth Annual Convention, Boston, Massachusetts, June 28, 1940.

† Westinghouse Electric and Manufacturing Company, Bloomfield, New Jersey.

PART I—WATER COOLING

Generally speaking, the efficiency of cooling of a hot wall by moving fluid depends on the physical constants of the fluid, its velocity, and the dimensions of the cooling arrangement. In vacuum tubes with external anodes, cooling also depends,—in a degree not to be neglected,—on the anode wall thickness and the internal tube structure, as these parameters determine patterns of heat distribution throughout the anode. Heat generated on the inside surface of the anode flows through its walls, is transferred to the moving liquid and carried by it away from the tube. From heat engineering it is known that all factors constituting the mechanism of *heat transfer* from the wall to the liquid are connected by the following relation:[1]

$$\left(\frac{hD}{k}\right) = 0.024\left(\frac{D\rho V}{\mu}\right)^{0.8} \times \left(\frac{C_p\mu}{k}\right)^{0.4}. \tag{1}$$

If the individual factors are measured in any consistent system of units, the three parenthetic expressions in this equation are dimensionless. In our discussion centimeter-gram-second units are used, therefore the meaning of the symbols is as follows:

h = rate of heat transfer in calories per second per square centimeter per degree centigrade

[1] William H. Adams, "Heat Engineering," McGraw-Hill Book Company, Inc., New York, N. Y., and London, England, 1933, p. 165.

k = thermal conductivity of fluid in calories per second per centimeter per degree centigrade
ρ = density of fluid in grams per cubic centimeter
μ = viscosity of fluid in grams per centimeter second (poises)
C_p = specific heat of fluid in calories per gram per degree centigrade
V = average velocity of the fluid in centimeters per second
D = equivalent diameter of the cross section of the fluid channel in centimeters

If h is known, the total anode dissipation can be represented as the product of three quantities.

$$P_h = S\,T_a\,h \text{ calories per second} = 4.2\,S\,T_a\,h \text{ watts} \qquad (2)$$

where S is the total heated area of the anode and T_a is the anode temperature above that of the cooling water

It is important to point out that (1) is applicable only to cases of "turbulent" flow in contradistinction

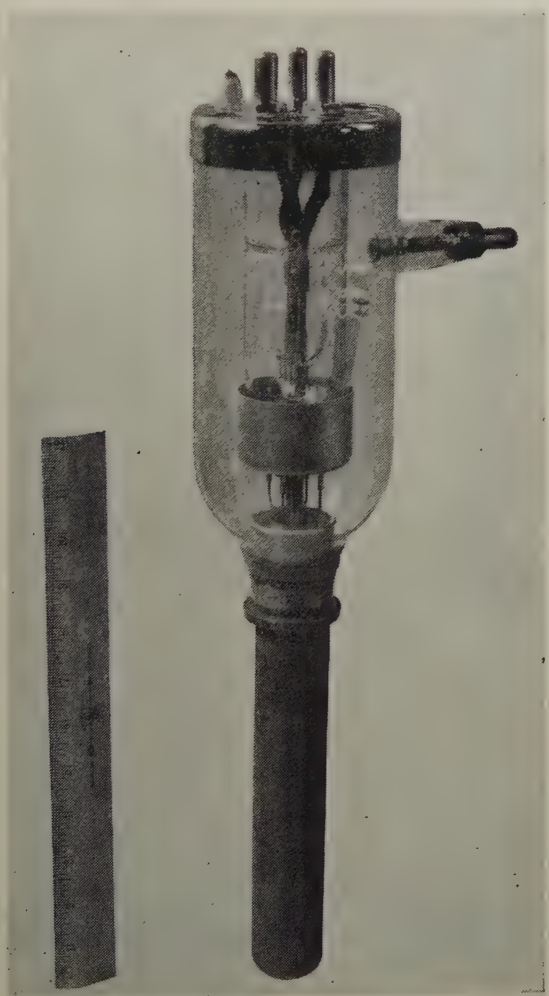

Fig. 1—Type 891 water-cooled tube.

to the "parallel," "laminar," or "viscous" flow. In each individual case one can decide whether the flow is turbulent or viscous either by direct observation on the transparent model of the jacket, or by using the well-known criterion, the so-called, *Reynolds* number given by

$$Re = \frac{D\rho V}{\mu}. \qquad (3)$$

One can notice at once that Re is nothing else but the second dimensionless member in (1). About 60 years ago Osborn Reynolds established the fact that with

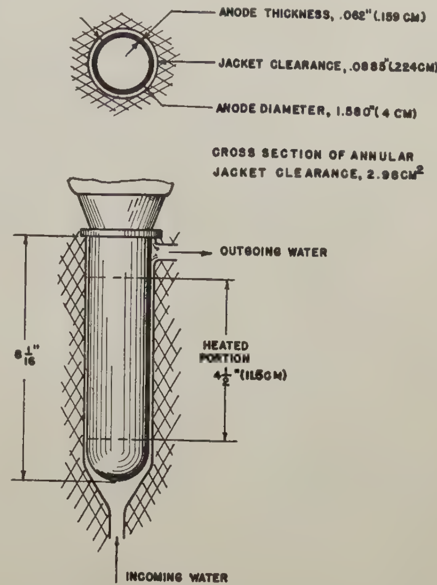

Fig. 2—Anode dimensions.

Re smaller than 2100 the flow is always viscous; with Re greater than 4000 it is turbulent. With intermediate values of Re the flow is unstable and may change from turbulent to viscous and *vice versa*. This law holds for any fluid and it has been repeatedly verified by many experimenters.

In order to obtain a clearer picture of the amount of cooling that can be achieved on vacuum tubes, and also in order to study the role of the individual factors involved in the cooling mechanism, we shall apply (1) to the well-known 891 or similar types of water-cooled tubes regarding which numerous experimental data are available.

The general view of this tube is represented in Fig. 1; the principal dimensions of its anode and standard jacket are given in Fig. 2. The recommended rate of water flow is from 3 to 8 gallons per minute, and the safe plate dissipation with 4 gallons per minute, and a uniform heat distribution (such as is approximately realized in class C operation) is 10 kilowatts; to this, 1320 watts necessary for lighting the filament must be added. Experimentally, it has been found that under the specified conditions the water just begins to "hiss."[2,3] Direct observation through a glass water jacket shows that at this point minute steam bubbles are formed at the anode surface and are carried away by the water.

[2] I. E. Mouromtseff and H. N. Kozanowski, "Comparative analysis of water-cooled tubes as class B audio amplifiers," Proc. I. R. E., vol. 23, pp. 1246–1248; October, 1935.
[3] I. E. Mouromtseff and H. N. Kozanowski, "Analysis of operation of vacuum tubes as class C amplifiers," Proc. I. R. E., vol. 23, pp. 769–771; July, 1935.

In the following, by using (1) on the chosen example, we shall calculate h, the rate of heat transfer from the anode wall to the cooling water. However, in order to justify the application of (1) we must first check whether the flow under the specified conditions is turbulent. The two physical constants affecting the Reynolds number are water density ρ and viscosity μ; both vary with temperature. We assume that the initial water temperature is, $t_i = 25$ degrees centigrade; then, from the rate of water flow, 4 gallons per minute (254 cubic centimeters per second), and the figure of dissipated power, 11.3 kilowatts, we shall determine that the outgoing water will have temperature $t_e = 37.5$ degrees centigrade. Hence, the average water temperature $t_{\text{ave}} = 31$ degrees centigrade. From physical tables it is found that at this temperature

$$\rho = 0.996 \text{ gram per cubic centimeter}$$
$$\mu = 0.0078 \text{ poise (gram per centimeter second)}. \quad (4)$$

Water velocity calculated by division of the rate of flow, 254 cubic centimeters per second over the cross-section area of the flow, 2.98 square centimeters, is

$$V = 85 \text{ centimeters per second.} \quad (5)$$

Finally, the equivalent diameter of the annular clearance between the anode and the jacket (Fig. 2), calculated as explained below, is

$$D_e = 0.45 \text{ centimeter.} \quad (6)$$

Using the numerical data one arrives at the Reynolds number

$$Re = 0.45 \times 85/0.778 \times 10^{-2} = 4940. \quad (7)$$

Hence, the flow is turbulent, and therefore (1) is applicable to the case under investigation.

As to the diameter D_e, by definition[4], it is equal to four times the *hydraulic radius* of the cross-sectional area of water flow, the hydraulic radius being defined as the ratio between the area and the wetted perimeter of the cross section. In the particular case of the annular cross section, the equivalent diameter is equal to the difference of the jacket and the anode diameters, or to twice the spacing between the jacket and the anode, $2\epsilon = 0.45$ centimeter.

In order to find the numerical value of the rate of heat transfer, in addition to the already determined quantities, one must know heat conductivity k and specific heat of water C_p. From physical tables we have

$$k = 0.00145 \text{ calorie per centimeter second per degree centigrade}$$
$$C_p = 1 \text{ calorie per gram per degree centigrade.} \quad (8)$$

Inserting (4) to (8) into (1) we finally obtain

$$h = 0.1355 \text{ calorie per second per square centimeter per degree centigrade.} \quad (9)$$

[4] William H. Adams, see pp. 117 and 235 of footnote 1.

This is the rate of heat transfer from anode to water in the case under discussion; more generally, the calculated figure also shows the order of magnitude of heat transfer per unit area (1 square centimeter) of water-cooled anodes under more or less conventional conditions. When h and the total heated area of the anodes are known, one can calculate the anode temperature simply by using (2). In discussions similar to ours, it is generally more convenient for various theoretical derivations to consider a 1-centimeter long anode zone. From the total power of anode dissipation and the length of its "hot" portion we find that dissipation per unit length of anode is[5]

$$m = 11{,}320/4.2 \times (11.5 + 1.24)$$
$$= 212 \text{ calories per second} \quad (10)$$

where 0.62 centimeter is added on each end of the filament length to take care of the cooling effect of the anode ends; this will be explained in some later part of the paper. On the other hand, the amount of heat transferred to water within the same zone is

$$e = h \times \pi d = 0.1355 \times 4\pi$$
$$= 1.7 \text{ calories per second per degree centigrade.} \quad (11)$$

In the state of equilibrium the relation exists

$$m = eT_a. \quad (12)$$

Therefore,

$$T_a = 212/1.7 = 124.5 \text{ degrees centigrade.} \quad (13)$$

and the actual anode temperature above freezing point is

$$T_{0a} = 124.5 + 31 = 155 \text{ degrees centigrade.} \quad (14)$$

This is considerably in excess of the boiling temperature of water. Some direct measurements made by various experimenters[6] confirm that the anode temperature at sufficiently high dissipation is above the boiling point. Still, on first thought it seems to be somewhat puzzling how water can be in contact with such a hot surface and not boil. The explanation is to be looked for in the following facts: First, practical measurements of permissible tube dissipation are usually carried out with the anode insulated from the ground by "water coils" both on the inlet and outlet sides. These coils are made of rather long pieces of rubber hose and incur considerable pressure drop when water is flowing; actually from 20 to 60 pounds water pressure is usually required to pass water at the recommended rate through vacuum tubes. Thus, the pressure inside the jacket, which is in series with the two coils and between them, may be as high as 30 pounds and more. The boiling point at this condition reaches the

[5] In this expression, the factor 1/4.2 converts watts into calories per second.

[6] R. LeRossignal and E. W. Hall, "The development of large radio transmitting valves," *Gen. Elec. Co. Jour.* (British), vol. 7, p. 185; August, 1936.

value of 135 degrees centigrade or more. Second, "spheroidal" state of water probably precedes the outright boiling. Cold water coming in contact with a hot surface forms an extremely thin film of superheated steam at the surface so that there may be no direct contact between the water and the anode wall; this film is continuously destroyed and renewed due to turbulency of flow. An increase in heat flow above the "safe limit" results in more energetic formation of steam bubbles, that is, in *boiling*, which frequently can be accompanied by mechanical vibration of the hose and even of the tube itself. It is considered undesirable to permit water to boil as this usually results in scale formation and finally anode puncture due to its local overheating.

Now, we shall more closely discuss the effect of variation of the individual factors appearing in (1) and the limitation imposed by them.

Water Velocity

The most important factor in (1) is water velocity V, because in practice it is the only factor which can be varied by the operator at will and varied within rather wide limits. In our example the recommended water-flow limits are from 3 to 8 gallons per minute. Accordingly, the heat-transfer figure theoretically can be varied from

$$h_3 = h_4(3/4)^{0.8} = 0.108 \text{ calorie per second per square centimeter per degree centigrade} \quad (15)$$

to

$$h_8 = h_4(8/4)^{0.8} = 0.235 \text{ calorie per second per square centimeter per degree centigrade} \quad (16)$$

hence, permissible dissipation should vary in the same ratio as heat-transfer figures, that is, proportionately to $h_3:h_4$ and $h_8:h_4$. So, for 3- and 8-gallon-per-minute rate of water flow the dissipation limit will be 8 and 16 kilowatts, respectively. However, if one looks into the published technical data of the tube, one will find that there is no practical need in dissipation higher than approximately 10 kilowatts because other limitations (in voltage, electronic emission) make it useless. Yet higher rates of water flow are necesssary because in a great majority of cases of operation heat distribution in the anode is nonuniform. Then, as is demonstrated elsewhere,[7] dissipation limit may vary in proportion only to 0.4th power of water velocity instead of 0.8th as implied by (1). This will be discussed later on in connection with the effect of tube structural parameters.

In this place, it may be repeated that the immediate effect of an increase of water velocity is the intensification of *turbulency* of flow; a more turbulent flow makes a greater inroad into the thin stationary film of water (or steam) ever present at the anode wall, and thus increases heat exchange between the wall and the water. The existence of slowly moving or stationary layers of liquid in the vicinity to the wall even in a turbulent flow has been established by direct measurements by many experimenters.[8]

It is obvious that turbulency of the flow can increase not only due to increased water velocity but also due to the formation of steam bubbles. Therefore, the higher the anode temperature, the greater is the rate of heat transfer. However, for the reasons given before it is not desirable to carry this too far and to permit water to boil. It is also logical to admit that the turbulency of flow can be also intensified by properly designed baffling surfaces built in the path of the water, or by other "mechanical" means.

Clearance Between Anode and Jacket

With a fixed rate of water flow Q_a cubic centimeters per second, variation of the annular clearance ϵ between the anode and the jacket affects two factors: velocity of water V and the equivalent diameter D_e. Each of these factors independently affects turbulency as may be seen from (3). However, for a given anode size the Reynolds number is practically independent of the width of clearance (if clearance is generally small compared to the anode diameter d_a). Indeed, water velocity increases with decreasing clearance practically in inverse proportion, while the equivalent diameter of the annular cross section decreases in direct proportion to it; hence, the net effect is almost nil. In our numerical example $\epsilon = 0.0885$ inch and the Reynolds number, $Re = 4940$. One can show that even with an infinitesimal spacing (ϵ = nearly 0) the Reynolds number will increase only slightly. In this limiting case

$$Re_0 = 2\epsilon Q_a/\epsilon\pi d_a\mu = \frac{2 \times 254}{\pi \times 4 \times 0.0078} = 5200. \quad (17)$$

In other words, with a large or a small clearance, turbulency stays the same if the number of gallons per minute is maintained the same. This, however, does not mean that the heat transfer h remains the same. By combining similar factors of different dimensionless groups in (1) one will find that h is proportional to the 0.8th power of velocity and inversely proportional to $D^{0.2}$. Hence, for smaller clearance heat transfer becomes larger, mainly, due to an increased velocity. Experiments show that improvement in cooling does not quite follow the expected law, when the clearance becomes very small. In fact, it has been found that for each particular set of operating conditions there is an optimum value of clearance ϵ, such that either for larger or smaller clearances the efficiency of cooling drops. The experiments on a standard tube with a $1\frac{1}{2}$-inch anode showed that the optimum clearance varied from 0.020 to 0.015 inch depending on the rate of water flow. Of course, in ordinary designs of water-cooled

[7] I. E. Mouromtseff, "The influence of grid focusing effect on plate dissipation limit of a vacuum tube," *Communications*, vol. 20, p. 11; December, 1938.

[8] William H. Adams, see p. 106 of footnote 1.

tubes these extremely small clearances can be considered as impracticable. The reason for existence of the optimum clearance must be looked for in the fact, mentioned previously, of existence of almost stationary films of liquid at the walls. When the thickness of the water wall becomes comparable with the thickness of these stagnant films the turbulency decreases and the flow may even become laminar, in spite of a higher velocity.

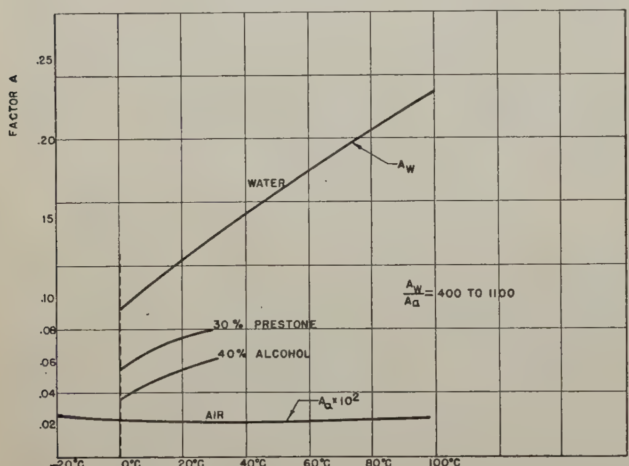

Fig. 3—Factor A versus fluid temperature.

Factor A shows combined effect of physical constants on rate of heat transfer

$$h = 0.024\frac{v^{0.8}}{d^{0.2}} \cdot \frac{\rho^{0.8}k^{0.6}c^{0.4}}{\mu^{0.4}} = 0.024\frac{v^{0.8}}{d^{0.2}}\ A \text{ cal/sec} \cdot \text{cm}^2/^\circ\text{c}$$

Physical Constants of Liquid

From the four constants appearing in (1), water density ρ and specific heat C_p can be considered practically independent of water temperature; either of these constants is equal to unity. The other two constants, heat conductivity k and viscosity μ, vary with temperature. Their over-all effect on rate of heat transfer is shown in Fig. 3, upper curve.

In order to illustrate the discussed relation better, we shall assume that with the same power dissipation, 11,320 watts, the temperature of the incoming water is 7 degrees centigrade. The values of k and μ to be used in (1) are

$$k = 0.00136 \text{ calorie per centimeter per second per degree centigrade.}$$

$$\mu = 0.0124 \text{ poise.} \tag{18}$$

The calculated heat-transfer figure is, then

$$h = 0.1075 \text{ calorie per second per square centimeter per degree centigrade} \tag{19}$$

and the anode temperature

$$T_a = 169 \text{ degrees centigrade.} \tag{20}$$

Thus, we arrive at an apparent paradox: in spite of much colder water (7 instead of 25 degrees centigrade) the anode temperature is higher by 14 degrees centigrade. Moreover, due to an increased viscosity, the Reynolds number in the case of the 7-degree-centigrade water becomes practically nonturbulent. This will cause a further reduction in the rate of heat transfer. No wonder that in this condition water at the anode surface may start boiling, and one will be forced to limit the permissible dissipation.

In addition to the temperature sensitivity, viscosity of water may also vary with pressure; and since the pressure in the water jacket may vary from case to case to a considerable degree, the cooling effect may be somewhat different in spite of the apparent similarity of other conditions in various experiments.

The role of the physical constants becomes particularly important if one decides to use liquids other than water, for example, transformer oil, kerosene, or one of the known antifreeze solutions. This may be warranted by superior insulating properties of oils, or by the necessity to install a transmitter in a room without heating. Table I gives constants for the two most popular antifreeze liquids, prestone and alcohol. From the table one can see that except for density of prestone the constants of both solutions differ from those of water so that all of them tend to reduce the rate of heat transfer. Particularly important is viscosity which with solutions with medium content of antifreeze is from 2 to 3 times higher than with water. This means that in order to have the same turbulence as with water the rate of the flow must be doubled or trebled.

TABLE I
Physical Constants of Cooling Liquids

	Mixture %	Boiling Point °C	Freezing Point °C	Density			Viscosity			Specific Heat, C_p			Heat Conductivity, k		
				30°C	10°C gm/cm³	0°C	30°C	10°C centipoises	0°C	30°C	10°C cal/gm/1°C	0°C	30°C	10°C cal/sec/cm/1°C	0°C
Water	100	100	0	1	1	1	0.8	1.35	1.8	1.0	1.0	1.0	0.00145	0.00138	0.00132
Prestone	10	101	−4	1.010	1.014	1.016	1.0	1.75	2.5	0.99	0.99	0.99			
	30	102	−16	1.034	1.042	1.046	1.75	3.1	4.5	0.90	0.88	0.87	(0.001)		
	50	106	−37	1.058	1.07	1.075	3.0	5.5	8.0	0.83	0.79	0.79			0.000635
Alcohol	10	93.5	−5	0.979	0.984		1.16	2.18	3.31	1.0	1.0	1.0	0.00130	0.00122	0.00116
	40	83.5	−29	0.928	0.942		2.02	4.39	7.14	0.92	0.91	0.90	0.00093	0.00088	0.000.85
	100	80		0.78	0.80	0.81	1.00	1.47	1.77	0.64	0.60	0.54	0.000433	0.000433	0.00433

If necessary to choose from the two solutions, prestone must be preferred as alcohol easily evaporates at comparatively low temperatures, and its constants are summarily less favorable for heat transfer than those of prestone. The over-all effect of prestone and alcohol for low temperatures is plotted in Fig. 3.

The physical constants of oils, generally speaking, are also such that the heat-transfer figure for oils is less than for water. Therefore with the same dissipation the anode temperature is always higher for oil than for water. With the temperature approaching 200 degrees centigrade oil begins to "sludge"; this contaminates the anode surface and consequently the rate of heat transfer drops markedly from its initial value. Nevertheless, oils possess one indispensable advantage, high insulating property which makes long insulating water coils unnecessary. Therefore, in cases when dissipation is not too high, or where perfect insulation is of prime importance (as for example in X-ray tubes), oil cooling may become justifiable. One of the best liquids of this kind seems to be kerosene.

The Role of the Vacuum-Tube Structure

If the anode of a vacuum tube is heated perfectly uniformly, the anode diameter d and the cathode length L are the only structural parameters determining the dissipation limit. If the permissible maximum temperature is $T_{\max}$, the dissipation limit is

$$P_0 = \pi d\, L\, h\, T_{\max} \tag{21}$$

where h is heat-transfer figure to be calculated from (1) and $T_{\max}$ is the anode temperature above that of the cooling water. However, it is known that due to the focusing effect of the grid in many cases of operation heat is generated in the anode nonuniformly; heat patterns depend on grid meshes and on the location of individual filament strands with respect to the grid stays. As a result, the average anode temperature T_{ave}, cannot be allowed to reach the permissible maximum; hence, the anode dissipation limit becomes less than with a uniform heat distribution. Usually closely spaced grid windings of thin wire affects but very little the temperature distribution; the entire blame for nonuniformity is to be put on the heavy longitudinal grid stays. It has been shown[9] that in the typical case of electron beams concentrated along the mid-line between the shadows of adjacent grid stays (points A, B, C, D in Fig. 4) the average anode temperature is given by the expression

$$T_{\text{ave}} = T_{\max}(\tanh Q)/Q. \tag{22}$$

The temperature $T_{\max}$ prevails at the points, A, B, C, and D, where heat is generated by impinging electrons; quantity Q depends on heat-transfer figure h and the tube structural parameters in the following way:

$$Q = \sqrt{h/\delta\, k} \times \pi d/2n. \tag{23}$$

[9] I. E. Mouromtseff, see p. 12 of footnote 7.

Here d = anode diameter (4 centimeters)
δ = anode wall thickness (0.159 centimeter = 1/16 inch)
n = number of grid stays (4)
k = heat conductivity of copper (0.9 calorie per centimeter per second per degree centigrade)
h = heat-transfer figure (0.1355 calorie per square centimeter per second per degree centigrade)

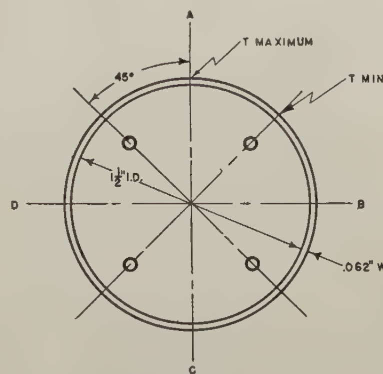

Fig. 4—Focusing effect of grid stays in the 891 tube.

Accordingly, if there is grid focusing effect, the anode dissipation limit will be reduced in proportion to

$$T_{\text{ave}}/T_{\max} = (\tanh Q)/Q. \tag{24}$$

Using numerical values in parenthesis, which are the figures of our practical example of the 891 tube, one will find that

$$Q = 1.53 \quad \text{and} \quad \tanh Q = 0.91 \tag{25}$$

here

$$\tanh Q/Q = 0.595. \tag{26}$$

This means that because of the grid focusing effect the permissible plate dissipation is to be reduced by 40.5 per cent. The reduction can be even greater if the filament strands are not symmetrically located with respect to the grid "windows."

Close examination of (22) and (23) reveals that variation of any factor in (23) should effect a simultaneous increase or decrease of both the numerator and denominator of (22). However, the hyperbolic tangent of a function changes more slowly than the function itself. Therefore, the net change of T_f/T_{ave} is governed by the variation of quantity Q in the denominator. This is especially true if the value of tanh Q is nearly unity (which is the case in our example). Thus, one may rule that in order to decrease the nonuniformity of temperature distribution resulting from the grid focusing effect one has to increase either the anode wall thickness δ or the number of grid stays n. The latter statement must be supplemented by the consideration of the cathode structure; it must be disposed of in such a manner that all grid "windows" are uniformly utilized by the electrons. In addition, one may also note that the larger the anode diameter, the greater is

temperature nonuniformity with the same number of grid stays. As to the effect of heat-transfer figure h, one arrives at the conclusion that its increase amplifies the nonuniformity of temperature distribution; and, since in a given arrangement one can change h by changing water velocity, one must realize that the faster the water is passed through the tube the more pronounced are heat spots on the anode. Nevertheless, in spite of this the *total* power dissipation increases generally with the rate of water flow. This follows from the expression for total heat dissipation

$$P_f \text{ total} = \pi d\, l\, h\, T_{\text{ave}} \tag{27}$$

or

$$P_f \text{ total} = 2n\sqrt{h\delta k}\, \tanh\left(\sqrt{h/\delta\, k} \times \pi d/2n\right). \tag{27a}$$

With water-cooled tubes of conventional designs the hyperbolic tangent in this expression, as already mentioned, is usually very close to unity; therefore the dissipation limit in operation with pronounced grid focusing effect increases proportionally to the square root of the heat-transfer figure, or proportionally to the 0.4th power of water velocity V.

In connection with (21) and (10) the question may be asked: "Is the length of the anode hot portion exactly equal to that of the filament structure, or is it longer due to the heat spreading throughout the 'cold ends'?" A theoretical treatment of this problem is given elsewhere;[10] in application to our numerical example it can be shown that the contribution of the cold ends is equivalent to an increase of the heated portion by approximately 0.6 centimeter at each end.

PART II—FORCED-AIR COOLING

Introductory Notes

In recent years, approximately since 1935, water-cooled tubes in a number of new transmitters built in this country and, later on, in Europe were supplanted by tubes with forced-air cooling. Air-cooled tubes can be advantageously used in all cases when there is a danger of ambient temperature dropping below the freezing point. In some other cases they can be furnished with inexpensive individual blowers, thus eliminating the necessity of water piping and of the use of water coils insulating the high-voltage water-cooled anodes from the ground.

Air cooling, the same as water cooling, is not a new engineering problem; yet its application to high-power vacuum tubes is a new and sufficiently specific problem to warrant its careful study both theoretically and experimentally in order to establish general rules for the systematic design of air coolers. The problem of designing an efficient air cooler for a given type of vacuum tube with an external anode may be formulated in several different ways. Thus, one may wish to design a cooler of the smallest mechanical dimensions for a definite maximum power dissipation. Or *vice versa*, one may start with the largest permissible diameter of a cooler and calculate the feasible maximum dissipation. One may also need a cooler representing not more than a certain specified resistance pressure, in order to employ a distinct type of air blower available on the market. In the case of a portable air cooler its weight becomes an important factor. Finally, the cost of the individual coolers may influence the choice of the design. One should note that in all cases the maximum permissible anode temperature is a critical factor, as it directly affects the dissipation ratings. However, this temperature cannot be specified once and forever and for all designs, because it depends on physical properties of materials involved in the design and on the degree of outgassing vacuum-tube parts. Obviously, there is no single solution of the postulated problem in general, but for each particular set of requirements one can find the best answer or an optimum design for the cooler.

It may be of interest to mention that as far back as 1931 an air-cooling jacket for the 863 tube (closely resembling the 891), was designed and tested at East Pittsburgh; it was intended for a 5-kilowatt transmitter. This project is interesting because the air cooler formed a part of the transmitter equipment, and the tube could be replaced in it as in an ordinary water jacket. In a few words, this air jacket can be described as follows: It was machined from a $3\frac{1}{2}$-inch aluminum bar; its total weight was less than 4 pounds. The central bore was drilled to fit the $1\frac{1}{2}$-inch tube anode. A number of longitudinal slots was milled on the outside of the cylindrical bar. Due to a longitudinal cut, the jacket could be easily brought about and clamped tightly around the anode. Cooling air was supplied at a rate of 90 cubic feet per minute from the source of about 0.4 pound pressure. The described jacket permitted approximately 2.5 kilowatts total anode dissipation with the anode temperature at about 160 degrees centigrade. For protection from oxidation the anode of the tube was gold-plated. The device did not find much practical application as the transmitter designers needed greater anode dissipation if forced-air cooling had to compete with water cooling.

In this part of the paper general principles of designing air coolers are, first, outlined; then, the principles are applied to the calculation of a cooler for one of the popular types of tubes; finally, various factors influencing cooler designs are discussed.

General Principles

A conventional air cooler consists of a core with a central bore for the tube and of a set of vertical fins extending in radial direction and secured to the outer surfaces of the core. All parts are usually made of copper because of its good thermal conductivity. A general view of an 891 tube soldered in an air cooler is

[10] I. E. Mouromtseff, "Temperature distribution in vacuum tube coolers with forced air cooling," *Jour. Appl. Phys.*, vol. 12, pp. 491–497; June, 1941.

shown in Fig. 5; its horizontal and vertical cross sections are schematically represented in Fig. 6.

Generally speaking, the amount of power dissipation by a cooler P_h is proportional to each of the following three factors:

1. Average temperature difference between fins and air, $T^0_{f\,ave}$.
2. Rate of heat transfer from copper to air, h calories per second per square centimeter per degree centigrade.
3. Total area of the cooling surface, S square centimeters.

In short, the power dissipated is

$$P_h = T_{f\,ave} \times h \times S \text{ calories per second.} \tag{28}$$

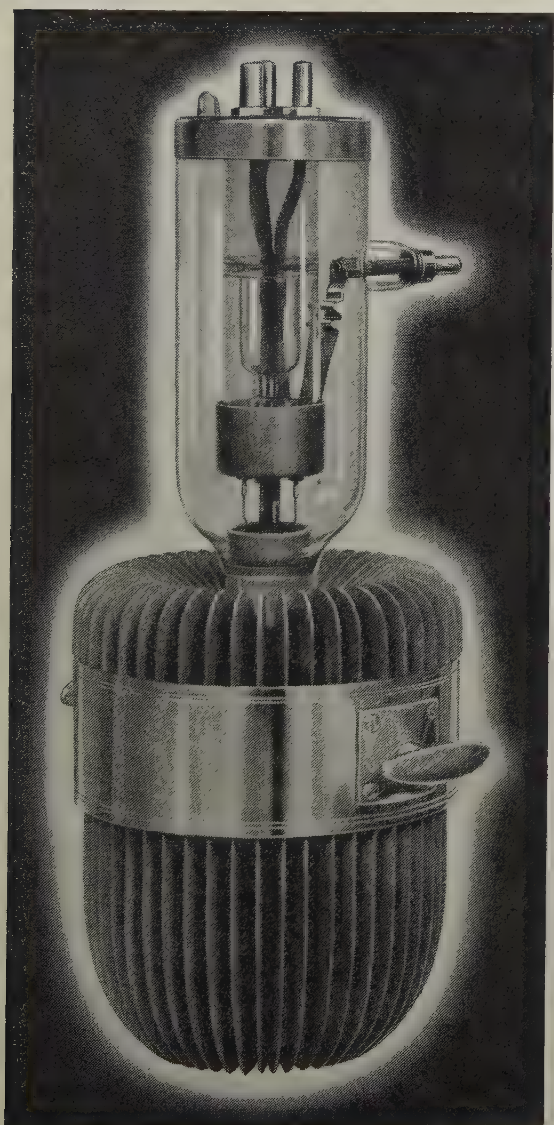

Fig. 5—Type 891 tube adapted for air cooling.

For a given ambient temperature t_a, the largest possible value of fin temperature $T_{f\,ave}$ is restricted by the maximum permissible anode temperature $T_{a\,max}$, the major part of which is constituted by fin temperature. The *actual* anode temperature in operation establishes itself as function of the power dissipated in the cooler. It can be computed by summing up individual temperature differences in the path of heat flow from the tube to the cooling air; to this sum the ambient temperature must, of course, be added. Obviously, at no time and at no place can the actual anode temperature be permitted to exceed the safe maximum anode temperature $T_{a\,max}$. As such, one can designate 20 or 30 degrees centigrade below the dangerous temperature at which either the solder bond between the tube and

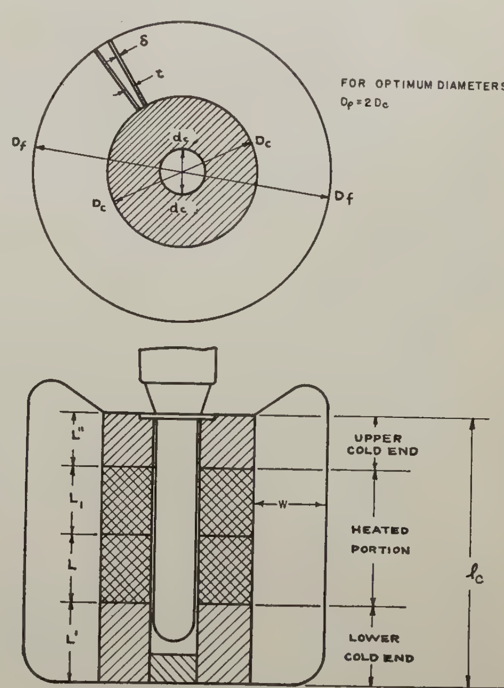

Fig. 6—Optimum design of 891R and similar air coolers.

the cooler can be weakened, or the vacuum inside the tube becomes affected by gas liberated from overheated tube parts. Thus for example, with pure tin solder, 160 degrees centigrade can be specified as $T_{a\,max}$, because at 180 degrees centigrade tin begins to soften; if heated to this level even occasionally, the solder finally melts at some points and causes a puncture of the anode wall. With normally exhausted tubes it appears safe to adopt 230 degrees centigrade as the anode temperature limit; in such cases, of course, a solder with a higher melting point has to be used; cadmium proved to be very satisfactory for this purpose.

The second factor in (28), *the rate of heat transfer* h can be calculated from the expression similar to (1), in which physical constants for water are substituted for by similar constants for air

$$h = 0.024 \frac{k}{D}\left(\frac{D\rho V}{\mu}\right)^{0.8}\left(\frac{C_p\mu}{k}\right)^{0.4}. \tag{29}$$

By inspection of this expression one may conclude that the only factor in the designer's hands for controlling the rate of heat transfer is air velocity. The higher the velocity the more efficient is the cooling. Its upper limit may be set either by an objectionable whistling noise produced by air escaping from the ducts, or, more

likely, by a rapidly increasing pressure required to force the air through the cooler; this pressure increases as the square of velocity. An excessive pressure may preclude the use of certain types of good commercial blowers available on the market. In addition, power required for driving the blower increases proportionally to the cube of the air velocity. One may assume that 3000 centimeters per second (6000 feet per minute) is the highest velocity to be recommended for practical applications.

Equivalent diameter of the ducts D in (29) is calculated as four times the ratio of the duct cross-sectional area to its perimeter. Its variation from cooler to cooler has not much influence on the rate of heat transfer as it enters in (29) only with an exponent of 0.2.

Individual physical constants appearing in the same equation vary with air temperature. However, if grouped together, they form a factor whose value remains almost constant within a wide range of temperatures. This factor A_a is plotted in Fig. 3 as a function of air temperature; it rises slightly toward the freezing point; otherwise for all practical cases it can be assumed approximately 0.0215×10^{-2}, so that (29) in applications to air can be modified as follows:

$$h = 0.024 \frac{V^{0.8}}{D^{0.2}} A = 5.15 \times 10^{-6} \frac{V^{0.8}}{D^{0.2}} \cdot \qquad (30)$$

Note: The dimension of the factor A is colories per second$^{0.2}$ per centimeter$^{2.6}$ per degree centigrade.

As in most of the practical designs, $D^{0.2}$ is not too much different from unity; the later formula can be simplified still further to read

$$h = 5.15 \times 10^{-6} V^{0.8}. \qquad (31)$$

As to the third factor in (28), the total cooling area of fins S is one of the important factors determining the merits of a cooler design. The larger it is the better. However, once the size of the cooler is chosen, there is a definite maximum cooling area inherent in the design: it depends on mechanical limitations of the cooler structure. These are the minimum fin thickness δ and the minimum spacing t between the fins at their root, that is, at the core surface. Thus, independent of the general design of the cooler, the smallest *fin pitch* around the periphery of the core is $(\delta + t)$; therefore, with the core diameter D_c the largest feasible number of fins is

$$n_{\max} = \pi D_c / (\delta + t). \qquad (32)$$

If, then, D_f is the cooler diameter, the total cooling area of the fins is

$$S = 2(D_f - D_c) \times \pi l D_c / (\delta + t). \qquad (33)$$

Since the fin length is usually fixed by the tube length l, the feasible maximum of S can be found from

$$\frac{\partial S}{\partial D_c} = 0. \qquad (34)$$

Solution of this equation gives

$$D_c = D_f / 2. \qquad (35)$$

This holds for any fixed figure of fin pitch. As to the role of the over-all cooler diameter D_f it may be concluded *a priori* that the larger the diameter, the more power can be taken care of by the cooler, all other conditions being equal. However, at the end of this section we shall more closely enter upon the optimum radial extension of fins. One may generally note that due to a great difference in values of factor A shown in Fig. 3, the total cooling area of an air cooler must be much larger than in a water jacket, if anode dissipation of the same order of magnitude is to be taken care of in both cases. In a practical design the size of the cooler is limited by the general design of the transmitter and its radio-frequency circuit.

Numerical Example of Cooler Design

In this section a method of calculation of an air cooler is outlined on the example of the 891-R and similar tubes.

For convenience of numerical calculation we first assume that power dissipation per centimeter length of the "hot" portion of the anode (Fig. 6) is constant and equal to 1000 watts, which corresponds to the total anode dissipation 11,500 watts. With this assumption we calculate maximum anode temperature for air flow rate of 1500 centimeters per second. (3000 feet per minute). Then, in view of proportionality between power dissipation and anode temperature above the ambient, the permissible dissipation for each individual rate of air flow is obtained by setting the anode temperature limit for example at 230 degrees centigrade and by reducing or increasing the initially assumed power dissipation in proportion to the new anode temperature. It is convenient to refer all calculations to the cooler zone of unit length.

Taking into consideration the discussion of the previous section and with reference to Fig. 6, we shall adopt the following structural data in Table II for the cooler:

TABLE II

	Inches	Centimeters
D_f = outer fin diameter	7.5	19.1
D_c = outer core diameter	3.75	9.53
d_c = inner core diameter	1.63	4.14
δ = fin thickness	0.0625	0.159
t = fin spacing at root	0.075	0.191
T = fin spacing at free end	0.150	0.381
t_{ave} = fin spacing, average	0.1125	0.286
w = fin width (in radial direction)	1.88	4.78
l_c = fin length (in axial direction)	9.0	22.8
n = fin number 86		
L' = length of lower cold end	2.70	6.85
L'' = length of upper cold end	1.72	4.38
$L+L'$ = length of heated portion	4.53	11.50

From these data one can compute several quantities necessary for further discussion. These are

Total "heated" perimeter of air ducts:

$$p = 2nw = 820 \text{ centimeters}. \qquad (36)$$

Total cross-sectional area of air ducts:

$$A = \frac{\pi}{4} D_f^2(1 - 1/4) - n\delta w$$
$$= 150 \text{ square centimeters.} \quad (37)$$

Hydraulic radius of individual ducts:

$$r_h = A/p = 0.18 \text{ centimeter.} \quad (38)$$

Equivalent diameter of individual ducts:

$$D = 4r_h = 0.72 \text{ centimeter.} \quad (39)$$

Total cooling area of fins in a unit zone:

$$S = 2nw = 820 \text{ square centimeters.} \quad (40)$$

Rate of air flow though the cooler:

$$q_a = vA = 1500 \times 150$$
$$= 225{,}000 \text{ cubic centimeters per second}$$
$$= 475 \text{ cubic feet per minute.} \quad (41)$$

The physical constants for air at 60 degrees centigrade are:

$\rho = 1.06 \times 10^{-3}$ gram per cubic centimeter is the air density.
$k = 6.25 \times 10^{-5}$ calorie per second per centimeter per degree centigrade is the thermal conductivity of air.
$C_p = 0.24$ calorie per gram per degree centigrade is the specific heat of air.
$\mu = 1.95 \times 10^{-4}$ gram per second per centimeter is the air viscosity.

As indicated in the previous section, instead of using individual physical constants, one can conveniently operate with the factor A_a plotted in Fig. 3. The estimated average air temperature will be 60 degrees centigrade if we assume an ambient temperature of 45 degrees centigrade.

Before proceeding with further calculation we shall check whether under the specified conditions the air flow is turbulent. The Reynold's number is

$$Re = D\rho v/\mu = 5860. \quad (42)$$

Hence, the flow is turbulent, and for the calculation of the rate of heat transfer from fins to air, we can apply either of the equations (29), (30), or (31). We obtain, first

$$h = 0.00193 \text{ calorie per second per square centimeter per degree centigrade.} \quad (43)$$

From this figure and from the total cooling area one will find the total rate of heat transfer for the entire unit zone:

$$e_f = hS = 1.57 \text{ calories per second per degree centigrade.} \quad (44)$$

Remembering that heat generated within the same zone is

$$m = 1000 \text{ watts} = 240 \text{ calories per second} \quad (45)$$

one can determine the *average fin temperature* T_f above air from the equilibrium condition:

$$m = e_f \times T_{f\,\text{ave}}$$
$$T_{f\,\text{ave}} = 153 \text{ degrees centigrade.} \quad (46)$$

Due to the radial heat flow through the fins, temperature is maximum at the fin roots and gradually falls toward their free ends (see Fig. 7). The temperature distribution in the fin is given in the law derived elsewhere:[11]

$$t_x = T_{f\,\text{ave}} \cosh (Q_f - q_{fx})/\cosh Q_f. \quad (47)$$

The relation between the average fin temperature, $T_{f\,\text{ave}}$ and $T_{f\,\max}$ (which at the same time is the temperature of the core, T_c), according to the same derivation (7), is:

$$T_{f\,\text{ave}} = T_{f\,\max}(\tanh Q_f)/Q_f \quad (48)$$

or

$$T_{f\,\text{ave}} = T_c(\tanh Q_f)/Q_f. \quad (49)$$

In the last three expressions, Q_f, as shown below, depends on rate of heat transfer h; fin thickness δ; their length w; and heat conductivity of copper $k_c = 0.9$ calorie per second per centimeter per degree centigrade.

$$Q_f = qw = w\sqrt{2h/\delta\, k_c}. \quad (50)$$

Using the numerical values from the previous discussion one obtains

$$q_f = 0.164 \text{ centimeter}^{-1}$$
$$Q_f = 0.784 \quad (51)$$
$$\tanh Q_f = 0.653$$
$$(\tanh Q_f)/Q_f = 0.833 \quad (52)$$

and finally,

$$T_{f\,\max} = 153/0.833 = 184 \text{ degrees centigrade.} \quad (53)$$

In order to determine the anode temperature T_a, we must yet find the temperature drop in the core ΔT_c and in the layer of solder ΔT_s. The thickness of solder we assume to be 1 millimeter (0.040 inch). Using dimensions given in the beginning of this section we find

$$T_c = m \times 1/2\pi k_c \times ln(D_c/d_c)$$
$$= 35 \text{ degrees centigrade} \quad (54)$$

$$T_s = n \times 0.1/\pi d_c k_s = 12.3 \text{ degrees centigrade.} \quad (55)$$

Here $k_s = 0.225$ designates thermal conductivity of cadmium solder.

In addition, we must check the average air temperature $\Delta t_{a\,\text{ave}}$, above ambient. This will be found from the total dissipation $P_h = 2760$ calories per second and the rate of air flow $q_a = 225{,}000$ cubic centimeters per second.

$$\Delta t_{\text{ave}} = P_h/2q_a\rho C_p = 24 \text{ degrees centigrade.} \quad (56)$$

[11] See equation (1) on p. 491 of footnote 10.

Finally, the anode temperature will be determined by simple addition of all calculated partial temperature drops in various parts of the cooling system:

$$T_a = 45 \text{ degrees centigrade} + \Delta t_{\text{ave}} + T_{f\max} + \Delta T_c + \Delta T_s$$
$$= 45 + 24 + 184 + 35 + 12.3$$
$$= 300 \text{ degrees centigrade.} \qquad (57)$$

This is in excess of $T_{a\max} = 230$ degrees centigrade which we adopted as the permissible maximum anode temperature at any point. However, the calculated temperature, 300 degrees centigrade, corresponds to a situation seldom encountered in practice and certainly not in our concrete example. Indeed, it is calculated in supposition that all heat generated in any unit zone of the cooler is transferred to the cooling air within the same zone; in other words, thus far in the calculation we neglected longitudinal heat flow through the core from the directly heated portion to its cold ends and, hence, we neglected the contribution to the heat dissipation by the cooler's "cold ends." Logically, one can predict that the heavier the core the more substantial is this help. Mathematical treatment of this problem is given elsewhere.[10] Briefly, it can be summarized as follows: The effect of "cold ends" is manifested, first, in a general reduction of temperature along the entire heated portion of the cooler. In addition, from the middle of the heated portion the temperature decreases toward the cold ends. In a symmetrical structure the maximum temperature occurs exactly at the geometrical middle. With unequal lengths of ends the maximum moves toward the shorter end; its exact location can be established by calculat on. Without reproducing the theoretical derivation we shall use here only its final results. The important maximum temperature at about the middle of the directly heated portion of the core (omitting temporarily the consideration of the radial temperature drop in the core) is generally given by:

$$T_{c\max} = m/e_c - (m/e_c - t_b)/\cosh Q. \qquad (58)$$

Here, quantity m/e_c is the core temperature calcated in the earlier assumption that there is no longitudinal temperature drop in the core (no cold ends).

m, as before, is heat generated per unit length.

e_c is the rate of heat transfer for the entire unit zone, referred to the outer surface of the core per unit zone. It can be determined from (44) and (46) and the condition of continuity of heat flow:

$$e_c T_c = e_f T_f \qquad (59)$$

t_b is the temperature at the boundary between the "heated" and "cold" portions of the core.

Q is the quantity similar to Q_f of (50) pertaining however, to the heated portion of the core; viz,

$$Q = qL \qquad (60)$$

and

$$q = \sqrt{e_c/a_c k_c} \qquad (61)$$

with a_c designating the annular cross section of the core; L, the length of the heated portion between the points with temperature maximum and t_b, and k_c, heat conductivity of copper.

The boundary temperature for each end is given by

$$t_b' = m/e_c \times 1/(1 + \tanh Q'/\tanh Q) \qquad (62)$$

and

$$t_b'' = m/e_c \times 1/(1 + \tanh Q''/\tanh Q)$$

Here,

$$Q' = qL' \quad \text{and} \quad Q'' = aL'' \qquad (63)$$

with q the same as per (61) and L' and L'' representing the lengths of the two cold ends. Obviously, maximum temperature $T_{c\max}$ calculated for both ends of the core must be the same.

By a trial calculation one can easily establish that the maximum core temperature lies at a distance of 6.2 centimeters from the longer and 5.3 centimeters from the shorter cold end. Then, inserting the available data into (62) and (58) we obtain

$$t_b' = 91.3 \text{ degrees centigrade}$$
$$t_b'' = 99.8 \text{ degrees centigrade} \qquad (64)$$

and

$$T_{c\max} = 124.25 \text{ degrees centigrade.}$$

This temperature is to be compared to 184 degrees centigrade of (52). Obviously, the actual heat flow in a radial direction through the unit zone comprising $T_{c\max}$ is less than the initially assumed figure, 240 calories per second, in proportion to the calculated temperatures:

$$f_{\max} = 240 \times 124.5/184 = 162.5 \text{ calories per second.} \qquad (65)$$

This permits us to compute the actual maximum radial temperature drop across the core at the hottest cross section; it will be reduced from the former figure (equation (53)) in the same proportion:

$$T_{c\max} = 35 \times 124.5/184 = 23.6 \text{ degrees centigrade.} \qquad (66)$$

As to the temperature drop through the solder wall one must assume that it stays unaffected by the derived distribution of heat flow; indeed, heat generation in the anode is unaffected by it, and one may assume that longitudinal heat equalization takes place entirely in the core, as the anode wall is relatively thin. Also, unaffected by the longitudinal temperature distribution, air temperature above the ambient remains as it depends only on the total heat dissipation. Thus, the correct maximum anode temperature is

$$T_{a\max} = 45 + 24 + 124.25 + 23.6 + 12.3$$
$$= 230 \text{ degrees centigrade.} \qquad (67)$$

This temperature is exactly equal to the established permissible $T_{a\max}$. Hence, the assumed total dissipation $= 11.5$ kilowatts is the correct maximum permissible dissipation for the designed cooler under the

assumed operating conditions. One may note that the calculated power-dissipation figure equals the limit usually specified for the 891 tube with water cooling. This indicates that, if necessary, air coolers can be designed so that practically the same dissipation ratings can be applied to a tube as with water cooling. The calculated radial temperature distribution within the hottest section of the cooler is represented graphically in Fig. 7.

It may be of interest to note that in a cooler with no cold ends, the permissible dissipation should have been reduced from the originally assumed total dissipation, 11,500 watts, in proportion to the maximum permissible anode temperature and the calculated anode temperature above ambient, that is,

$$P_{h\,\max} = 11.5 \times (230 - 45)/(295 - 45) = 8.3 \text{ kilowatts.} \qquad (68)$$

The corresponding cooler would have a length exactly equal to that of the heated portion of the anode. Obviously, for efficient cooling such a structure normally should be avoided; however, one may be forced into it if the filament structure occupies practically the entire length of the anode.

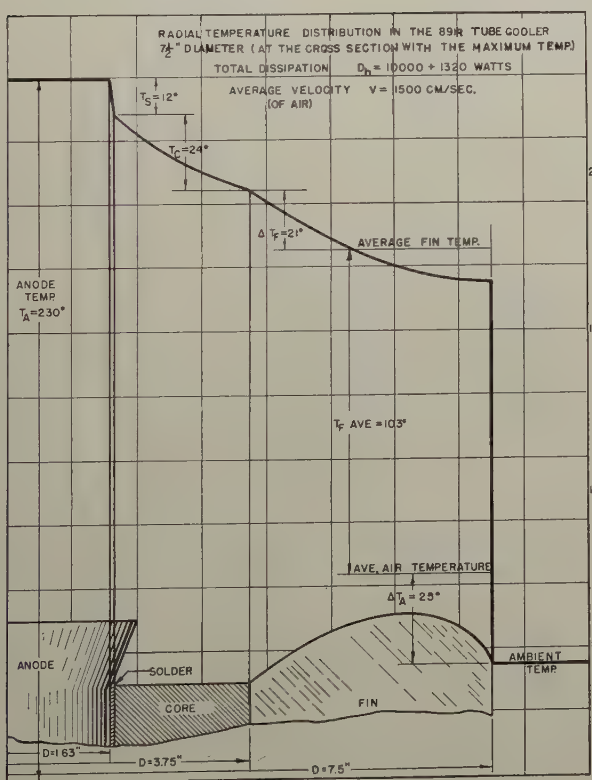

Fig. 7—Radial temperature distribution in the 891R tube cooler.

Aerodynamical Properties of the Air Cooler

In the design of a water jacket for vacuum tubes one does not give much consideration to the pressure drop in the jacket as this normally is only a small portion of the total pressure generally available at the station and necessary for forcing water through long insulating water coils. For example, with 3 gallons per minute recommended for the 891 and similar tubes, the pressure drop across the jacket is only 2 pounds per square inch, while the available pressure is seldom less than 25 pounds per square inch. Things are quite different with air coolers. The resistance pressure of a cooler and the rate of air flow inherently determine the kind of

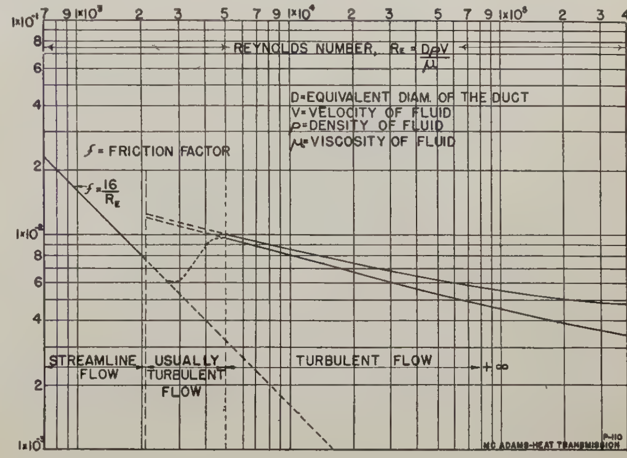

Fig. 8—Fanning friction factor versus Reynolds number.

blower and power necessary for forcing the air through the cooler. For a given cooler design as mentioned before, air pressure required from a blower increases in proportion to the square and power to the cube of air velocity.

Resistance pressure of the jacket proper consists of friction loss in the ducts H_f and of contraction loss H_c due to a sudden change of the cross section of the air flow at the entrance into the cooler; adding to this the velocity head H_v, one obtains the total pressure H_{total} necessary to propel air through the jacket with the desired velocity, v centimeters per second.

Friction loss is given by the expression[12]

$$H_f = f l_c \rho v^2 / 2 g r_h. \qquad (69)$$

Contraction loss is [13]

$$H_c = k \rho v^2 / 2g \qquad (70)$$

and *velocity head*

$$H_v = \rho v^2 / 2g. \qquad (71)$$

The meaning of the symbols is as follows:

v = air velocity in centimeters per second; $v = 1500$ centimeters per second.

g = gravitational acceleration; $g = 981$ centimeters per second squared.

ρ = air density; at 40 degrees centigrade, $\rho = 1.2 \times 10^{-3}$ gram per cubic centimeter.

l_c = total length of the cooler; $l_c = 22.75$ centimeters.

f = friction coefficient; for the calculated $Re = 5860$, $f = 0.0093$, (see Fig. 8).

[12] William H. Adams, see p. 109 of footnote 1.
[13] William H. Adams, see p. 121 of footnote 1.

k = a factor depending on A/A_1, if A is the total cross-sectional area of the air ducts, and A_1 the total area of the cooler cross section. (See Fig. 9.) In our case $A/A_1 = 0.52$ and $k = 0.285$.

r_h = hydraulic radius of individual ducts of the cooler; $r_h = 0.18$ centimeter.

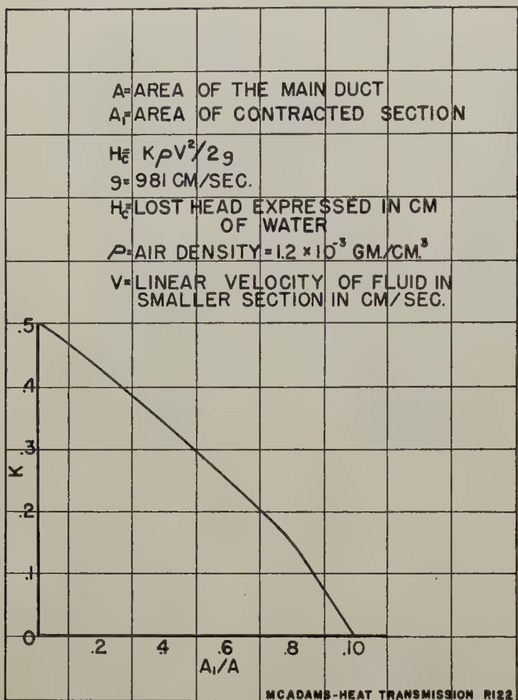

Fig. 9—Plot of K versus A_1/A for calculation of contraction loss.

Substituting the indicated numerical values just given for the symbols in the last three expressions, we obtain:

$$H_f = 1.55 \text{ centimeters} \quad H_c = 0.392 \text{ centimeters} \quad \text{and}$$

$$H_v = 1.36 \text{ centimeters.} \tag{72}$$

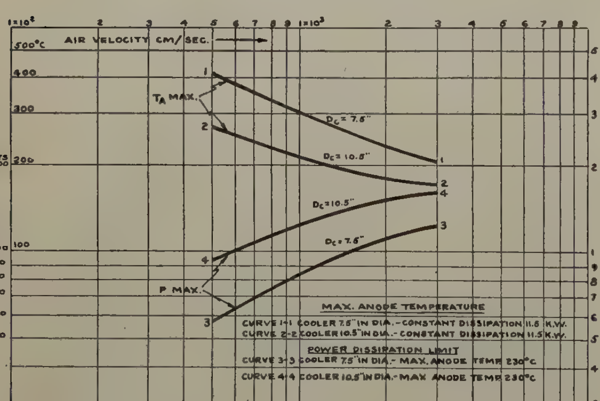

Fig. 10—Maximum anode temperature and power dissipation limit versus air velocity.

The minimum pressure required from the blower

$$H_{\text{total}} = 3.34 \equiv 1.315 \text{ inches.} \tag{73}$$

Minimum power requirement in horsepower is to be computed from the expression

$$HP = 0.157 \times 10^{-3} Q_a H''_{\text{total}} \tag{74}$$

where Q_a is the rate of air flow in cubic feet per meter (in our case $Q = 475$ cubic feet per meter), while H_{total} is the total pressure in inches of water. In our numerical examples, $HP_{\min} = 0.5$. This is without considering the efficiency of the blower. In many cases, knowing the required values of Q_a and H, one can readily find all necessary data for a suitable blower in industrial catalogues.

Discussion of Some Special Problems in Cooler Designing

Variation of Air Velocity

Considering (28) and (29) one may expect that permissible dissipation is proportional to the 0.8th power

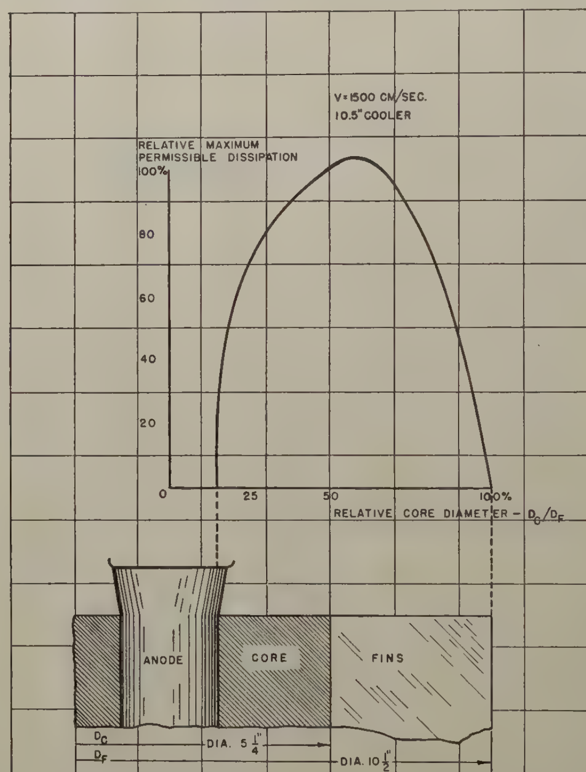

Fig. 11—Permissible power dissipation versus core diameter.

of air velocity. However, due to the radial temperature drop in fins (see (49)) and due to the effect of the cooler's "cold ends," the actual proportionality exponent lies between 0.8 and 0.4. The greater the velocity, the smaller is the exponent. Fig. 10 contains curves of calculated permissible dissipation and maximum anode temperature for the 7.5-inch cooler of our numerical example and also for another cooler, 10.5 inches in diameter, designed for the same tube. Both are coolers of "optimum" dimensions.

Optimum Design

Earlier in this discussion it was shown that for a given outside diameter of the cooler D_f, a maximum dissipation can be expected for a design in which the core diameter is approximately $D_c = D_f/2$. This conclusion is based on a derivation in which the average fin temperature alone is considered, as it usually

constitutes the major part of the total temperature difference between the anode and the air. However, temperature drop in various parts of the cooler (layer of solder, radial drop in the core, etc.,) may influence the final results and may change the above ratio. In order to check how close the derived figure, 1/2, is to the actual relation, calculation has been carried out on several cooler designs. The results showed that by adhering to the 50 per cent core-diameter rule, one will always be within only a few per cent of the feasible maximum dissipation, the actual maximum falling between 0.5 D_f and 0.55 D_f. In Fig. 11 a curve is plotted for the 10.5-inch cooler, representing permissible dissipation as a function of core diameter.

The requirement of the maximum cooling area in an optimum design implies also that with a given core diameter the fin number must be the greatest feasible. Their thickness and spacing, as mentioned in an earlier section, is governed primarily by the mechanical strength and convenience of manufacturing and handling the cooler. Experience shows that with coolers of medium and large sizes 1/16 inch is apparently the practical low limit for fin thickness; spacing between the fins can be equal to their thickness, or better, be somewhat wider. However, in some cases it may be found that instead of brazing stamped fins to the core, it is more economical to mill longitudinal slots on the outer surface of a larger copper cylinder.[14] The fins formed by this method are heavier than stamped fins; also, when deep slots are required they must be wider than root spacing between the adjacent stamped and soldered fins. As an example, practicable dimensions for *slotted* designs are given in Table III.

TABLE III

Milled Slots					
Cooler diameter, inches	4	6	8	10	12
Slot depth, inches	1	1.5	2	2.5	3
Slot width, inches	0.0625	0.080	0.100	0.125	0.1875
Spacing at slot bottom, inches	0.046	0.088	0.109	0.120	0.138
Fin number, approximate	58	56	60	64	58
1/16-inch Stamped Fins					
Fin number, approximate	46	68	92	114	140

It is evident that the larger the cooler diameter the greater is the total cooling area of a "fin" design as compared to the "milled-slot" design. Hence, relatively higher dissipation limits can be obtained with finned designs, all other conditions being similar. With smaller coolers the milled type may prove to be preferable. The data given in Table III are only approximately estimated figures.

Maximum Radial Fin Length

In the "optimum design" the fin length is equal to one quarter of the cooler diameter D_f, and the fin number n is proportional to the same. Hence, the larger the cooler the more dissipation can be taken care of by it. However, the increase of fin length has its limit beyond which it does not contribute to further improvement of cooling. This becomes evident from the following reasoning. Suppose we gradually increase the fin length without changing their number. By combining (49), (28), and (36), we can represent core temperature as function of structural and operational parameters by

$$T_c = \frac{mq}{2nh} \times \frac{1}{\tanh wq}. \tag{75}$$

From this, permissible dissipation per unit length m can be written as

$$m = T_c n\sqrt{2h\delta k_c} \times \tanh wq. \tag{76}$$

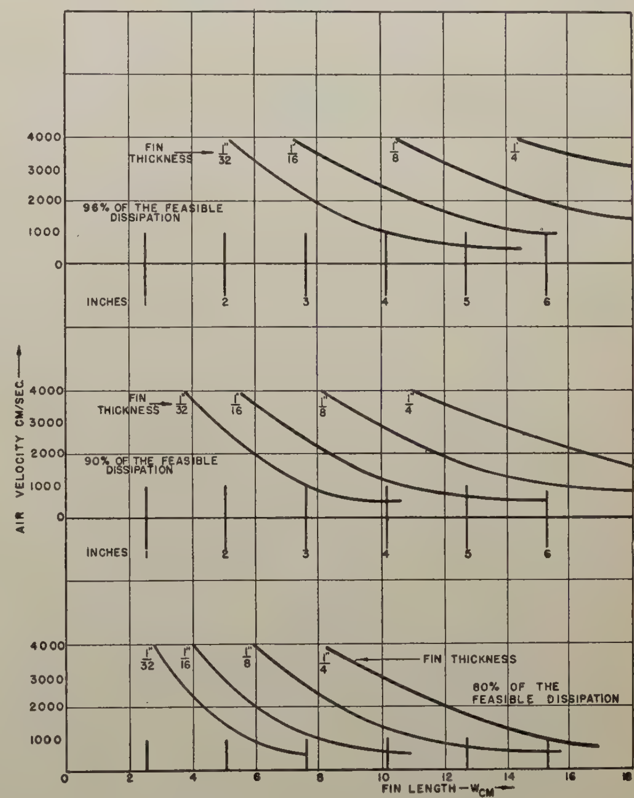

Fig. 12—Useful fin length versus air velocity.

Here, according to the earlier designation

h = the rate of heat transfer from fins to air
δ = the fin thickness
k_c = the thermal conductivity of copper
w = the fin length (in radial direction)
$q = \sqrt{2h/\delta k_c}$

One must remember that h depends on air velocity and is proportional to $V^{0.8}$.

If we assume all factors to be constant except w, permissible dissipation will be proportional to $\tanh wq$, which, at $wq = 3$, practically reaches its limiting value, unity. Hence, there is no sense in choosing fins longer than

$$w = 3/q. \tag{77}$$

Moreover, by examining tables of hyperbolic functions one can notice that a reduction of wq by 50 per cent

[14] Van de Beek, "Air cooled transmitting valves," *Philips Tech. Rev.*, vol. 4, p. 124; May, 1939.

from this limiting value, that is to 1.5, would reduce tanh wq and m only by 10 per cent.

From (77) it is also obvious that the greater the air velocity (hence, h, the rate of heat transfer) the shorter becomes the useful length of fins, all other conditions being similar. The fin thickness δ also influences the useful fin length. This length calculated from (77) for several different fin sizes is plotted in Fig. 12 versus air velocity for an assumption of 95, 90, and 80 per cent utilization of the total feasible cooling capacity of the fins. From these curves one can conclude for example, that with a velocity of 3000 centimeters per second very little can be contributed by 1/16-inch fins by ex-

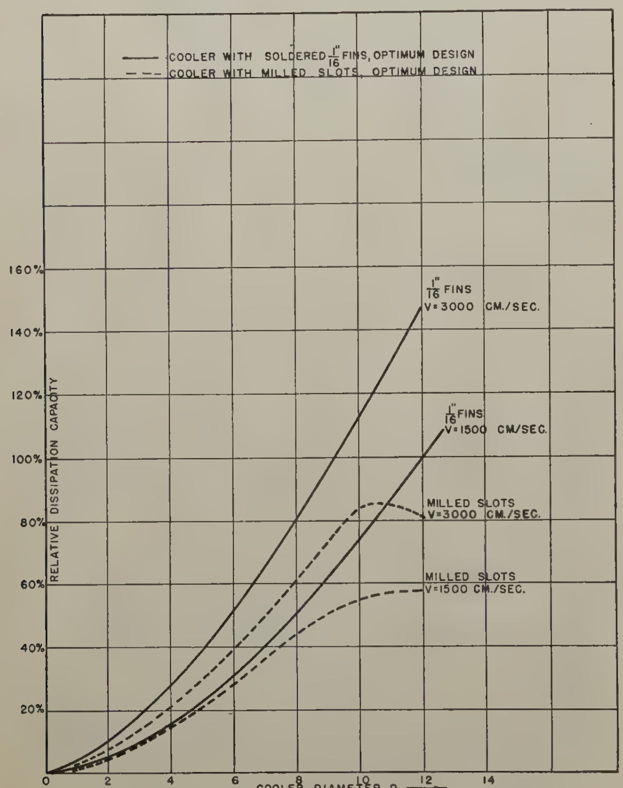

Fig. 13—Relative power dissipation versus cooler diameter.

tending their length in excess of $3\frac{1}{2}$ inches and even 3 inches. The similar limiting length for a 1/32-inch thick fin is only $2\frac{1}{2}$ inches and 2 inches.

In Fig. 13 the curves are plotted to show comparative dissipation limit in coolers of various sizes with soldered 1/16-inch fins and, also, with milled slots. The relatively low dissipation with the larger coolers of the latter type is due to the fact that the fin number in these coolers, because of greater depth and greater spacing of slots, comes out almost independent of the cooler size. Equation (76) is used in this calculation. The curves also show that by doubling the air velocity one can increase permissible dissipation only by 48 per cent. Consideration of the effect of the cold ends would modify this ratio in favor of lower air velocities by a few per cent.

Cold Ends

From a close examination of (58) and (62) one may draw the following conclusions in regards to the effect of the cold ends: (1) with a given length of the anode "hot" portion L_1 (that is, with a constant Q), cold ends tend to reduce maximum anode temperature, hence, to increase permissible dissipation; (2) the effect of cold ends reaches a maximum when tanh Q' or tanh qL' becomes equal to unity; (3) with this optimum length of the cold ends, their effectiveness drops as the length of the hot portion L increases; (4) cold ends completely cease to influence permissible dissipation when the length of the hot portion becomes such that $Q=qL$ reaches the value of 4.6 or even 3.0; with the first figure the maximum anode temperature is only 1 per cent below the uniform anode temperature calculated in the absence of the cold ends; with $Q=3$ this difference is 5 per cent. This can be derived from the same equation by putting tanh $Q'=1$; (5) in estimating the cold-end effect one must keep in mind that both Q and Q' are proportional to q, and this is proportional to 0.4th power of air velocity and inversely proportional approximately to the square of the core thickness.

Conclusions

Reviewing the results of various derivations arrived at in this paper, which are in agreement with direct experiments, one may state that within practical limits water and forced-air cooling can both be used in equal measure on vacuum tubes with external anodes. The decision whether one or the other type of cooling is preferable in any particular tube application depends on the general design of the transmitter, relative cost of the installation, and on certain specific conditions of operation. Thus, forced-air cooling becomes indispensable in unheated spaces where the ambient temperature is hovering about freezing point, or below it. Air cooling is also a logical solution if fresh water is scarce, as for example on shipboard. On the other hand, water jackets are more compact than air coolers; also, water-cooled tubes possess the important advantage of being easily replaceable in their jackets, thus permitting the jackets to be built into the transmitters. Air-cooled tubes cannot be simply inserted in their coolers; they must be very carefully soldered into the cooler core to form an intimate contact between the anode and the cooler. Generally, it is considered impracticable to burden station personnel with this slow and rather critical operation, especially when cadmium solder is used. Therefore, air-cooled tubes, as a rule, are transported and handled with their bulky and sometimes very heavy coolers as a unit; this procedure is expensive and inconvenient. Attempts have been made to design air coolers consisting of two component parts: (1) a thin inner core, soldered around the anode at the factory; (2) an outer part of the core with fins, built into the transmitter. Then, only the tube with a relatively light shell can be transported and handled.

The difficulty in this case lies in establishing a reliable and uniform thermal contact between the removable and stationary parts of the cooler; in fact, this requires extremely accurate machining of the contact surfaces which logically would have a slightly tapered form. Experience shows that a special mechanism would be required in this case for removing an old or a defective tube from its seat, as the portable and stationary parts of the cooler in operation frequently sweat together at some spots, due to localized heat. This fact is rather disappointing, because it makes it necessary to reclean the stationary cooler surface mechanically each time the tube is changed.

Among other points of relative merits of air versus water cooling one may reiterate that, if desired, air-cooled tubes can be furnished with individual cooling units consisting of a small air blower driven by a small electric motor, while water cooling always implies an elaborate water supply and drainage system. Finally, one may remark that, as a rule, air-cooled tubes behave better in operation than water-cooled tubes with respect to "arcing" back." This is, probably, due to a more favorable temperature distribution within the tube, influencing the distribution of adsorbed gas; with air-cooled tubes the anode is at a much higher temperature than the glass blanks which are intensely cooled by the outgoing air. In a water-cooled tube the anode is the coldest surface inviting condensation of residual gases; these may eventually be released in operation and cause instantaneous local increase in pressure, hence, an arc.

Calculations and direct experience show that either with water or forced-air cooling one may count on a safe dissipation of 500 to 750 watts per square inch of the "heated" anode portion, provided heat is generated *uniformly* throughout the hot surface. Nonuniformity of heat generation, such as is caused by grid focusing effect, as mentioned in this paper, may reduce the permissible dissipation with water-cooled tubes by as much as 50 per cent and even more. Air-cooled tubes are in a much more favorable position in this respect as heavy-walled cores allow for better heat equalization in the longitudinal or circumferential directions, that is, perpendicular to the main heat flow in the radial direction. In the case of air-cooled tubes the figure of reduction in permissible heat dissipation would usually not exceed 20 per cent; mostly it is below this figure.

For similar reasons (restricted heat flow in a longitudinal direction), the presence of the "cold ends" in water-cooled anodes practically does not contribute to the anode cooling, while "cold ends" in an air cooler play a very important role by increasing the total cooling surface, thus making up for the much lower rate of heat transfer per unit area from metal to air as compared with water. However, there is a limit to the length of the "cold ends" beyond which they cease to contribute further to cooling efficiency.

The effect of "cold ends" is less pronounced for higher rates of heat transfer, that is, for higher air velocities.

Regarding the number and the length of fins we may reinterate the findings of this paper that for greater dissipation a greater number of thinner fins is desirable. For a given cooler size and given fin pitch at the core surface, an "optimum design" will have the core diameter equal to one half of the total cooler diameter. Also, there is a limit to the fin length beyond which there is no further contribution to the cooling effect of the cooler. This limiting length is the shorter the greater the air velocity and the thinner the fins.

In conclusion, it may be mentioned that as a rule the material for air coolers is copper, because of its high thermal conductivity. However, coolers made of copper are relatively heavy. Therefore, a natural question arises: why not use aluminum for the same purpose? Among ordinary material, the thermal conductivity of aluminum is next to that of copper; it amounts to about 50 per cent, while aluminum weight is less than 25 per cent of that of copper.

In general, aluminum coolers are quite feasible. However, at this time, lack of an easy method of soldering copper anodes into an aluminum cooler prevents the realization of this desirable innovation on a wide scale. One must also keep in mind that the temperature drop in the metal parts of a cooler (core, fins) is greater with aluminum than with copper; therefore, the average fin temperature, hence, total heat dissipation, will be lower with an aluminum than with a copper cooler of similar dimensions and with the same permissible anode temperature.

Correction

Correction to "The Calculation of Ground-Wave Field Intensity Over a Finitely Conducting Spherical Earth," by K. A. Norton. Footnote 13 which appears on page 625 of the December, 1941, issue of the PROCEEDINGS, states "The graph paper used for drawing these figures was Keuffel and Esser Company graph paper No. 30731, which consists of log-log cycles with dimensions identical to those in Figs. 2, 4, 7, and 11." The number of the graph paper should read K&E 358-127 for the thin sheets and for the heavy sheets, K&E 359-127G.

Institute News and Radio Notes

Board of Directors

The Board of Directors met on March 4 and those present were A. F. Van Dyck, president; Austin Bailey, A. B. Chamberlain, C. C. Chambers, I. S. Coggeshall, H. T. Friis, Alfred N. Goldsmith, C. M. Jansky, Jr., J. K. Johnson, F. E. Terman, B. J. Thompson, H. M. Turner, H. A. Wheeler, L. P. Wheeler, and H. P. Westman, secretary.

The resignation of Mr. Crawford as assistant secretary was announced.

It was agreed that the names of members, as of December 1, 1941, residing in enemy and enemy-controlled countries would be included in the YEARBOOK.

Executive Committee

The Executive Committee met on March 3. Those present were A. F. Van Dyck, chairman; I. S. Coggeshall, Alfred N. Goldsmith, R. A. Heising (guest), F. B. Llewellyn, B. J. Thompson, and H. P. Westman, secretary.

Approval was granted of sixty-four applications for admission to Associate, two for admission to Junior, and forty-three for admission to Student grade.

There were sixteen applications for admission to Member and nine for transfer to Member approved.

The resignation of Mr. Crawford as assistant secretary was accepted.

On March 17, a meeting of the Executive Committee was held and was attended by A. F. Van Dyck, chairman; I. S. Coggeshall, Alfred N. Goldsmith, R. A. Heising (guest), F. B. Llewellyn, B. J. Thompson and H. P. Westman, secretary.

Broadcast Engineering Conference

The Fifth Annual Broadcast Engineering Conference which was held from February 23 to 27 at Columbus, Ohio, was highly successful in the opinion of those who attended it. The leadership of the conference was in the hands of W. L. Everitt of The Ohio State University who was assisted by L. C. Smeby, director of engineering of the National Association of Broadcasters, and A. F. Van Dyck, president of the Institute. These two organizations co-operated with The Ohio State University in the holding of the conference this year.

The conference was primarily devoted to a consideration of the problems which confront broadcast stations under wartime conditions. The program was given in full in the February, 1942, issue of the PROCEEDINGS.

Besides the sessions on the campus, two evenings of entertainment were scheduled; a popular scientific lecture by Dr. Phillips Thomas of the Westinghouse Electric and Manufacturing Company, and the annual banquet which was attended by nearly two hundred guests.

Section Meetings

ATLANTA

Discussion on "The Radio Engineer's Part in the National Defense Program," January 30, 1942.

BOSTON

"The Communication System of the Tropical Radio Telegraph Company," by C. C. Harris, chief engineer, Tropical Radio Telegraph Company, November 14, 1941.

"Analogies Between Photography and Radio," by Donald G. Fink, *Electronics*, January 23.

"The Coronavisor," by H. W. Babcock, Radiation Laboratory, Massachusetts Institute of Technology, February 19.

BUFFALO-NIAGARA

"Radio Interference," by Herbert W. Staderman, Buffalo-Niagara Electric Company, February 18.

"Photoelectric Intrusion Protection," by Carl C. Smith, Hydro-Electric Commission of Ontario, March 9.

"Field Strength Measurements of Broadcast Stations," by Leroy F. Fiedler, Buffalo Broadcasting Corporation, March 9.

CHICAGO

"Equivalent Circuits for Vacuum-Tube Amplifiers," by G. D. Robinson, U. S. Navy, February 20.

"Description of New CBS Transmitter WABC," by J. L. Middlebrooks, Columbia Broadcasting System, February 20.

CINCINNATI

"Physical and Chemical Forces," by Karl K. Darrow, Bell Telephone Laboratories, January 22.

"Light and Darkness in Defense," by Samuel G. Hibben, Westinghouse Electric and Manufacturing Company, January 21.

"High-Frequency Therapy Apparatus," by Carl K. Gieringer, Liebel-Flarsheim, February 17.

CLEVELAND

"The Role of Radio in Air Transportation," by E. P. Buckthal, Communications Laboratory, United Air Lines, February 26.

CONNECTICUT VALLEY

"Trends in Receiving-Tube Design," by Robert L. Kelly, RCA Manufacturing Company, January 15.

EMPORIUM

"Spectrographic Analysis in the Manufacture of Radio Tubes," by Stuart Parsons, Hygrade Sylvania Corporation, February 26.

INDIANAPOLIS

"Noise Suppression in Frequency Modulation," by H. J. Reich, University of Illinois, February 20.

MONTREAL

"Shore-to-Ship Communication," by L. T. Bird, Canadian Marconi Company, February 18.

"Color Television," by P. C. Goldmark, Columbia Broadcasting System, March 11.

PHILADELPHIA

"Some Problems of Disk Recording," by C. J. LeBel, Audio Devices, Inc., March 5.

PITTSBURGH

"The Brush Surface Analyzer and Other Industrial Applications," by Charles K. Gravley and H. S. Kartsher, Brush Development Company, February 9.

TORONTO

"Color Television," by P. C. Goldmark, Columbia Broadcasting System, March 9.

"Frequency-Modulation - Receiver - Design Principles," Dudley E. Foster, Rogers-Majestic (1941), Ltd., Toronto, March 23.

TWIN-CITIES

General discussion of the recent Broadcast Engineering Conference held at Ohio State University relating to the problems of the communication engineer as a result of the war, by H. Skifter, chief engineer, KSTP; M. Jensen, chief engineer, WCAL; O. Prestholdt, chief engineer, WLOL, March 18.

WASHINGTON

"Impedance Measurements at Frequencies from 1 to 100 Megacycles," by Robert F. Field, General Radio Company, March 9.

Eta Kappa Nu Awards

Dr. Cledo Brunetti (A'37), assistant professor of electrical engineering at Lehigh University and now on leave of absence for defense work, has been named by Eta Kappa Nu, the electrical engineering honor society, as the outstanding young electrical engineer for 1941. This award is made annually to an engineer not more than ten years out of college nor over 35 years of age in recognition of "meritorious service in the interest of his fellow men."

Dr. Brunetti was born in Virginia, Minnesota, on April 1, 1910. He worked his way through the University of Minnesota, receiving the B.E.E. degree in 1932 and the Ph.D. degree in 1937. From 1932 to 1936 he was a teaching Fellow and during

the next year an instructor in the electrical engineering department of the university. In 1937 he went to the faculty of Lehigh University as an instructor, becoming an assistant professor of electrical engineering in 1939. During the summers of 1939 and 1940 he was a research associate at the radio laboratory of the National Bureau of Standards. Since May, 1941 he has served there as a radio physicist and is on leave of absence from Lehigh University.

Dr. Brunetti has contributed extensively to the technical press and a number of his papers have appeared in the PROCEEDINGS.

Two certificates of honorable mention are presented by Eta Kappa Nu and this year were received by Institute members,

DR. CLEDO BRUNETTI

George F. Leydorf of the Crosley Corporation and Simon Ramo of the General Electric Company.

George F. Leydorf (A'26) was born in Perrysburg, Ohio, on April 24, 1908. He was trained at Ohio State University, receiving a Bachelor's degree in electrical engineering in 1931 and a Master's degree in science in 1933. He then joined the broadcast division of the Crosley Corporation and shortly thereafter became director of the technical staff.

Dr. Ramo (A'38) was born in Salt Lake City, Utah, on May 7, 1913. He received a Bachelor's degree in electrical engineering from the University of Utah in 1933 and in 1936 had conferred on him by the California Institute of Technology the Ph.D. degree, magna cum laude.

He joined the engineering staff of the General Electric Company in 1936 and has worked on high-frequency engineering and electron-optics problems. He has contributed to the PROCEEDINGS and to other engineering publications.

Membership

The following indicated admissions and transfers of memberships were approved by the Board of Directors on March 4, 1942.

Transfer to Member

Aiya, S. V. C., Poona 4, India
Canon, H. B., 1523 Woodbine Ct., Deerfield, Ill.
Davis, G. C., 501–507 Munsey Bldg. Washington, D. C.
Findley, Paul B., 463 West St., New York, N. Y.
Gebhard, L. A., Naval Research Laboratory, Anacostia, D. C.
Herrick, R. H., 1033 W. Van Buren St., Chicago, Ill.
Hoffman, R. B., 36 S. Munn Ave., East Orange, N. J.
Hood, J. T., 4816 N. Illinois St., Indianapolis, Ind.
Labin, E., 25 Fifth Ave., New York, N. Y.
Sykes, R. A., Bell Telephone Laboratories, Inc., 180 Varick St., New York, N. Y.

Admission to Member

Aboussleman, W., 122 Woodlawn Ave., Collingswood, N. J.
Anderson, H. V., Radio Station WJBO, 444 Florida St., Baton Rouge, La.
Boswau, H. P., 2447 E. Erie Ave., Lorain, Ohio
Chesnut, R. W., Bell Telephone Laboratories, Inc., 463 West St., New York, N. Y.
Condon, E. U., Westinghouse Research Laboratories, East Pittsburgh, Pa.
Davis, R. J., Towson and Morris Ave., Lutherville, Md.
Ferguson, J. G., Bell Telephone Laboratories, Inc., 463 West St., New York, N. Y.
Findley, P. B., Bell Telephone Laboratories, Inc., 463 West St., New York, N. Y.
Kendall, B. W., Bell Telephone Laboratories, Inc., 463 West St., New York, N. Y.
Licuanan, F. H., Jr., 28 Alfonso XIII, San Juan, Rizal, Philippines
Mathes, R. C., Bell Telephone Laboratories, Inc., 463 West St., New York, N. Y.
Sherman, J. M., 5033 Portland Ave., S., Minneapolis, Minn.
Sweeny, C. P., 16 Jackson Ave., Chatham, N. J.
Wagner, W. J., Box 1040, Anchorage, Alaska
Whitney, M. E., 308 Corinthian Ave., Willow Grove, Pa.
Young, M. G., University of Delaware, Evans Hall, Newark, Del.

Admission to Associate

Alden, E. E., Radio Station WIRE, Indianapolis, Ind.
Amundsen, R. C., 4 Gilbert Ave., East Norwalk, Conn.
Anderson, E. J., 1331 Schley St., Butte, Mont.
Bartha, S. J., 3326 W. Crystal St., Chicago, Ill.
Bewig, K. W., 107 W. South St., Crown Point, Ind.
Bierach, K. F.. Jr., 561 Tech. S. S., Barracks 151, Scott Field, Ill.
Biga, J. J., 3412 Montrose Ave., Chicago, Ill.
Bromley, R. A., Box 123, Hamlin, W. Va.
Bryson, R. W., 26 Alleghany Ave., Towson, Md.
Cahill, J. P., 23 Bramcote Dr., Beeston, Notts., England
Caswell, J. N., 127-02 109th Ave., South Ozone Park, N. Y.
Chambers, G. R., 3116—18 St., N. W., Washington, D. C.
Cohen, J., 430 Lamont St., N. W., Washington, D. C.
Conner, F. B., 65 Waverly Ave., Dayton, Ohio
Davidson, C., 696 Broadway, Long Branch N. J.
DeVore, L. T., 717 S. Fountain Ave., Springfield, Ohio
Dickerson, B. C., 913 Colonial Ave., Norfolk ,Va.
Dimmer, R. P., 3315 W. Monroe St., Chicago, Ill.
Epstein, J., 132 W. Maple Ave., Moorestown, N. J.
Ferrier, D. T., 92 Winchester Rd., Arlington, Mass.
Furst, U. R., 2256 N. Cleveland Ave., Chicago, Ill.
Gorham, J. E., 320 Bath Ave., Long Branch, N. J.
Gresham, W. S., Jr., Box 1384, Indianapolis, Ind.
Guiles, C. H., 102 Anchor Way, East Hempstead, L. I., N. Y.
Handleman, M., 33 Beeching St., Worcester, Mass.
Hassler, E. B., 2332 N. Central Park Ave., Chicago, Ill.
Hibbard, L. U., 16 Phoenix St., Lane Cove, Sydney, N.S.W., Australia
Kelley, J. J., WFBL Bldg., Syracuse, N. Y.
Kennedy, F. H., Jr., 1702 Tower Petroleum Bldg., Dallas, Texas
Killgore, H. S., 25 Prospect Pl., New York, N. Y.
Kirshner, D. R., 2011 Grand Concourse, New York, N. Y.
Kroll, R. T., 212 Murray St., Ann Arbor, Mich.
Lindenberg, E. C., 1442 N. Farwell Ave., Milwaukee, Wis.
Lyon, J. A. M., c/o Ebasco Services, Inc., 2 Rector St., New York, N. Y.
Martin, J. F. P., 137 Peterborough St., Boston, Mass.
Moulic, W. E., Jr., c/o *Radio Today*, 480 Lexington Ave., New York, N. Y.
Nadeau, A. G., 11 St. Benoit St., Quebec, Que., Canada
Odden, R. B., 1008 S. Adams St., Marion, Ind.
Pate, C. W., 214 Mossbrae Apartments, Dunsmuir, Calif.
Pratt, J. W., Jr., 207 Ingleside Ave., Catonsville, Md.
Pritchard, W. S., 750 Huron Rd., Cleveland, Ohio
Rehfisch, T. J., Northampton Polytechnic, St. John St., London E.C. 1, England
Richards, G. W., Route 5, Box 189, 29490 Gloederd, Mount Clemens, Mich.
Robertson, H. G., 36 Norwood Rd., Toronto, Ont., Canada
Rohidas, P., Jr., The Gramophone Company, Ltd., Box 118, Bombay, India
Rumbaugh, J. R., 628 Wood St., Houma, La.
Scarborough, H. B., Georgia School of Technology, Atlanta, Ga.

Seaton, J. W., 1426—21 St., N. W., Washington, D. C.
Sherwood, H. R., 35-448 Eighth St., Jackson Heights, L. I., N. Y.
Smith, S. R., Box 2162, Georgia School of Technology, Atlanta, Ga.
Smith, W. L., 10110 Pierce Dr., Woodmoor, Silver Spring, Md.
Stonger, W. L., WFBL Bldg., Syracuse, N. Y.
Suffield, F. G., 2636 N. Charles St., Baltimore, Md.
Sullivan, T. J., 24 Ozark St., Springfield, Mass.
Vizanko, D., 1518 S. Fith, Springfield, Ill.
Vogeler, R. A., 6650 S. Cicero Ave., Chicago, Ill.
Wallin, G., 631 Sheridan Rd., Chicago, Ill.
Wayer, C. F., Jr., Box 440, Anchorage, Alaska
Weber, G. L., 4358 N. Pershing Dr., Arlington, Va.
Wilson, E. S., 1265 Culver Rd., Rochester, N. Y.
Withrow, W. E., 4209 Longfellow St., Hyattsville, Md.
Wood, J. O., 15 Stoddard Rd., Hingham, Mass.
Woodward, T. M., Jr., 354 E. Fifth St., Emporium, Pa.
Yetter, E. W., 4901 Stenton Ave., Philadelphia, Pa.

Institute Committees, 1942

Admissions

H. M. Turner, *Chairman*

C. B. Aiken, G. T. Royden
H. H. Beverage, Melville Eastham
I. S. Coggeshall, Lloyd Espenscheid
F. W. Cunningham, L. C. F. Horle

Awards

Ralph Bown, *Chairman*

A. B. Chamberlain, C. B. Jolliffe
Melville Eastham, F. B. Llewellyn
G. E. Gustafson, F. E. Terman
C. M. Jansky, Jr., H. A. Wheeler

Board of Editors

Alfred N. Goldsmith, *Chairman*

R. R. Batcher, H. F. Olson
P. S. Carter, G. W. Pickard
L. M. Clement, Haraden Pratt
E. W. Engstrom, C. A. Priest
W. L. Everitt, L. J. Sivian
P. C. Goldmark, L. C. Smeby
F. W. Grover, B. J. Thompson
C. M. Jansky, Jr., H. A. Wheeler
J. D. Kraus, L. P. Wheeler
F. B. Llewellyn, L. E. Whittemore
S. S. Mackeown, G. W. Willard
E. L. Nelson, William Wilson
C. J. Young

Constitution and Laws

Austin Bailey, *Chairman*

I. S. Coggeshall, L. C. F. Horle
R. A. Heising, H. M. Turner
H. R. Zeamans

Executive

A. F. Van Dyck, *Chairman*
Haraden Pratt, *Vice Chairman*

I. S. Coggeshall, F. B. Llewellyn
Alfred N. Goldsmith, B. J. Thompson
H. P. Westman, *Secretary*

Membership

F. E. Terman, *Chairman*

V. J. Andrew, F. W. Cunningham
C. M. Burrill, A. V. Eastman
J. M. Clayton, Noel Eldred
R. I. Cole, W. L. Everitt
E. D. Cook, D. G. Fink
E. W. Herold, K. S. Van Dyke
C. M. Jansky, Jr., H. M. Wagner
J. G. Kreer, Jr., Ernst Weber
J. P. Minton, H. A. Wheeler
R. L. Snyder, Jack Yolles
Sarkes Tarzian

New York Program

Keith Henney, *Chairman*

C. B. Aiken, F. A. Hinners
Wilson Aull, Jr., G. T. Royden
A. B. Chamberlain, B. E. Shackelford
E. J. Content

Nominations

H. H. Beverage, *Chairman*

Ralph Bown, J. K. Johnson
W. L. Everitt, W. W. Lindsay, Jr.
C. M. Jansky, Jr., Haraden Pratt
L. P. Wheeler

Papers

William Wilson, *Chairman*
F. B. Llewellyn, *Vice Chairman*

H. A. Affel, D. K. Martin
J. L. Callahan, Knox McIlwain
N. P. Case, H. R. Mimno
A. B. Chamberlain, G. G. Muller
J. K. Clapp, A. F. Murray
I. S. Coggeshall, Benjamin Olney
F. W. Cunningham, H. O. Peterson
R. B. Dome, J. R. Poppele
W. G. Dow, Simon Ramo
E. B. Ferrell, F. X. Rettenmeyer
F. W. Grover, P. C. Sandretto
O. B. Hanson, S. A. Schelkunoff
J. V. L. Hogan, D. B. Sinclair
F. V. Hunt, H. M. Turner
Harley Iams, Dayton Ulrey
L. F. Jones, W. C. White
J. G. Kreer, Irving Wolff
F. R. Lack, J. W. Wright
H. C. Leuteritz, H. A. Zeamans

Papers Procurement

D. D. Israel, *Chairman*

W. L. Barrow, D. E. Noble
E. L. Bowles, A. A. Oswald
J. E. Brown, J. R. Poppele
R. S. Burnap, P. C. Sandretto
E. L. Chaffee, W. L. Schwesinger
J. D'Agostino, B. E. Shackelford
E. T. Dickey, H. C. Sheve
A. V. Eastman, L. C. Smeby
D. E. Foster, Karl Spangenberg
Virgil M. Graham, H. M. Turner
O. B. Hanson, A. F. Van Dyck
F. V. Hunt, H. A. Wheeler
H. S. Knowles, L. P. Wheeler
H. K. Morgan, R. M. Wise

Public Relations

O. H. Caldwell, *Chairman*

E. K. Cohan, D. D. Israel
D. G. Fink, I. J. Kaar
G. W. Gilman, F. X. Rettenmeyer
George Grammer, Lincoln Walsh
O. B. Hanson

Registration of Engineers

H. B. Richmond, *Chairman*

J. K. Johnson, E. L. Nelson

Sections

R. A. Heising, *Chairman*

C. N. Anderson, L. C. F. Horle
I. S. Coggeshall, J. H. Miller
E. D. Cook, F. A. Polkinghorn
Virgil M. Graham, G. T. Royden
L. P. Wheeler

Tellers

A. B. Chamberlain, *Chairman*

R. S. Burnap, Beverly Dudley
C. E. Scholz

Technical Committees

Annual Review

L. E. Whittemore, *Chairman*

W. M. Angus
W. G. Cady
O. H. Caldwell
J. L. Callahan
J. H. Dellinger
Keith Henney
I. J. Kaar
D. E. Noble
E. G. Ports
H. A. Wheeler

Electroacoustics

G. G. Muller, *Chairman*

S. J. Begun
F. V. Hunt
V. N. James
Knox McIlwain
George Nixon
Benjamin Olney
H. F. Olson
H. H. Scott
L. J. Sivian

Electronics

R. S. Burnap, *Chairman*

E. L. Chaffee
H. P. Corwith
K. C. DeWalt
W. G. Dow
R. L. Freeman
T. T. Goldsmith, Jr.
L. B. Headrick
S. B. Ingram
Ben Kievit, Jr.
I. E. Mouromtseff
L. S. Nergaard
G. D. O'Neill
H. W. Parker
H. J. Reich
C. M. Wheeler
J. R. Wilson

Facsimile

J. L. Callahan, *Chairman*

J. C. Barnes
W. A. R. Brown
G. V. Dillenback, Jr.
W. G. H. Finch
John Hancock
J. V. L. Hogan
H. C. Knutson
Paul Lefko
R. E. Mathes
J. W. Milner
J. R. Poppele
C. J. Young

Frequency Modulation

D. E. Noble, *Chairman*

J. E. Brown
C. C. Chambers
W. F. Cotter
Murray Crosby
W. L. Everitt
R. F. Guy
C. M. Jansky, Jr.
V. D. Landon
H. B. Marvin
B. E. Shackelford
D. B. Smith
L. P. Wheeler
Warren White

Piezoelectric Crystals

W. G. Cady, *Chairman*

C. F. Baldwin
W. L. Bond
J. K. Clapp
W. P. Mason
J. M. Wolfskill
K. S. Van Dyke

Radio Receivers

W. M. Angus, *Chairman*

G. L. Beers
W. M. Breazeale
W. F. Cotter
Harry Diamond
W. L. Dunn
H. B. Fischer
H. C. Forbes
D. E. Foster
C. J. Franks
David Grimes
J. K. Johnson
Garrard Mountjoy
H. O. Peterson
A. E. Thiessen
R. M. Wilmotte

Radio Wave Propagation

J. H. Dellinger, *Chairman*

S. L. Bailey
C. R. Burrows
W. A. Fitch
G. D. Gillett
H. R. Mimno
K. A. Norton
H. O. Peterson
H. P. Thomas
Warren White

Standards

H. A. Wheeler, *Chairman*

W. M. Angus
C. T. Burke
W. G. Cady
C. C. Chambers
Virgil M. Graham
L. C. F. Horle
I. J. Kaar
D. E. Noble
E. G. Ports
A. E. Thiessen
H. M. Turner

Symbols

H. M. Turner, *Chairman*

R. R. Batcher
M. R. Briggs
C. R. Burrows
E. L. Chaffee
E. T. Dickey
O. T. Laube
E. W. Schafer

Television

I. J. Kaar, *Chairman*

H. S. Baird
R .R. Batcher
J. E. Brown
A. B. DuMont
D. E. Foster
P. C. Goldmark
T. T. Goldsmith, Jr.
A. G. Jensen
L. M. Leeds
H. M. Lewis
A. V. Loughren
H. T. Lyman
A. F. Murray
R. E. Shelby
D. B. Sinclair
D. B. Smith

Transmitters and Antennas

E. G. Ports, *Chairman*

Raymond Asserson
M. R. Briggs
W. W. Brown
Harry Diamond
F. A. Gunther
Raymond Guy
W. E. Jackson
J. F. Morrison
J. C. Schelleng
Robert Serrell
D. B. Sinclair
Warren White
J. E. Young

Institute Representatives in Colleges

Alabama Polytechnic Institute: Woodrow Darling
Alberta, University of: J. W. Porteous

British Columbia, University of: H. J. MacLeod
Brooklyn, Polytechnic Institute of: F. E. Canavaciol

California Institute of Technology: S. S. Mackeown (Alternate, William Pickering)
California, University of: L. J. Black
Carleton College: C. A. Culver
Carnegie Institute of Technology: R. T. Gabler
Case School of Applied Science: P. L. Hoover
Cincinnati, University of: W. C. Osterbrock
Colorado, University of: J. M. Cage
Columbia University: J. B. Russell
Connecticut, University of: V. S. Carson
Cooper Union: J. B. Sherman
Cornell University: True McLean

Drexel Institute of Technology: R. T. Zern
Duke University: W. J. Seeley

Florida, University of: Joseph Weil

Georgia Institute of Technology: M. A. Honnell

Harvard University: E. L. Chaffee

Idaho, University of: Hubert Hattrup
Illinois Institute of Technology: P. G. Andres
Illinois, University of: H. J. Reich
Iowa, University of: R. C. Kent

Johns Hopkins University: Ferdinand Hamburger, Jr.

Kansas State College: Karl Martin
Kansas, University of: S. E. Clements
Kentucky, University of: E. B. Doll

La Plata: Jean Arnaud
Lawrence Institute of Technology: H. L. Byerlay
Lehigh University: H. C. Knutson
Louisiana State University: Taintor Parkinson

Maine, University of: W. J. Creamer, Jr.
Manhattan College: J. F. Reintjes
Maryland, University of: G. L. Davies
Massachusetts Institute of Technology: W. H. Radford and E. Guillemin
McGill University: F. S. Howes
Michigan, University of: L. N. Holland
Minnesota, University of: H. E. Hartig
Montana State College: G. J. Fiedler

Nebraska, University of: F. W. Norris
Newark College of Engineering: Solomon Fishman
New Mexico, University of: H. L. Jones
New York, College of the City of: Maxwell Henry
New York University: Philip Greenstein
North Dakota, University of: E. J. O'Brien
Northeastern University: G. E. Pihl
Northwestern University: A. B. Bronwell
Notre Dame, University of: H. E. Ellithorn

Ohio State University: W. L. Everitt
Oklahoma Agricultural and Mechanical College: H. T. Fristoe
Oregon State College: A. L. Albert

Pennsylvania State College: G. H. Crossley
Pennsylvania, University of: C. C. Chambers
Pittsburgh, University of: R. C. Gorham
Princeton University: J. G. Barry
Purdue University: R. P. Siskind

Rensselaer Polytechnic Institute: H. D. Harris
Rose Polytechnic Institute: H. A. Moench
Rutgers University: J. L. Potter

Southern California, University of: J. K. Nunan
Southern Methodist University: R. E. Beam
Stanford University: Karl Spangenberg
Stevens Institute of Technology: F. C. Stockwell

Texas, University of: E. W. Hamlin

Toronto, University of: B. de F. Bayly
Tufts College: J. L. Barnes

Union College: F. W. Grover
United States Military Academy: E. C. Gillette, Jr.
United States Naval Academy: G. R. Giet
Utah, University of: O. C. Haycock

Virginia Polytechnic Institute, W. A. Murray

Washington, University of: A. V. Eastman
Washington University: R. S. Glasgow
Wayne University: G. A. Carter
Western Ontario, University of: G. A. Woonton
West Virginia University: R. C. Colwell
Wisconsin, University of: Glenn Koehler
Worcester Polytechnic Institute: H. H. Newell
Wyoming, University of: Carl Brown

Yale University: H. M. Turner

Institute Representatives on Other Bodies

A.I.E.E.—Subcommittee on Radio of the Committee on Applications to Marine Work............T. E. Nivison and J. L. Preston
American Documentation Institute..........C. M. Jansky, Jr.
Committee on Applied Physics..........William Wilson
Council of the American Association for the Advancement of Science..........J. C. Jensen
Engineering Index National Committee..........Melville Eastham
Joint Co-ordination Committee on Radio Reception of the N.E.L.A., N.E.M.A., and R.M.A..........C. E. Brigham
National Advisory Council on Radio in Education, Committee on Engineering Developments..........
..........Lloyd Espenschied, Alfred N. Goldsmith, C. W. Horn, L. M. Hull, and R. H. Marriott
National Television Systems Committee..........Alfred N. Goldsmith (H. A. Wheeler, alternate)
Panel 2..........Alfred N. Goldsmith, Chairman
Panel 4..........E. G. Ports
Panel 8..........Knox McIlwain
New York City Advisory Board on Industrial Education..........H. P. Westman
Planning Committee, National Conference on Educational Broadcasting, American Council on Education..........
..........C. M. Jansky, Jr., C. B. Jolliffe, and E. L. Nelson
U.R.S.I. (International Scientific Radio Union) Executive Committee..........C. M. Jansky, Jr.
U. S. National Committee, Advisers on Electrical Measuring Instruments..........Melville Eastham and Harold Olesen
U. S. National Committee, Advisers on Symbols..........L. E. Whittemore and J. W. Horton

American Standards Association

Standards Council..........Alfred N. Goldsmith (H. P. Westman, alternate)
Board of Examination..........H. P. Westman
Electrical Standards Committee..........H. M. Turner (H. P. Westman, alternate)
Sectional Committee on Acoustical Measurements and Terminology..........E. D. Cook and H. F. Olson
Sectional Committee on Definitions of Electrical Terms..........Haraden Pratt
Subcommittee on Vacuum Tubes..........B. E. Shackelford
Sectional Committee on Electric and Magnetic Magnitudes and Units..........J. H. Dellinger
Sectional Committee on Electrical Installations on Shipboard..........I. F. Byrnes and V. R. Russ
Sectional Committee on Electrical Measuring Instruments..........Wilson Aull
Sectional Committee on Graphical Symbols and Abbreviations for Use on Drawings..........Austin Bailey (H. P. Westman, alternate)
Subcommittee on Communication Symbols..........H. M. Turner
Sectional Committee on Letter Symbols and Abbreviations for Science and Engineering..........H. M. Turner
Subcommittee on Letter Symbols for Radio Use..........H. M. Turner
Sectional Committee on National Electrical Safety Code, Subcommittee on Article 810, Radio Broadcast Reception Equipment..........
..........E. T. Dickey (Virgil M. Graham, alternate)
Sectional Committee on Preferred Numbers..........A. F. Van Dyck
Sectional Committee on Radio..........Alfred N. Goldsmith, Chairman; Haraden Pratt, and L. E. Whittemore
Sectional Committee on Radio-Electrical Co-ordination..........J. V. L. Hogan, C. M. Jansky, Jr., and L. E. Whittemore
Sectional Committee on Specifications for Dry Cells and Batteries..........H. M. Turner
Sectional Committee on Standards for Drawings and Drafting Room Practices..........Austin Bailey
Section Committee on Vacuum Tubes for Industrial Purposes..........B. E. Shackelford

Books

Chart Atlas of Complex Hyperbolic and Circular Functions (Third Edition), by A. E. Kennelly, 1924.

Published by Harvard University Press Cambridge, Massachusetts. 30 large pages of charts. 20×20 inches. Price $6.00.

This volume, originally published in 1914, is a valuable collection of large graphical charts giving the direct and inverse hyperbolic and circular functions of a complex variable. The large size of the charts contributes to the accuracy of reading. For convenience in plotting, the angles are expressed in quadrants instead of radians. One of the variables is plotted on rectangular co-ordinates, the other is plotted in contour lines. In special cases, the contours form the polar co-ordinates of the familiar circle diagrams. The principal application of these charts is in the field of transmission lines and filters.

H. A. Wheeler
Hazeltine Service Corporation
Little Neck, L. I., N. Y.

Tables of Complex Hyperbolic and Circular Functions, (Second Edition), by A. E. Kennelly, 1927.

Published by Harvard University Press, Cambridge, Massachusetts. 240 pages. $6\frac{3}{4}\times 9\frac{1}{2}$ inches. Price $6.00.

This volume, originally published in 1914, is mainly a collection of numerical tables of hyperbolic functions of the complex variable. About one third of the book is devoted to an explanation of the tables and their use, with special attention to interpolation and correcting factors. This section gives instructions for plotting the functions in charts.* Also it closes with a collection of 238 formulas of the relations among hyperbolic functions, their series expansions, derivatives, and integrals.

H. A. Wheeler
Hazeltine Service Corporation
Little Neck, L. I., N. Y.

* A. E. Kennelly, "Chart Atlas of Complex Hyperbolic Functions," 1914–1924, preceding review on this page.

Theory of Gaseous Conduction and Electronics, by F. A. Maxfield and R. R. Benedict

Published by McGraw-Hill Book Company, 330 West 42 Street, New York, N. Y. 465+xiv pages+17-page index. 241 figures. $6\frac{1}{4}\times 9\frac{1}{4}$ inches. Price, $4.50.

As to general plan, this text in each chapter presents certain principles of electronic behavior, and then illustrates these principles by discussing specific devices in which they are used. For example, gaseous-conduction rectifiers, including thyratrons and ignitrons, are taken up in the latter part of a chapter on the "Arc Discharge," while photoelectric devices are discussed toward the end of the chapter on "Electron Emission." The text proper opens with a treatment of electric-field principles. There follow several chapters treating the behavior of charged particles in evacuated regions, also in regions containing gases, then chapters respectively on spark formation, and the behavior of glow discharges and of arc discharges.

The text is plentifully illustrated with cuts of equipment, diagrams illustrating the electronic behaviors being analyzed, and circuit diagrams. There is very considerable qualitative discussion of the behavior of circuits in which electronic devices are used, but relatively little detailed circuit analysis. The book is a good illustration of the present trend toward use of the m-k-s system of units. The reasons for the choice of this system of units are explained early in the text.

By far the greater part of the book is taken up with the discussions of the various electronic mechanisms associated with gaseous conduction. The presentation of the basic and generally important facts of the molecular theory of gases in relation to gaseous conduction is especially good. The background of Paschen's spark-over law is built up simply and well, although with only a very general reference to the important part that is believed to be played by secondary photoelectric emission at the cathode.

In the last chapter there is a very good discussion of a closely related group of applications, including arc-back in mercury-arc rectifiers, the principles of behavior of circuit-interrupting devices, and of lightning arresters, together with certain aspects of the internal behavior of ignitrons and thyratrons. This treatment reflects the very considerable industrial experience Dr. Maxfield has had in work in this field.

A knowledge of the more common electrical-engineering principles, and a reasonably satisfactory facility with calculus, provide sufficient background for study of the text. There are very many useful, illustrative problems.

W. G. Dow
University of Michigan
Ann Arbor, Michigan

Contributors

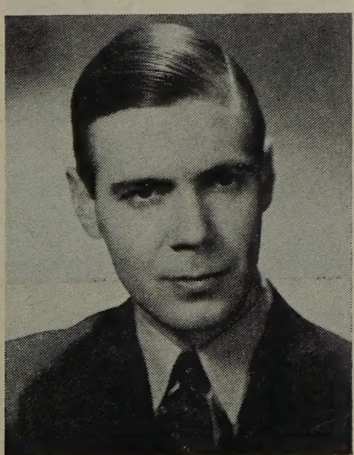

John N. Dyer

John N. Dyer (J'30–A'32) was born in Haverhill, Massachusetts, on July 14, 1910. He received the B.S. degree in 1931 from Massachusetts Institute of Technology. In September, 1933, he joined the Columbia Broadcasting System staff and was assigned to the Byrd Antarctic Expedition as chief communications engineer to handle the Columbia Broadcasting System broadcasts. Returning in 1935, he did ultra-high-frequency work in the general engineering department. At the close of 1936 he was transferred to the television engineering department and is now assistant chief engineer.

❖

S. Frankel (A'37) was born in New York City on October 6, 1910. He received the B.A. degree in electrical engineering at the Rensselaer Polytechnic Institute in 1931, the M.A. degree in mathematics in 1934, and the Ph.D. degree in mathematics in 1936. He was an instructor in mathematics at Rensselaer Polytechnic Institute from 1931 to 1933.

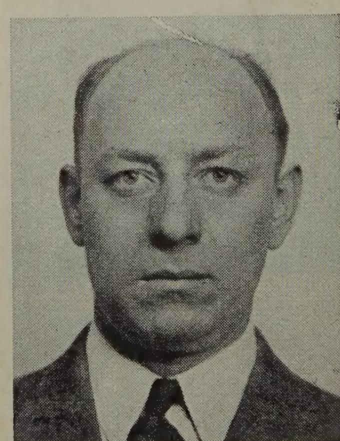

S. Frankel

During 1936–1937 Dr. Frankel was a sound-recording engineer with the Brook-

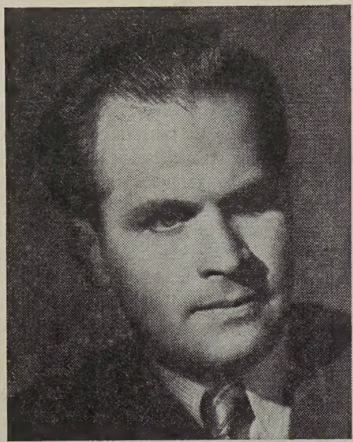

PETER C. GOLDMARK

lyn Vitaphone Corporation, and in 1937–1938 an assistant engineer in the design and development of electronic flight instruments with the Eclipse Aviation Corporation, at Bendix, New Jersey.

Since 1938, he has been an engineer in the design and development of radio transmitters with the Federal Telegraph Company, Newark, New Jersey.

He is a member of Sigma Xi.

❖

Peter C. Goldmark (A'36–M'38) was born on December 2, 1906 at Budapest, Hungary. He received the B.Sc. degree in 1930 from the University of Vienna and the Ph.D. degree in physics in 1931. Dr. Goldmark was in charge of the Television Department of Pye Radio, Ltd., Cambridge, England, from 1931 to 1933; consulting engineer in New York City, 1933 to 1935. Since 1935 he has been chief television engineer at the Columbia Broadcasting System.

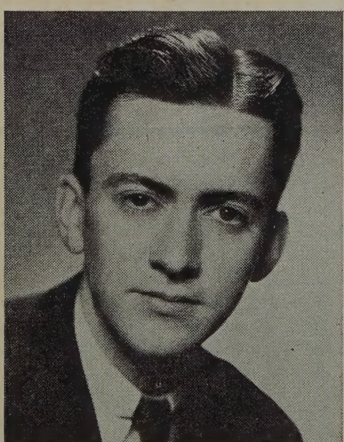

J. M. HOLLYWOOD

John M. Hollywood (J'30–A'32) was born at Red Bank, New Jersey, on February 4, 1910. He received the B.S. degree in communications in 1931 and the M.S. degree in electrical engineering in 1932 from Massachusetts Institute of Technology. From 1933 to 1935 Mr. Hollywood was with the Electron Research Laboratories; from 1935 to 1936 with the Ken-Rad Tube Corporation engaged in cathode-ray-tube development; and from 1936 to the present time, with the Columbia Broadcasting System working on television development.

❖

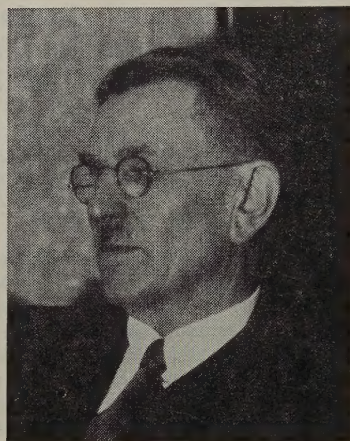

I. E. MOUROMTSEFF

Ilia Emmanuel Mouromtseff (A'34) was born in December, 1881, at St. Petersburg, Russia. He received the M.A. degree from the Engineering Academy at St. Petersburg in 1906 and the Diploma-Ingenieur degree from the Institute of Technology at Darmstadt, Germany, in 1910. Mr. Mouromtseff was in the radio laboratory of the Russian Signal Corps in 1911. He has been a member of the technical staff of the Westinghouse Electric and Manufacturing Company since 1923.

❖

E. R. Piore (A'38) received the B.A. in physics in 1930 and the Ph.D. degree in physics in 1935 from the University of Wisconsin. He was assistant instructor in physics at the same University from 1930 to 1935, and from 1935 to 1938 he was a research physicist at the electronic research laboratories of the RCA Manufacturing Company, Inc. Since 1938 Dr. Piore has been a member of the Columbia Broadcasting System television engineering department as engineer-in-charge of the television laboratories. He is a member

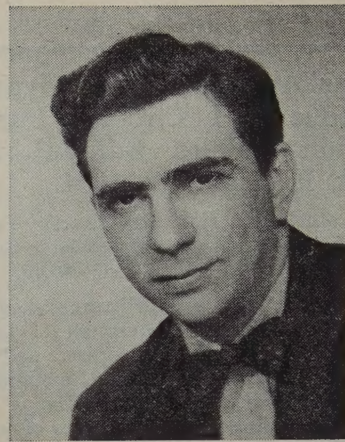

E. R. PIORE

of the American Physical Society and Sigma Xi.

❖

F. R. Stansel (A'26–M'33) was born in Raleigh, North Carolina, on August 7, 1904. He received the B.S. in E.E. degree from Union College in 1926, the M.E.E. degree from the Polytechnic Institute of Brooklyn in 1934, and the D.E.E. degree from the same institution in 1941. In 1926 he joined the Bell Telephone Laboratories and until 1936 was engaged at their Whippany laboratory in the development and design of high-power radio transmitters for broadcast and transoceanic service. Since 1936 Dr. Stansel has been engaged in the development and design of special testing equipment.

He is a member of the American Institute of Electrical Engineers.

❖

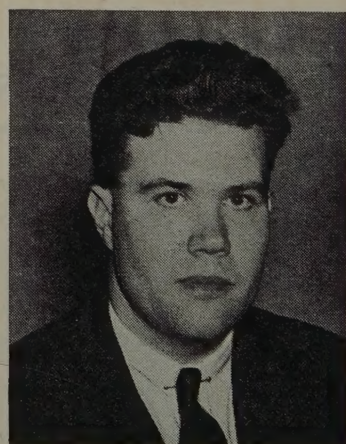

F. N. STANSEL